2008

A Novel Phosphorylation Site in the Telomeric Protein TRF2 is Regulated by the ATR Kinase and Plays a Role in Relieving Replication Stress at the Telomere

Kristina Hoke

A NOVEL PHOSPHORYLATION SITE IN THE TELOMERIC PROTEIN TRF2 IS REGULATED BY THE ATR KINASE AND PLAYS A ROLE IN RELIEVING REPLICATION STRESS AT THE TELOMERE

A Thesis Presented to the Faculty of

The Rockefeller University

In Partial Fulfillment of the Requirements for

the Degree of Doctor of Philosophy

by

Kristina Hoke

June 2008

A NOVEL PHOSPHORYLATION SITE IN THE TELOMERIC PROTEIN TRF2 IS REGULATED BY THE ATR KINASE AND PLAYS A ROLE IN RELIEVING REPLICATION STRESS AT THE TELOMERE

Kristina Hoke, Ph.D.

The Rockefeller University 2008

Phosphatidyl inositol 3-kinase-like kinases (PIKKs) have a well documented function at yeast telomeres. Although several lines of evidence suggest that members of the PIKK family also play a role in vertebrate telomere biology, little is known about their specific functions. We report that the human shelterin component, TRF2, overexpressed in 293T cells, is phosphorylated on serine 368 (S368) in a caffeine and wortmannin sensitive manner. Phosphorylation is induced by hydroxyurea (HU) and ultraviolet (UV) radiation but not Ionizing Radiation (IR). Knockdown studies indicate that ATR is the primary kinase responsible for TRF2 S368 phosphorylation, while the mTOR kinase is implicated as a negative regulator of the phosphorylation event. In order to study the function of phosphorylation of TRF2 on S368, we replaced endogenous TRF2 in MEFs with TRF2 containing mutated S368 (S366 in mouse). TRF2 S366 mutants fulfilled the major telomeric protective functions of TRF2 and prevented cell cycle arrest, formation of telomere dysfunction induced foci, overhang loss, telomere fusions, and telomere sister chromatid exchanges. TRF2 S368 mutants

were able to influence telomere length homeostasis in certain settings in both human and mouse cells. In mouse cells, expression of TRF2 containing a phosphomimetic mutation at position 366 (S366E) caused dramatic telomere lengthening; in human cells, overexpression of S368 mutants did not reproduce the rapid telomere shortening caused by overexpression of wildtype TRF2, indicating that these mutants may not be able to promote t-loop HR. Telomeres exhibited an unusual sensitivity to aphidicolin: 25-28% of 53BP1 foci induced by aphidicolin treatment colocalized with telomeric DNA. Expression of TRF2 S366E improved survival of MEFs after aphidicolin treatment. Cells expressing TRF2 S366E also exhibited fewer chromatid breaks and 53BP1 foci after aphidicolin treatment, and the percentage of 53BP1 foci which colocalized with telomeres was decreased by a small but significant amount. Finally, we show that a phosphomimetic mutation at position 368 weakens the interaction between TRF2 and TIN2, suggesting that phosphorylation of TRF2 on S368 may relieve replication stress at the telomere by modifying the conformation of shelterin to allow the replication fork to more easily pass.

Acknowledgments

Foremost I wish to thank my advisor, Dr. Titia de Lange, for her excellent mentorship. In spite of her many responsibilities and commitments she always made herself available to answer my questions and offer expert guidance and assistance, both theoretical and practical. She has set extremely high standards for scientific rigor that will guide me in my future career. I would also like to thank her for the occasional loan of designer shoes and gowns.

I would also like to thank the members of my thesis committee: Chair Dr. David Allis, Dr. John Petrini, and Dr. Hironori Funabiki for the invaluable advice and perspective they have provided over the years. They always managed to simultaneously challenge and encourage me at our yearly committee meetings. I would also like to express my appreciation to Dr. Eric Brown, for traveling from the University of Pennsylvania to serve as the external examiner on my thesis committee.

To the past and present members of the de Lange lab, I would like to express my appreciation for making the lab a pleasant and scientifically stimulating (and very neat and orderly) work environment. I would particularly like to thank Dr. Diego Loayza for my initial training. Dr. Hiro Takai, Dr. Sara Buonomo, Dr. Eros Lazzerini-Denchi, and Dr. Agnel Sfeir were also exceedingly generous with their scientific knowledge, advice, and reagents. I would like to thank the former and current graduate students of the de Lange lab, Josh Silverman, Rich Wang, Dirk Hockemeyer, Nadya Dimitrova, Megan van

Overbeek, Jan-Peter Daniels, Wilhelm Palm and Peng Wu for their camaraderie and generosity with scientific advice and reagents. I would especially like to thank my fellow graduate student, Jill Donigian, for all her support, both scientific and personal over the years.

Stew Barnes deserves special recognition for being exceedingly knowledgeable and helpful about all computer-related issues. I would also like to thank Stephanie Blackwood for helping me many times to obtain important reagents. Stephanie Blackwood, Rita Rodney, Kaori Takai, Eliana Forero, and Heathers Parsons have made the lab run smoothly, making it a great place to do science. I am also indebted to Lola MacRae for her help formatting and proofreading my thesis. I would also like to thank the Rockefeller University Dean's Office for their guidance during the dissertation process.

I would also like to thank Dr. Daria Colombo and Dr. Saud Sadiq. Finally, I want to thank my parents Jim and Kathy Hoke and my sister Lara Hoke for their love and support throughout my education. A special thanks goes to my partner Paul Antonson for his unflagging love, support, and encouragement.

Table of Contents

List of Figures

List of Abbreviations

ALT	Alternative Lengthening of Telomeres
APB	ALT associated PML Body
AT	Ataxia Telangiectasia
BAC	Bacterial Artificial Chromosome
CO-FISH	Chromosome Orientation FISH
DC	Dyskeratosis Congenita
DSB	Double Stranded Break
FACS	Fluorescence Activated Cell Sorting
FISH	Fluorescence *In Situ* Hybridization
HR	Homologous Recombination
IF	Immunofluorescence
KO	Knock-Out
MEF	Mouse Embryonic Fibroblast
MMS	Methyl Methanesulfonate
NBS	Nijmegan Breakage Syndrome
NER	Nucleotide Excision Repair
NHEJ	Non-Homologous End Joining
NMD	Nonsense-mediated RNA Decay
OA	Okadaic Acid
OB/OB	Oligonucleotide/Oligosaccharide Binding
ORC	Origin Replication Complex
PFGE	Pulsed Field Gel Electrophoresis
PIKK	Phosphatidyl Inositol 3-Kinase-like Kinase
PML	Promyelocytic Leukemia
RCT	Rap1 C Terminal
RFB	Replication Fork Barrier
SCD	SQ/TQ Cluster Domain
TIF	Telomere Dysfunction Induced Foci
TRD	Telomere Rapid Deletion
T-SCE	Telomere Sister Chromatid Exchange

Chapter 1: Introduction

CHROMOSOME STRUCTURE AND REPLICATION

Most prokaryotic genomes consist of a single circular chromosome, while the larger and more complex genomes of eukaryotes are usually composed of multiple linear chromosomes. Linear chromosomes contain a single centromere, which range from approximately 100 base pairs in budding yeast to several megabases in humans[1]. Centromeres are composed of specialized chromatin that forms the basis for the assembly of kinetochores, the points at which spindle microtubules attach[1]. Centromeres generally consist of short tandem DNA repeats, the sequences of which are not well conserved across species, however mammalian centromeric chromatin contains a centromere-specific variant of histone H3, distinguishing it from bulk chromatin[2].

Chromosomes are chiefly replicated by conventional semi-conservative DNA replication. Replication of chromosomal DNA begins when the Origin Replication Complex (ORC) binds to an origin of replication and recruits the machinery required for DNA replication[3]. Several thousand origins of replication have been identified in *S. cerevisiae*, but identification of mammalian origins has been much more difficult, and less than 20 veritable origins are defined[3]. At the ends of linear chromomsomes, the mechanisms of DNA replication predict that the lagging strand will be incompletely replicated due to the requirement for an RNA primer, a predicament dubbed the 'end replication problem'[4,5]. A second

problem presented by linear chromosomes is the constituitive presence of DNA ends in the nucleus. Because DNA ends normally indicate the occurrence of double-stranded DNA breaks (DSBs) and cells have stringent mechanisms to detect and respond to their presence, the DNA damage response machinery must be able to distinguish chromosome ends from DSBs. Telomeres, nucleoprotein structures located at the tips of the linear chromosome, mitigate the end replication problem and prevent chromosome ends from being detected as DNA damage.

TELOMERE STRUCTURE

Telomeres consist of GC-rich DNA repeats bound by specific proteins. Vertebrate telomeres are composed of multiple repeats of the 6 nucleotide sequence 5'-TTAGGG-3'. The sequence of most eukaryotic telomere repeats is similar or the same as the vertebrate telomere repeat sequence. For example, the hypotrichous ciliate telomere repeat is 5'-TTTTGGGG-3'[6], the flowering plant *Arabidopsis thaliana* telomere repeat is 5'-TTTAGGGG-3'[7], and the silkworm *Bombyx mori* telomere repeat is 5'-TTAGG-3'[8].

Human telomeric tracts are 5-15 kb in length[9 10]. In the laboratory mouse, *Mus musculus*, telomeric tracts are much longer, often greater than 30 kb. However, the telomeres of *Mus spretus* and several other species of mouse are closer in length to human telomeres, in the range of 4-12 kb, indicating that significant interspecies variability in telomere length is possible, at least in

rodents[11 12]. At the very end of the eukaryotic telomere, the G rich strand protrudes past the terminus of the C rich strand to form a structure called the G-tail or G-overhang[13]. In humans the vast majority of C rich telomeric strands end with the sequence 3'-ATC-5' suggesting that the processing of the C strand terminus is tightly regulated[14]. In contrast, the terminus of the G rich telomeric strand is much less precise but the termini, 5'-GGTTAG-3', 5'-GGGTTA-3', or 5'-AGGGTT-3' occur with higher frequency than the other possible permutations[14].

T-loops, lariat-like DNA structures in which the 3' overhang of the telomere strand invades a more proximal portion of the double-stranded telomere can form at chromosome termini[15 16]. T-loops have been documented at the telomeres of humans, mice, chickens, trypanosomes, and the hypotrichous ciliate *Oxytricha fallax*[15 17 18 19], suggesting that they may be a near-universal feature of chromosome termini. The resemblance of the t-loop to a DNA recombination intermediate[15] raises the possibility that the homologous recombination (HR) machinery may be involved in their formation[20] and that tight regulation of HR may be required at the telomere to prevent unscheduled resolution of these structures[21].

The presence of nucleosomes has been demonstrated at the telomeres of both vertebrates and invertebrates[22 23 18]. However, several observations indicate that telomeric chromatin has different properties than bulk chromatin. The telomeric mononucleosome is hypersensitive to micrococcal nuclease and the linker of telomeric nucleosomes is minimal[22 23 24]. Also, the micrococcal nuclease

digestion pattern of human telomeres in cells with short telomeres is more diffuse than that of bulk chromatin, suggesting the presence of nucleosome free regions or altered chromatin structures[24].

TELOMERASE AND DISEASE

Telomerase

An activity that adds telomere repeats to GT-rich primers was identified in the ciliate *Tetrahymena*[25]. The enzyme responsible for this activity, telomerase, contains an RNA component[26] called hTR, or hTERC in humans[27], and a protein component with reverse transcriptase activity,[26 28 29 30] hTERT in humans[31 32] (Fig 1-1). In budding yeast, the core components of telomerase associate with several accessory proteins including Est1 which is involved in telomerase recruitment[33 34]. Three putative human homologs of Est1 have been recently identified, two of which associate with telomerase[35 36]. Recent biochemical purification showed that catalytically active human telomerase consists of two molecules each of hTERT, hTR, and the H/ACA box binding protein dyskerin[37]. Telomerase must act to counter the terminal sequence loss due to the end replication problem and active degradation of the telomere. Evidence that telomeres are subject to active degradation comes from the observation that in human and mouse cells lacking telomerase, telomeres shorten at a rate of 50-150 bp/end/cell division, rather than the 3-5 bp/end/cell division predicted by the end replication problem[38].

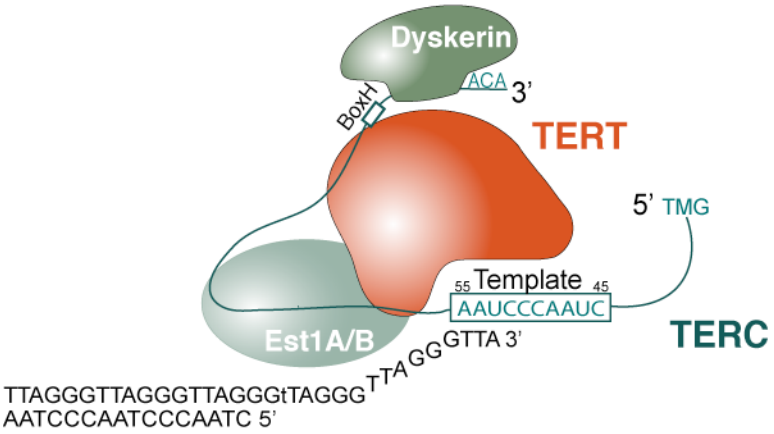

Figure 1-1: Human telomerase.
Catalytically active human telomerase consists of two molecules each of the reverse transcriptase hTERT, the RNA template hTERC, and the ribonucleoprotein dyskerin. The accessory proteins Est1A and Est1B may be involved in regulating telomerase recruitment and activity.

Senescence

Primary human fibroblasts grown in culture eventually stop dividing[39], a phenomenon known as replicative senescence. Telomeres shorten as fibroblasts age[10] and yeast with a mutation causing their telomeres to progressively shorten enter a senescence-like state[33]. These observations led to the proposal that replicative senescence is regulated by telomere shortening. Replicative senescence was definitively linked to telomere shortening when it was shown that introduction of hTERT into telomerase-negative cells causes telomere elongation and cellular immortalization[40].

Disease states related to telomerase function

The implications of telomere-mediated replicative senescence for cancer and aging were readily identified[41]. In humans, telomerase activity is low in somatic cells after embryonic development, with the exception of highly

proliferative cells such as bone marrow cells[42]. However, most cancer cells have regained telomerase expression[43] and most of those that have not use a recombination-based mechanism called Alternative Lengthening of Telomeres (ALT)[44] to lengthen their telomeres and circumvent telomere-mediated replicative senescence.

Genetic models as well as human disorders have highlighted the importance of telomere-mediated replicative senescence in human health. Late generation mice that lack the telomerase RNA component are susceptible to spontaneous malignancies, have shortened lifespans, and exhibit phenotypes related to limited cell proliferative capacity such as poor wound-healing[45 46 47 48]. Accumulating evidence indicates that the symptoms of the premature aging and cancer susceptibility disease, Werner Syndrome, are due to telomere dysfunction [49 50 51 52]. The human disease, dyskeratosis congenita (DC), characterized chiefly by skin abnormalities and bone marrow failure[53], is caused by mutations in the RNA component of telomerase[54] or in dyskerin, a ribonucleoprotein that binds and contributes to the maturational processing of hTERC[55] and is a component of catalytically active telomerase[37]. The phenotypes of DC can be attributed to defective telomere maintenance, limiting the proliferative capacity of skin and blood cells[56]. Mutations in the RNA component of telomerase can also lead to a life-threatening form of anemia[57] presumably by limiting the proliferative capacity of the bone marrow.

TELOMERE BINDING PROTEINS

The Shelterin Complex

In humans, chromosome ends are protected and regulated by the shelterin complex, which is made up of six proteins that localize primarily to the telomere and whose primary function is telomeric: TRF1, TRF2, Rap1, TIN2, TPP1, and Pot1[58] (Fig. 1-2A). Shelterin is anchored to the double-stranded TTAGGG repeats by TRF1 and TRF2[59 60 61 62 63]. TRF1 and TRF2 are linked together by TIN2[64,65], which also binds and recruits TPP1 to the telomere[66 67]. TPP1 binds POT1[68 66 67], which can bind single-stranded telomeric DNA[69 70]. All six components of shelterin can be found in a single complex[64 71] but evidence suggests that TRF1 and TRF2, and their direct binding partners, can exist in separate complexes as well[64,72].

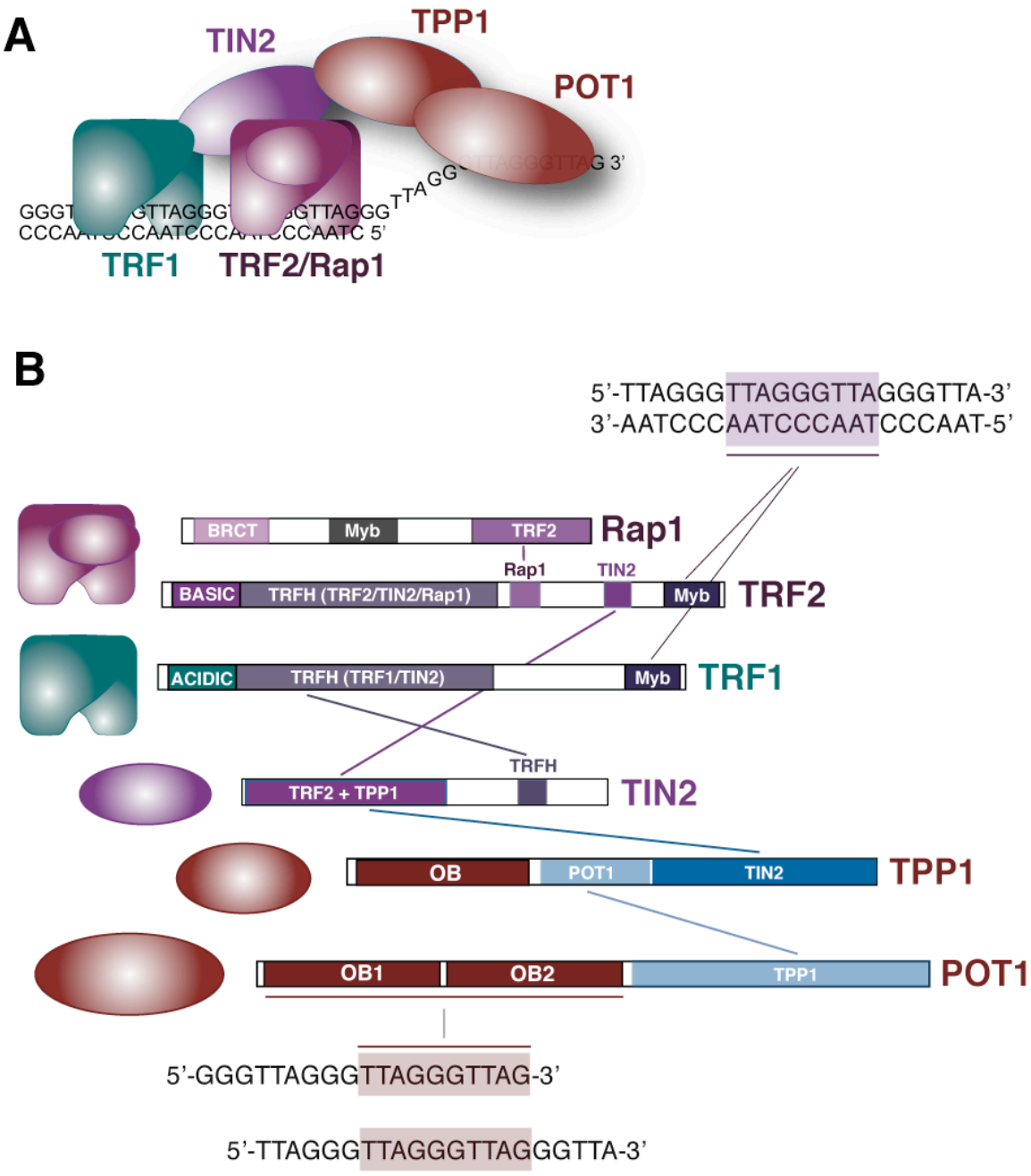

Figure 1-2: The Shelterin Complex
(A) Schematic of the shelterin complex on telomeric DNA. Human telomeres are protected and shaped by shelterin, a complex of six proteins which localize primarily to the telomere and whose primary function is telomeric.
(B) Domain structure of shelterin components. Interactions among shelterin components are indicated. Interactions between shelterin components and telomeric DNA repeats are indicated by diagonal lines.

TRF1

The first human telomeric protein to be discovered, TRF1, was isolated from nuclear extracts based on its ability to bind telomeric DNA[59]. TRF1 is an essential gene; its genetic deletion results in early embryonic lethality in the mouse[73]. TRF1 has an N terminal acidic domain, a homodimerization domain, a flexible domain, and a C terminal DNA binding domain containing myb-related motifs[60 61]. TRF1 binds double-stranded telomeric DNA as a dimer and both myb domains of dimeric TRF1 are required for DNA binding[61]. However there is no constraint on distance or orientation for the telomeric binding sites of the two DNA-binding domains of a TRF1 dimer[74].

TRF1 overexpression in the tumor cell line HT1080, results in telomere shortening while expression of a dominant negative allele of TRF1, which removes endogenous TRF1 from telomeres, causes telomeres to lengthen[75]. TRF1 affects the telomerase pathway; when TRF1 is overexpressed in telomerase-negative primary human fibroblasts it has no effect on telomere dynamics[76].

TRF2

TRF2 was identified in the database based on its homology with TRF1[60 62]. The TRFH domains, which mediate homodimerization of TRF1 and TRF2, are very closely related. However, heterodimerization between TRF1 and TRF2 does not occur[60]. The crystal structures of the TRFH domains shows that differences at key residues sterically hinder formation of heterodimers between

TRF1 and TRF2[77]. Furthermore, the composition of potential protein interaction surfaces, not involved in the dimer interface, differs significantly between TRF1 and TRF2, raising the possibility that these surfaces mediate interaction with different factors[77].

A striking difference between TRF1 and TRF2 is that while the N-terminal 50 amino acids of TRF1 are highly acidic, the corresponding region of TRF2 is very basic. The flexible or "hinge" domains, which lie between the TRFH and myb domains, are also quite different[60], raising the possibility that these regions are involved in the functional differences between TRF1 and TRF2. The crystal structures of the TRFH domains revealed that the alpha helices forming an individual TRFH domain fold back on each other so that the N and C terminus are located near each other in space[77], potentially positioning the N-terminal acidic and basic domains of TRF1 and TRF2 respectively in close proximity to the more C terminal hinge and DNA binding domains of the TRF proteins.

TRF2 can influence telomere length in telomerase negative cells and is required to prevent telomeres from being recognized as DNA damage. These functions of TRF2 will be discussed in detail below.

Rap1

The TRF2 interacting protein Rap1 was found in a two-hybrid screen using TRF2 as bait[78]. The telomeric localization of Rap1 is dependent on TRF2[78] and in the absence of TRF2, Rap1 is destabilized[79]. Human Rap1 contains an N-terminal BRCT domain, central myb domains, and a RCT (Rap1 C Terminus)

domain as do the Rap1 orthologs of *S. cerevisiae* and *S. pombe*[78]. Overexpression studies indicate that human Rap1 is a negative regulator of telomere length and also suggest that the BRCT domain of Rap1 influences telomere length homogeneity[80]. Whether Rap1 contributes to telomere end protection is currently unknown[81]. Unlike human Rap1, *S. cerevisiae* Rap1 binds directly to telomeric DNA[82] using its myb domains[83].

Like human Rap1*, S. pombe* Rap1[84] and *S. cerevisiae* Rap1[85] are negative regulators of telomere length. In *S. cerevisiae*, the Rap1 ortholog localizes to multiple sites in the genome in addition to telomeres and regulates the silencing of mating type loci and the transcription of several promoters[86].

TIN2

TIN2 was first identified as a TRF1 interacting factor involved in telomerase dependent telomere length regulation[87]. More recently it was shown that TIN2 can bind TRF1 and TRF2 simultaneously, and disruption of this interaction results in decreased telomeric TRF1 and TRF2, and a DNA damage response at telomeres[65 64]. The C terminus of TIN2 binds TRF1 within the TRFH domain[87], while the N terminus of TIN2 binds TRF2[65]. The crystal structure of the interaction between TIN2 and TRF1 was recently solved, revealing that amino acids 256-276 of TIN2 bind the loop region between alpha helices 3 and 4 of the TRF1 TRFH domain (Chen et al., in prep.). Surprisingly, in spite of the similarity of the TRFH domains of TRF1 and TRF2, the TRFH domain of TRF2 is not used for TIN2 binding, and a short region within the flexible hinge region

(amino acids 352-357) is required instead (Chen et al., in prep.). TIN2 also binds TPP1 and is required for its localization to the telomere[66 67 88]. Therefore TIN2 can influence the telomeric localization of all shelterin components. The link between TRF1 and TRF2 provided by TIN2 stabilizes both proteins and their binding partners at the telomere. TIN2 is also required for the telomeric localization of TPP1 which recruits the single-stranded telomeric binding protein Pot1 to the telomere.

TPP1/POT1

The telomeres of the hypotrichous ciliate *Oxytricha nova* are bound by Telomere End Binding Proteins alpha and beta (TEBPα and TEBPβ)[89 90]. The crystal structure of TEBPα and TEBPβ in complex with telomeric DNA shows these proteins use three oligonucleotide/oligosaccharide–binding folds (OB folds) to bind the single-stranded telomeric DNA and a fourth to interact with each other[91].

Homology with the N-terminus of TEBPα led to the identification of a single-stranded telomeric DNA binding protein in *S. pombe*[69]. This TEBPα ortholog was named Pot1 (Protection of Telomeres) because its deletion causes immediate degradation of telomeres with all surviving cells having completely circularized chromosomes[69].

On the basis of homology with *S. pombe* Pot1, human Pot1 was also identified[69]. The N-terminal OB fold of human Pot1 is required for binding of single-stranded telomeric DNA[70] however a mutant lacking this region, Pot1ΔOB,

still localizes to telomeres and causes rapid telomere elongation by preventing TRF1-mediated inhibition of telomerase[92]. In addition to playing a role in telomere length regulation in human cells, Pot1 also functions in telomere protection, described in more detail below.

Both human Pot1 and mouse Pot1a and Pot1b require interaction with the shelterin component TPP1 to localize to telomeres[68 66 67]. Structural and functional data indicate that the TPP1/POT1 complex is the evolutionary equivalent *of O. nova* TEBPα and TEBPβ[68 93 94].

TELOMERE PROTECTION BY TRF2

TRF2 prevents telomeres from activating the DNA damage response machinery

The consequences of TRF2 removal suggest that telomeres lacking TRF2 are perceived by the cell as DNA damage. TRF2 was initially inhibited by expression of a mutant form of TRF2 lacking both the N-terminal basic domain and the DNA binding myb domain, TRF2$^{\Delta B \Delta M}$, which acts as a dominant negative allele and removes TRF2 from telomeres[63]. When TRF2 is inhibited, many of the same proteins which localize to DSBs, are detectable at telomeres. These telomeric foci, named Telomere Dysfunction Induced Foci (TIFs) contain DNA damage response factors including 53BP1, phosphorylated histone H2AX (γH2AX), ATM phosphorylated on S1981, Mre11, Nbs1, and phosphorylated Rad17[95 96 79]. Underscoring their similarity to the DNA damage foci which form at DSBs, the efficient formation of TIFs after TRF2 inhibition requires the ATM

checkpoint kinase[95 96 97]. The ATM kinase is required for the appropriate cellular response to DSBs induced by ionizing radiation, including the formation of γH2AX foci at sites of damage[98] activation and stabilization of p53[99 100], and initiation of cell cycle checkpoints[101].

Growth arrest induced by inhibition of TRF2 led to a senescence-like phenotype in IMR90 primary fibroblasts and HTC75 fibrosarcoma cells[63] and apoptosis in several cell types including HeLa cells, primary T cells, and immortalized B cells[102]. Again paralleling the cellular response to DSBs, apoptosis in response to inhibition of TRF2 requires functional p53 and ATM[102].

Inhibition of TRF2 in primary fibroblasts induces a form of senescence which shares many characteristics with replicative senescence: expression of senescence-associated β-galactosidase, stabilization of p53, induction of p21, hypophosphorylation of Rb, and induction of p16[103]. Overexpression of TRF2 can also affect the induction of senescence. TRF2 overexpression causes primary fibroblasts to senesce with shorter telomeres than control cells with normal levels of TRF2[104]. One interpretation of these results is that induction of replicative senescence is not simply dictated by telomere length, but rather by the amount of TRF2 present at each chromosome end.

TRF2 protects telomeres from non-homologous end-joining

Telomere fusions resulting from TRF2 inhibition are dependent on DNA Ligase IV and Ku indicating that they are generated by non-homologous end joining (NHEJ)[105 79 106]. When telomeres fuse due to inhibition of TRF2, the

double-stranded part of the telomere remains largely intact and is detectable at sites of fusion, however the single stranded telomeric overhang is degraded[63] by the NER endonuclease ERCC1/XPF in human cells[107]. Removal of the 3' overhang is expected to be a prerequisite for the joining of telomeres by NHEJ[105]. The *S. pombe* TRF1 and TRF2 ortholog, Taz1, also protects telomeres from NHEJ-mediated telomere fusion[108].

TRF2 protects telomeres from Homologous Recombination

TRF2 overexpression results in telomere shortening[76,104]. Unlike TRF1, TRF2-induced telomere shortening can occur in the absence of telomerase[109 104]. The rapid telomere shortening observed when TRF2 is overexpressed may be due to the homologous recombination (HR) machinery acting on t-loops, in a process called t-loop HR. T-loop HR was proposed to explain the phenotype of overexpression of an allele of TRF2 which lacks the N-terminal Basic domain but retains the myb domain and localizes to telomeres, TRF2$^{\Delta B}$. TRF2$^{\Delta B}$ protects telomeres from NHEJ, but leads to telomere shortening and the formation of t-loop sized extrachromosomal telomeric circles[21]. As t-loops resemble an intermediate of homologous recombination and the phenotype of TRF2$^{\Delta B}$ was dependent on the Rad51 paralog, XRCC3, it was proposed that the telomeric deletions induced by TRF2$^{\Delta B}$ expression are due to the HR machinery acting on t-loops[21]. In yeast, a similar mechanism may explain the phenomena of Telomere Rapid Deletion (TRD) in which up to several kb of DNA are rapidly lost from telomeres[110 111].

TRF2 also acts in parallel with the NHEJ factor Ku to prevent homologous recombination between telomeres on sister chromatids, called Telomere Sister Chromatid Exchange (T-SCE)[106]. Loss of either TRF2 or Ku alone does not lead to increased rates of T-SCE, but combined loss of both proteins results in T-SCE at approximately 15% of chromosome ends[106]. The rapid deletion or elongation of individual telomeres caused by T-SCE could potentially lead to telomere dysfunction and telomere length deregulation. Evidence that a third form of HR threatens telomeric integrity was seen in cells that lack the Nucleotide Excision Repair factor ERCC1/XPF, which interacts with TRF2. ERCC1/XPF null MEFS contain a high frequency of Telomeric DNA-containing double minute chromosomes, structures which may result from a recombination event between telomeres and chromosome internal TTAGGG repeats[107].

The TRF ortholog Taz1 also seems to negatively regulate HR at telomeres, as a form of telomere elongation that is dependent on HR can only occur in the absence of Taz1[112]. Interestingly, a protein whose primary function is thought to be in homologous recombination, the Rad51 paralog, Rad51D, has been detected at telomeres and its absence leads to telomere shortening and telomere fusions[113]. Similarly, mouse cells without Rad54 have shorter telomeres and more frequent telomere fusions than wildtype controls, although this protein has not yet been detected at telomeres[114]. Taken together, these data indicate that while HR related processes are important for the normal functioning of

telomeres, possibly by facilitating the formation of t-loops, they must be tightly regulated, probably by TRF2, to protect the integrity of telomeres.

Potential mechanisms for TRF2-mediated telomere protection

TRF2 may contribute to the protection of telomeres in several different ways. TRF2 promotes the formation of t-loops, structures in which the 3' overhang of the telomere is literally hidden by strand invading the double-stranded part of the telomere[15 16]. TRF2 may also supplement the protection of telomeres provided by t-loops by binding and preventing the activation of the ATM kinase[115]. Karlseder et al. [115] observed that cells in which TRF2 is highly overexpressed do not respond appropriately to IR induced DNA damage. IR primarily activates the checkpoint kinase ATM, and several read-outs of ATM activation after IR are blunted in TRF2 overexpressing cells. These include stabilization of p53 and induction of its downstream targets p21, Bax, and Hdm2. Nbs1 phosphorylation on S343, a target of ATM, was also dampened in the presence of high levels of TRF2. Additionally, cells overexpressing TRF2 bypass the IR induced G2/M checkpoint at higher rates than control cells. Furthermore, it was shown that ATM and TRF2 interact by co-immunoprecipitation[115], allowing the possibility that TRF2 directly inhibits ATM through a physical interaction. The idea that a high local concentration of TRF2 at the telomere could inhibit the activation of the ATM kinase is consistent with the observation that signaling from DSBs induced near chromosome internal telomeric repeats is inhibited[116]. Telomeric deprotection upon loss of TRF2 could also be related to the

concomitant removal of its shelterin binding partners from telomeres, TIN2 and Rap1. The relative contribution of these non-mutually exclusive mechanisms for telomere protection by TRF2 is currently being explored.

TELOMERE PROTECTION BY POT1

RNAi-mediated inhibition of Pot1 in human cells leads to TIF formation in G1 and causes the 5' terminus of the telomere, which normally ends on the sequence $^{3'}$ATC$^{5'}$, to end on a random nucleotide within the $^{3'}$AATCCC$^{5'}$ repeat[117]. In mouse, both Pot1a and Pot1b contribute to the protection of telomeres, but loss of Pot1a causes a more severe telomere deprotection phenotype than loss of Pot1b[118]. Like TRF2, Pot1a and Pot1b act in parallel with Ku to prevent T-SCE; increased levels of T-SCE are seen in MEFs which are triply deficient in Pot1a, Pot1b, and Ku (Palm and de Lange, in prep.). Interestingly, loss of Pot1b but not Pot1a causes a marked increase in the single-stranded telomeric overhang, suggesting Pot1b may be involved in regulating exonucleolytic degradation of the C-rich telomere strand[118].

While the DNA damage response to removal of TRF2 from telomeres is chiefly dependent on the checkpoint kinase ATM, damage signaling after Pot1 removal requires the checkpoint kinase ATR[97]. ATR, and its binding partner ATRIP, are recruited to ssDNA bound by RPA[119], suggesting a model wherein the damage signal elicited by Pot1 removal is initiated by RPA binding to telomeric single-stranded DNA that would normally be bound by Pot1.

SHELTERIN ASSOCIATED FACTORS AND THEIR ROLE AT TELOMERES

TRF1 associated factors

The poly (ADP-ribose) polymerase, tankyrase, was identified in a yeast-2-hybrid screen using TRF1 as bait[120]. Tankyrase localizes to telomeres and ADP-ribosylation of TRF1 by tankyrase reduces TRF1 binding to telomeric DNA[120]. Overexpression of tankyrase causes telomere elongation[121] while its inhibition results in telomere shortening[122]. Tankyrase binds its partners using a conserved motif found in human TRF1 but not mouse TRF1[123], and tankyrase does not appear to be involved in telomere length regulation in mouse[122]. TRF1 may also negatively regulate telomere length through its interaction with PINX1, a protein that can inhibit telomerase *in vitro*[124]. However, the PINX1 homolog of *S. cerevisiae*, Gno1p, is involved in ribosomal RNA maturation but does not affect telomere length[125].

TRF2 associated factors

In addition to its binding partners Rap1 and TIN2, which are members of the shelterin complex, TRF2 interacts with several other factors which have prominent non-telomeric functions, many of which are involved in DNA metabolism. In spite of the role of TRF2 in preventing the NHEJ of telomeres, TRF2 interacts with the NHEJ proteins Ku and DNA-PK_{cs}[126 127 128]. The Mre11 complex, composed of Mre11, Rad50, and Nbs1, was found in TRF2 immunoprecipitates[129]. Nbs1 is only present at telomeres during S phase while Mre11 and Rad50 are present throughout the cell cycle[129]. Patients with

Nijmegen Breakage Syndrome (NBS) lack normal Nbs1 function and exhibit chromosome instability, cancer susceptibility, immunodeficiency, and radiosensitivity[130 131]. Fibroblasts from NBS patients exhibit shorter telomeres than fibroblasts of roughly the same passage from unaffected individuals[132]. The telomere length defect of NBS fibroblasts is rescued by expression of hTERT and Nbs1 together, but not by either protein alone[132], suggesting that the Mre11 complex is involved in the telomerase pathway. ATM and Mre11 function interdependently in the response to DSBs[133 134 135] and recent evidence suggests that ATM and MRN may also collaborate to regulate telomere length in human cells[136]. The Nucleotide Excision Repair Endonuclease ERCC1/XPF immunoprecipitates with TRF2 and is required for the removal of the 3' telomeric overhang after TRF2 inhibition in human cells[107]. As discussed above, ERCC1/XPF may also contribute to the prevention of homologous recombination between telomeres and chromosome internal telomeric repeats[107].

TRF2 also interacts with the RecQ helicases WRN and BLM and can stimulate their helicase activity on substrates resembling telomeric DNA[137 138]. RecQ helicases are believed to facilitate replication fork progression by disrupting obstructing DNA structures, including G quadruplex DNA, and may also play a role in the reinitiation of replication after fork collapse[139]. Impaired WRN function has deleterious consequences for telomeres that may be related to problems during telomere replication. Overexpression of a dominant negative WRN allele results in loss of lagging strand telomeres[52]. Late generation MEFs that are

doubly deficient for WRN and telomerase exhibit frequent sister telomere exchanges, one potential outcome of replication fork collapse within a telomere[140]. Additionally, primary fibroblasts which lack WRN function undergo premature senescence which can be reversed by expression of telomerase[49].

TRF2 was recently shown to interact with Apollo, a nuclease related to Artemis. Apollo localizes to telomeres and its knockdown results in senescence and TIF formation primarily in S phase[141 142]. An unusual phenotype observed when Apollo is inhibited is an increased frequency of telomere ends with two or more telomere signals[141], the significance of which is currently unknown. The C-terminus of Apollo binds the loop region between alpha helices 3 and 4 of the TRFH domain of TRF2 (Chen et al., in prep.).

REGULATION OF TELOMERASE BY SHELTERIN

A negative feedback mechanism that regulates telomere length in human cells was identified by overexpression of the shelterin component TRF1. Overexpression of TRF1 in the telomerase positive tumor cell line HT1080 causes telomeres to shorten despite unaltered telomerase activity[75]. The amount of TRF1 present at telomeres is proportional to telomere length[76 92] and TRF1 has no effect on telomerase activity *in vitro*[76] indicating that TRF1 is acting in *cis* at telomere ends to block telomerase action. More recently it was shown that the negative regulation of telomere length by TRF1 is mediated by Pot1[92]. A similar negative feedback mechanism appears to function in yeast, with Rap1 as the *cis*-

acting negative regulator of telomerase in *S. cerevisiae*[85] and Taz1 performing a similar role in *S. pombe*[143].

Telomerase must also be recruited to telomere ends, the importance of which was highlighted by a recent study showing that only 20-50 molecules of telomerase are present in the nuclei of human 293T cells[37]. In order for such a small number of molecules to localize to their rare substrate, the 3' overhang of telomeres, a powerful recruitment mechanism must exist. In mammals, recent evidence indicates that the shelterin component TPP1, which functions in the negative regulation of telomerase action by recruiting Pot1 to the telomere[66 67], is also involved in the recruitment and activation of telomerase[94 93].

RECOMBINATION-BASED MAINTENANCE OF TELOMERE LENGTH

Mammalian telomeres can be maintained in the absence of telomerase by a process known as Alternative Lengthening of Telomeres (ALT)[144]. Cells that maintain their telomeres using the ALT pathway have longer and more heterogeneous telomeres than related non-ALT cells[145 44 146]. By tagging telomeres with a specific DNA sequence, it was shown that a high level of intertelomeric recombinational events occur in ALT cells[147]. Cells that employ the ALT mechanism contain ALT-associated PML bodies (APBs) that contain telomeric DNA, TRF1, TRF2, and a number of proteins involved in DNA replication and recombination[148 144]. Most cancer cells that have not activated telomerase expression employ ALT to lengthen their telomeres[44].

PIKKs AND TELOMERES

The mammalian phosphatidyl inositol 3-kinase-like kinase (PIKK) family includes ATM, ATR, DNA-PK$_{cs}$, mTOR, SMG1, and the catalytically inactive TRRAP[149]. ATM, ATR, and DNA-PK$_{cs}$ have distinct but overlapping roles in maintaining genome integrity. ATM and ATR are the primary activators of the DNA damage response, phosphorylating multiple targets leading to cell cycle checkpoint activation and DNA repair[150]. While ATM and ATR can phosphorylate many of the same substrates including p53, Nbs1, and Rad17[151], they are activated by different types of DNA damage. Double-stranded DNA breaks (DSBs) are the most well characterized activator of ATM[152], while DNA damage related to replication stress primarily activates ATR[153]. Interestingly, ATM can be activated downstream of ATR in response to replication stress[154] and conversely, ATR can be activated in response to DSBs in an ATM dependent manner[155 156 157 158]. DNA-PK$_{cs}$ is largely dispensable for the signaling of DNA damage; in its absence, DNA damage checkpoints and downstream read-outs of the DNA damage response, such as phosphorylation and stabilization of p53, are intact[159]. However, DNA-PK$_{cs}$ and its binding partners, Ku70 and Ku86, are involved in the NHEJ-mediated DNA repair of double-stranded DNA breaks[160].

SMG1 was identified as the human ortholog of a *C. elegans* gene, involved in Nonsense-mediated mRNA Decay (NMD)[161]. In addition to its role in NMD, eliminating mRNAs containing premature stop codons, SMG1 is also involved in the maintenance of genome integrity. Cells deficient in SMG1 exhibit

increased sensitivity to IR, are unable to optimally phosphorylate and stabilize p53 in response to DNA damage, and exhibit evidence of spontaneous DNA damage in the form of foci of histone variant H2AX phosphorylated on serine 139 (γH2AX) and constituitive Chk2 phosphorylation[162]. mTOR, unlike other members of the PIKK family, is not directly implicated in the maintenance of genome integrity. Rather, it is involved in the complex regulation of cell growth in response to nutrient availability[163].

In yeast, PIKKs also play a role at telomeres. *S. cerevisiae* Tel1 and Tel2 were identified in an early screen for genes required for the maintenance of telomere length[164]. Tel1 is the yeast ortholog of the ATM kinase, however until recently the function of Tel2 was obscure. Data indicating that Tel2 is a master regulator of PIKK stability, and therefore required for Tel1 function, explains the requirement of Tel2 for telomere length maintenance (Takai et al., in press). In *S. cerevisiae,* Tel1 and Mec1 have been detected at telomeres[165] and Tel1 preferentially associates with the shortest telomeres[166 167 168]. In both *S. cerevisiae* and *S. pombe* Tel1 and Mec1 (Rad3 in *S. pombe*) are required for the maintenance of telomere length[169 170 171]. Tel1 and Mec1 could influence telomere length by phosphorylating factors involved in telomerase recruitment. Tel1 and Mec1 can phosphorylate Cdc13 within its telomerase recruitment domain, and mutation of these sites leads to telomere shortening[172] and Tel1 (but not Mec1) is required for the recruitment of telomerase components Est1p and Est2p in late S/G2[173].

Mre11 complex components are also required for telomere length maintenance, however deletion of Mre11 complex components in Tel1 deficient strains causes no additional telomere length defect indicating that Tel1 and the Mre11 complex function in the same pathway to regulate telomere length[174 175], a relationship that may be analogous to their partnership in the signaling of DSBs[133 134 135]. The preferential association of Tel1 with the shortest telomeres requires the *S. cerevisiae* Nbs1 ortholog Xrs2[166 167 168]. Recent data also suggests that ATM and the Mre11 complex may be involved in TRF1 mediated telomere length control in humans[136]. Intriguingly, HR mediated deletion of t-loops induced by expression of the mutant allele of TRF2, TRF2$^{\Delta B}$, requires Nbs1[21], suggesting that the Mre11 complex may be involved in this non-telomerase based mechanism of telomere length regulation.

As discussed above, ATM and ATR are involved in the signaling of dysfunctional telomeres, consistent with their role in the maintenance of genome integrity[102 97 95 96 176]. Although the role of PIKKs in the normal physiology of telomeres has not been well studied, some evidence suggests that members of this family are involved in telomere length regulation and protection in mammals. The disease Ataxia Telangiectasia (AT), in which ATM function is lost, is characterized by neurological deterioration, immunodeficiency, and cancer susceptibility[177 178]. The telomeres from cells of AT patients were reported to be shorter than age matched controls[179], however this study examined telomere length in lymphocytes, which proliferate in response to infection, making it likely

that the shortened telomeres observed in these cells was secondary to the higher frequency of infection in AT patients. However, in cultured cells, overexpression of truncated forms of ATM shorten telomeres[180] suggesting that ATM function may be able to directly influence telomere length. Additionally, telomerase deficient mice have shorter telomeres at earlier generations when DNA-PK is also absent[181]. A mild telomere deprotection phenotype has been observed in mice lacking DNA-PK[182 183] and Ku[184]. Recently it was shown that human cells lacking one allele of Ku86 exhibit telomere shortening and increased telomeric fusions[185]. However, TIF formation was not observed in Ku knockout MEFs, indicating that Ku is not required to protect telomeres in mouse[106]. Although a telomeric function of the SMG1 kinase has not been reported, a link between the NMD pathway and telomere biology was recently established when the NMD protein SMG-6 (Est1A) was shown to be the human homolog of the *S. cerevisiae* telomeric protein Est1, and found to associate with telomerase and play a role in telomere capping[35 36].

REPLICATION OF TELOMERIC DNA

Telomeric DNA presents several theoretical obstacles to the efficient passage of the replication fork. The G-rich strand of telomeric DNA can form quadruplex structures under certain conditions[186], which present an obvious obstacle to the passage of the replication fork[187]. Repeats can also lead to the formation of other unusual structures, such as H-DNA and “sticky” DNA, and also

may cause polymerase slippage[188]. Furthermore, telomere-specific DNA binding proteins might hinder the passage of the replication fork, such is the case with the well-studied *E. coli* Tus protein[189].

Several lines of evidence indicate that replication fork progression through telomeric DNA is hindered. Telomeric DNA is a poor substrate in the *in vitro* replication system of linear SV40 DNA[190] and EM analysis of synthetic model replication forks consisting of telomeric DNA show frequent fork regression, often resulting in four-stranded chickenfoot structures[191]. *In vivo*, replication forks proceed slowly through telomeric DNA in *S. cerevisiae*[192] [193]. In human cells synchronized with aphidicolin, BrdU incorporation into telomeric DNA occurs in two distinct phases during S phase, consistent with replication fork stalling during passage through telomeric DNA[20].

Chapter 2: TRF2 can inhibit ATM autophosphorylation

INTRODUCTION

When TRF2 is removed from telomeres, chromosome ends activate a DNA damage response that is dependent on the checkpoint kinase ATM[102 95 97]. TRF2 could mediate the inhibition of ATM at telomeres through several, non-mutually exclusive mechanisms. TRF2 may modify the chromosome terminus so that it does not resemble a DNA end, possibly by promoting the formation of t-loops - structures in which the 3' telomeric overhang is tucked into a more proximal duplex region of the telomere[15 16]. Secondly, it is possible that ATM activation upon TRF2 inhibition is actually due to the concomitant removal of the shelterin binding partners of TRF2; when TRF2 is genetically removed from mouse cells, Rap1 protein is reduced to nearly undetectable amounts[79] and TIN2 levels at the telomere drop by over 50%[68]. A final possibility is that TRF2 inhibits ATM activation directly.

Direct inhibition of ATM activation by TRF2 is supported by the finding that TRF2 and ATM physically interact[115]. Immunoprecipitation of ATM from primary human fibroblasts results in recovery of approximately 1% of endogenous TRF2. The veracity of this interaction is underscored by the finding that anti-ATM immunoprecipitates from fibroblasts that lack functional ATM do not contain TRF2, even when TRF2 is overexpressed. In co-immunoprecipitation experiments using purified baculovirus derived TRF2 and GST-tagged ATM

fragments, TRF2 bound two fragments of ATM spanning amino acids 1439 – 2138. This region contains the FAT (FRAP, ATM, TRAPP) domian, conserved in PIKKs, and the S1981 autophosphorylation site, discussed below.

Further supporting the hypothesis that TRF2 itself prevents activation of ATM, is the finding that ATM is not appropriately activated by ionizing radiation in cells expressing high levels of TRF2[115]. TRF2 overexpression blunts read-outs of ATM activation after IR, including phosphorylation and stabilization of p53 and induction of its downstream targets p21, Bax, and Hdm2. Nbs1 phosphorylation on S343, a target of ATM, was also diminished after IR in the presence of high levels of TRF2. Additionally, cells overexpressing TRF2 bypass the IR induced G2/M checkpoint at higher rates than control cells.

Autophosphorylation on S1981 was identified as a crucial event in ATM activation[194]. By exposing untreated fibroblasts to the cross-linking agent formaldehyde, it was shown that ATM normally exists as a dimer or higher order multimer. DNA damage leads to the dissociation of multimeric ATM into monomers, the active form of the kinase. Autophosphorylation on S1981 is detectable as early as 30 seconds after IR[194], and was shown to be crucial for the dissociation of multimeric ATM into its active, monomeric form, and subsequent ATM dependent signaling events[194].

Recently, controversy has arisen regarding whether autophosphorylation on S1981 is required for ATM activation. *In vitro*, ATM S1981 mutants were activated by DNA ends and the MRN complex as well as wildtype ATM[134].

Furthermore, in contrast to what was observed in human cells, mutation of the pertinent autophosphorylation site (S1987) in murine ATM did not affect its function[195]. Transgenic mice were generated that express ATM containing S1987 mutated to alanine (S1987A) on a BAC and these were backcrossed with $ATM^{-/-}$ mice to generate animals which only express ATM with the S1987A mutation. These transgenic mice develop normally and their cells exhibit normal cell cycle arrest and phosphorylation of ATM substrates after treatment with IR[195]. Furthermore, the mutant form of ATM localizes to DNA breaks[195]. The importance of the autophosphorylation event for the activation of ATM may be different in human and mouse, a view supported by the recent report that human ATM S1981 mutants localize to DSBs caused by the endonuclease PpoI[196]. Importantly, three additional ATM autophosphorylation sites have been discovered which are required for proper ATM signaling in response to DNA damage[197]. Regardless of whether autophosphorylation on S1981 is a requirement or a consequence of ATM activation, it serves as an early indicator of ATM activity, and is currently the most reliable method for detecting activation of ATM itself.

To determine whether TRF2 affects ATM signaling by acting on ATM itself or by acting at a point downstream of ATM in the signaling pathway, we examined the effect of TRF2 overexpression on autophosphorylation of ATM on S1981. The ability of TRF2 to influence ATM signaling could signify a hitherto unknown function of TRF2 in the DNA damage response. We address this

question by determining whether TRF2 relocates from telomeres to sites of DNA damage.

RESULTS

In order to study the effect of TRF2 overexpression on the IR induced autophosphorylation of ATM on S1981, ATM and TRF2, TRF1, or the empty plasmid vector were expressed by transient transfection in 293T cells. Expression of TRF2 by transient transfection in 293T cells was utilized because extremely high levels of overexpression can be achieved in this setting. ATM phosphorylation on S1981 can be detected after IR doses as small as 0.1 Gy and phosphorylation is maximal after treatment with 0.4 Gy IR[194]. In order to obtain a dose-dependent increase of ATM phosphorylation in response to IR, transfected 293T cells were exposed to 0, 0.3, or 0.6 Gy IR. ATM activation was monitored by western blotting with an antibody against ATM phosphorylated on S1981[194], here called αATM-P. ATM phosphorylation was robustly induced by IR in vector transfected control cells. In comparison, TRF2 overexpressing cells exhibited lower levels of phosphorylated ATM after IR (Fig. 2-1A). Western blot signals were quantified by densitometry. The relative level of ATM phosphorylated on S1981 (normalized to total ATM protein) at 0.3 Gy was 49% of the vector control value ($p = 0.002$, Student's t test; $n = 7$). ATM phosphorylation was not blunted in cells overexpressing another telomeric protein, TRF1, indicating that the effect is specific to TRF2. Overexpression of TRF2 also diminished the IR-induced ATM

autophosphorylation of endogenous ATM in IMR90 fibroblasts to 55% of vector control value at 0.3 Gy and 60% of vector control value at 0.6 Gy (Fig. 2-1B).

In order to elucidate the mechanism by which overexpressed TRF2 inhibits ATM, we attempted to analyze the effect of TRF2 on dissociation of the multimeric ATM complex induced by IR. However, we were unable to detect evidence of the ATM multimer by treating unperturbed cells with formaldehyde, precluding us from analyzing the effect of TRF2 on the dissociation of this complex.

To determine if the N-terminal basic domain, which is involved in the protection of telomeres from HR, is involved in the inhibition of ATM activation by TRF2, we expressed an allele of TRF2 lacking the N terminal basic domain, $TRF2^{\Delta B}$, in 293T cells by transient transfection. Surprisingly we found that expression of $TRF2^{\Delta B}$ resulted in significant destabilization of co-transfected ATM protein, preventing us from determining the effect of this allele on ATM activation.

These results raise the issue of whether TRF2 has a hitherto unknown role, modulating ATM activation after DNA damage, as has been proposed[198]. If this were the case, TRF2 would be predicted to localize to IR induced foci, where it would be in a position to influence ATM activation. However, it has previously been shown that endogenous TRF2 remains at telomeres and does not localize to IR induced foci[129]. We tested whether overexpressed TRF2 could be detected at such foci, and found that, likewise, it was not (Fig. 2-1C).

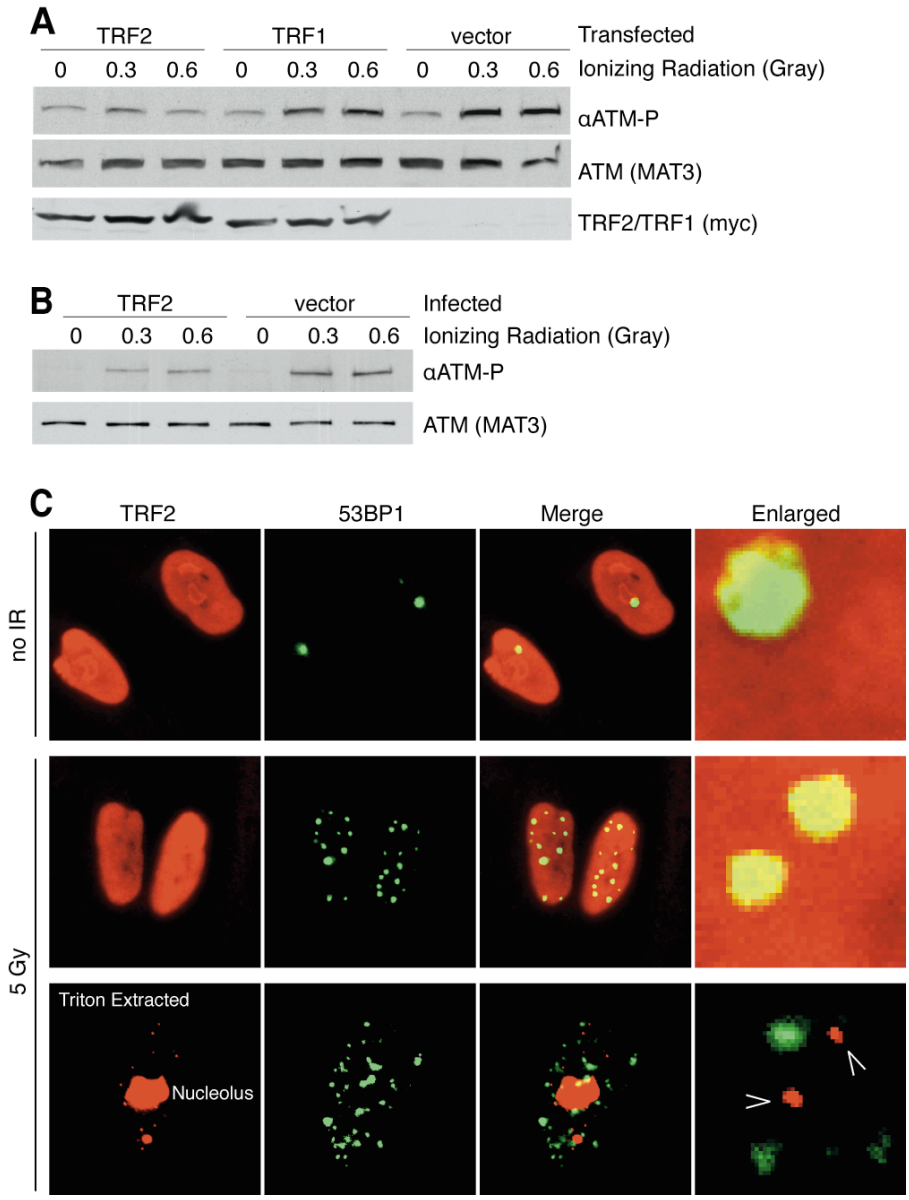

Figure 2-1: TRF2 inhibits activation of ATM by Ionizing Radiation.
(A) Overexpression of TRF2 inhibits IR-induced phosphorylation of transfected ATM in 293T cells. 293T cells co-transfected with ATM and either TRF2, TRF1, or vector were treated with the indicated doses of IR. After a 30 min. recovery, cells were harvested and western blot analysis was performed on whole-cell lysates.
(B) Overexpression of TRF2 inhibits IR-induced phosphorylation of endogenous ATM in primary fibroblasts. IMR90 primary fibroblasts infected with a retroviral construct expressing TRF2 or an empty virus were treated with the indicated doses of IR. After a 1 hr recovery, cells were harvested and ATM was immunoprecipitated from whole-cell lysates. Western blot analysis was performed on immunoprecipitated ATM.
(C) Overexpressed TRF2 does not localize to IRIFS. IMR90 primary fibroblasts infected with a retroviral construct expressing TRF2 were treated with 5 Gy IR. After a 90 min recovery, cells were fixed and processed for immunofluorescence with or without Triton X-100 extraction before fixation. Arrowheads denote foci of TRF2 signal previously demonstrated to represent telomeres. When overexpressed, some TRF2 is localized to nucleolus.

DISCUSSION

We have demonstrated that ATM autophosphorylation on S1981 after IR is inhibited by overexpression of TRF2. However, in our hands, TRF2, even when overexpressed, does not localize to IR induced foci, where it would be in a position to modulate ATM activation. Several other lines of evidence indicate that TRF2 is not normally involved in the response to DSBs. Importantly, TRF2 knock-out MEFs are proficient at NHEJ, repairing uncapped telomeres using this pathway[79]. HR also appears to be unimpeded in the absence of TRF2 as frequent telomere sister chromatid exchange occurs in cells that lack TRF2 and the NHEJ protein Ku[106]. Furthermore, both ATM and ATR signaling are active in MEFs after TRF2 has been deleted[79 97]. Because TRF2 does not play an obvious role in the normal response to DSBs, we surmise that the effect on ATM activation reflects an activity of TRF2 that is usually only employed at telomeres. In our transfection experiments, ATM was inhibited by extremely high levels of TRF2, at least 20-fold higher than the endogenous protein. Under the conditions used in these experiments, TRF2 was present not just at telomeres, but also at high levels throughout the nucleus[115]. Normally, TRF2 localizes primarily to the telomere, and thus would be able to act locally, preventing ATM from becoming active only near the chromosome end.

TRF2, as a member of the shelterin complex, prevents telomeres from being recognized as DSBs[58]. One way shelterin may function in this capacity is

by the formation of t-loops, hiding the single stranded overhang through a strand invasion in a proximal region of the double-stranded telomere[15 16]. However, even within the proposed t-loop, there are DNA structures that are predicted to activate a DNA damage response including ss-ds transitions, 3' and 5' ends, and single-stranded DNA. Preventing these structures from activating the DNA damage response may be achieved by direct inhibition of ATM by TRF2. We considered a model whereby TRF2, which is a dimer, would bind ATM dimers and prevent their dissociation, a step proposed to be crucial for ATM activation by Bakkenist and Kastan[194]. However, we were unable to determine whether TRF2 affects the dissociation of multimeric ATM in response to DNA damage, and currently the mechanism by which TRF2 inhibits ATM activation is unknown.

For the reasons discussed above, we have interpreted our data about the effect of TRF2 overexpression on ATM activation to represent a function of TRF2 that would normally be carried out at the telomere. Other groups have reached a different conclusion. Bradshaw et al.[198] show that TRF2 localizes to DNA damage induced by a high intensity laser. They go on to show that overexpression of TRF2 inhibits ATM S1981 phosphorylation and several downstream read-outs of ATM activity, essentially reproducing the results of Karlseder et al. Bradshaw et al. conclude that TRF2 has a non-telomeric function in the DNA damage response. The discrepancy regarding whether TRF2 localizes to sites of damage is probably due to the method Bradshaw et al. used to generate DNA damage, laser microbeam irradiation. The authors themselves

estimate that the laser microbeam produces DNA damage equivalent to approximately 80 Gy IR or 2800 DSBs per nucleus. This amount of DNA damage is clearly supraphysiological. ATM activation, as measured by S1981 phosphorylation, is detectable after 0.1 Gy IR (about 4 DSBs per nucleus) and maximal after 0.4 Gy[194]. The immense amount of damage created by the laser must cause a correspondingly supraphysiologic recruitment of DNA damage response factors. Because TRF2 is a known binding partner of many DNA damage response factors including the MRN complex[129], ERCC1/XPF[107], and WRN[138 137], it may be simply dragged along in the laser-induced DNA damage response tsunami. Another possible explanation for the discrepancy is raised by the finding that a mutant form of TRF2 lacking the N terminal basic domain, TRF2$^{\Delta B}$, does not localize to laser induced damage[198]. The basic domain of TRF2 was recently shown to interact with DNA structures in a sequence-independent manner[199 200] with a preference for three and four-way DNA junctions resembling those found in replication forks and homologous recombination intermediates[200]. These findings raise the possibility that the observed localization of TRF2 to laser induced DNA damage is a result of a non-specific interaction between the basic domain of TRF2 and unusual DNA structures induced by the laser.

Recently, a second study confirmed that TRF2 is recruited to high intensity laser induced damage, but also showed that TRF2 does not localize to DSBs produced by more conventional lower intensity lasers or IR from a Cs[137]

source[201]. These results indicate that the localization of TRF2 to DNA damage induced by the high intensity laser is due to the unique quality and magnitude of this type of DNA damage, and that TRF2 does not localize to DNA damage in biologically relevant settings[201].

Chapter 3: A novel TRF2 phosphorylation site is regulated by PI3K-like protein kinases

INTRODUCTION

The mammalian phosphatidyl inositol 3-kinase-like kinase (PIKK) family includes ATM, ATR, DNA-PK$_{cs}$, mTOR, SMG1, and the catalytically inactive TRRAP[149]. ATM, ATR, and DNA-PK$_{cs}$ have distinct but overlapping roles in maintaining genome integrity. ATM and ATR are the primary activators of the DNA damage response, phosphorylating multiple targets leading to cell cycle checkpoint activation and DNA repair[150]. While ATM and ATR can phosphorylate many of the same substrates including p53, Nbs1, and Rad17[151], they are activated by different types of DNA damage. Double-stranded DNA breaks (DSBs) are the most well characterized activator of ATM[152], while DNA damage related to replication stress primarily activates ATR[153]. Interestingly, ATM can be activated downstream of ATR in response to replication stress[154] and conversely, ATR can be activated in response to DSBs in an ATM dependent manner[155 156 157 158]. DNA-PK$_{cs}$ is largely dispensable for the signaling of DNA damage; in its absence, DNA damage checkpoints and downstream read-outs of the DNA damage response, such as phosphorylation and stabilization of p53, are intact[159]. However, DNA-PKcs and its binding partners, Ku70 and Ku86, are involved in the NHEJ-mediated DNA repair of double-stranded DNA breaks[160].

SMG1 was identified as the human ortholog of a *C. elegans* gene involved in Nonsense-mediated mRNA Decay (NMD)[161]. In addition to its role in NMD, eliminating mRNAs containing premature stop codons, SMG1 is also involved in the maintenance of genome integrity. Cells deficient in SMG1 exhibit increased sensitivity to IR, are unable to optimally phosphorylate and stabilize p53 in response to DNA damage, and exhibit evidence of spontaneous DNA damage in the form of γH2AX foci and constitutive Chk2 phosphorylation[162]. mTOR, unlike other members of the PIKK family, is not directly implicated in the maintenance of genome integrity. Rather, it is involved in the complex regulation of cell growth in response to nutrient availability[163].

In yeast, PIKKs also play a role at telomeres. *S. cerevisiae* Tel1 and Mec1 (orthologs of ATM and ATR, respectively) are present at telomeres in a cell-cycle dependent manner[165] and are involved in telomere length regulation[169]. Similarly, in the fission yeast *S. pombe*, Tel1 and the Mec1 homolog, Rad3, are required for maintenance of telomere length[170 171].

Consistent with their role in the DNA damage response, ATM and ATR are involved in the signaling of dysfunctional telomeres[102 97 95 176 96]. Although the role of PIKKs in the normal physiology of telomeres has not been well studied, some evidence suggests that members of this family are involved in mammalian telomere length regulation[179 180 181] and telomere protection[182 184 183]. Although a telomeric function for the SMG1 kinase has not been reported, a link between the NMD pathway and telomere biology was recently established when the NMD

protein SMG-6 was shown to be the human homolog of the *S. cerevisiae* telomeric protein EST1A, and found to associate with telomerase and play a role in telomere capping[35 36].

The only known requirement for PIKK phosphorylation is a serine or threonine followed by a glutamine (SQ or TQ)[151 202]. Many PIKK kinase targets have SQ/TQ motifs in groups known as SQ/TQ Cluster Domains (SCD)[203]. One example of a SCD containing protein is the *S. cerevisiae* telomere binding protein Cdc13, which has 10 SQ/TQ motifs in two clusters, and can be phosphorylated *in vitro* by Tel1 and Mec1[172]. The functional consequences of SQ/TQ phosphorylation are generally thought to include effects on protein-protein interactions. For example, ATR phosphorylates histone H2AX on S139 in response to replication stress[204] and ATM and DNA-PK do the same in response to DSBs[98 205 206]. The BRCT tandem domain of MDC1 specifically binds phosphorylated S139 of H2AX, and this interaction is required for the efficient recruitment of DNA damage response proteins to sites of damaged chromatin[207]. Several telomeric proteins have conserved SQ/TQ motifs. TRF1 has a conserved SQ site at amino acids 219-220 (within the dimerization domain), which can be phosphorylated by ATM[208]. Human TRF2 has three SQ/TQ motifs, T188, S368, and S380. S380 is not conserved in mouse, T188 is conserved in mammals but not all vertebrates, and S368 is found in all known vertebrate TRF2 proteins (Fig. 3-1). Recently it was reported that TRF2 is phosphorylated on T188 in response to IR[209]. We report that TRF2 can be phosphorylated on S368,

and show that this phosphorylation is both positively and negatively regulated by PIKKs. In the course of our studies, we document that antibodies targeting phosphorylated SQ/TQ residues within specific proteins, have a proclivity to cross-react with phosphoproteins other than their intended targets.

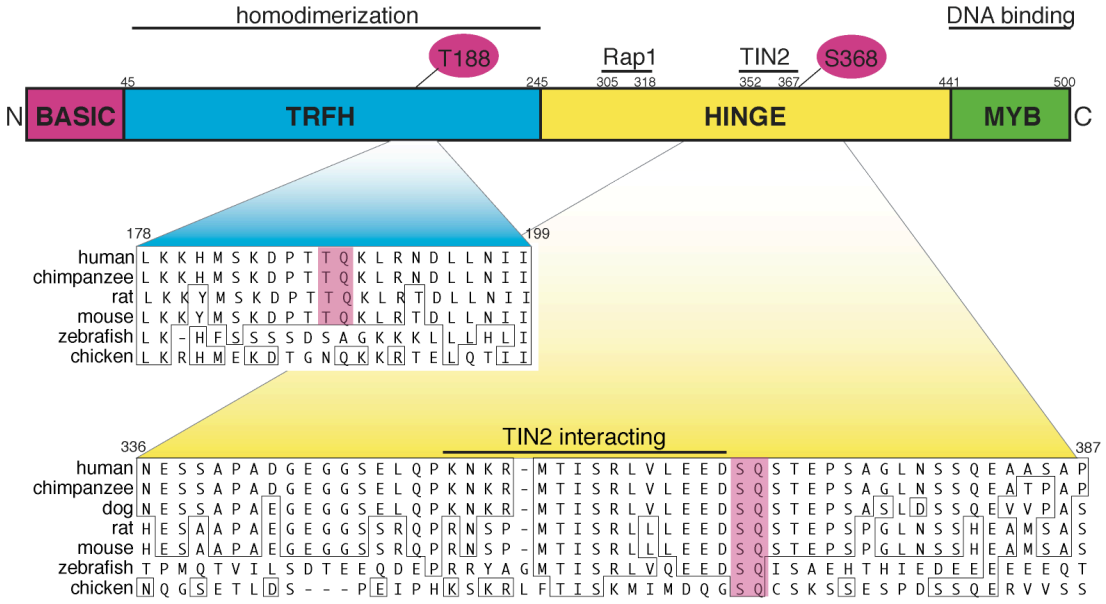

Figure 3-1: Conserved SQ/TQ motifs in the telomeric protein TRF2.
Schematic of human TRF2. The positions of conserved SQ/TQ motifs and minimal binding domains for TRF2 binding partners Rap1 and TIN2 are indicated. Relevant TRF2 sequences from the indicated organisms surrounding the conserved TQ and SQ motifs were aligned with ClustalW. Boxes indicate identical amino acids. The conserved TQ and SQ motifs are shaded in pink. The TQ motif at amino acids 188/189 is conserved in mammals, but not vertebrates. The SQ motif at amino acids 368/369 is conserved in vertebrates.

RESULTS

Human TRF2 is phosphorylated on S368 when expressed by transient transfection in 293T cells

As described in Chapter 2, TRF2 was overexpressed in 293T cells by transient transfection to determine its effect on the activation of ATM by IR. ATM activation was monitored by western blotting with a phosphospecific antibody against ATM phosphorylated on S1981, αATM-P. When TRF2 was overexpressed, but not a vector control or another protein such as TRF1, a strong band was evident on the αATM-P western blot that co-migrated with overexpressed TRF2 (Fig 3-2A). Examination of the amino acid sequence of TRF2 revealed that amino acids 361-375 were very similar to the peptide used to generate αATM-P (Fig 3-2B). Amino acids 361-375 are 57.1% identical and 64.3% similar to the ATM peptide. The pertinent serine at position 368 in human TRF2 is extremely well conserved, present in all known vertebrate TRF2 proteins (Fig. 3-1). In contrast, the only other conserved SQ/TQ motif in TRF2 (T188) is present in mammals but not in zebrafish or chicken. S368 is located in the flexible hinge domain of TRF2, and lies immediately adjacent to the minimal binding domain required for interaction between TIN2 and TRF2.

In order to determine if αATM-P was truly detecting TRF2 phosphorylated on S368, the serine was mutated to a glycine and this construct was expressed in 293T cells by transient transfection. Cells containing this mutant form of TRF2 did not exhibit a band with the MW of TRF2 on the αATM-P

western (Fig 3-2C). In order to confirm that the band represented TRF2 phosphorylated on S368, overexpressed TRF2 was immunoprecipitated from 293T cells and treated with lambda phosphatase (Fig. 3-2D). Phosphatase treatment abolished TRF2 reactivity with αATM-P. Highly concentrated purified human TRF2 produced in insect cells using the baculovirus expression system did not react with αATM-P on western blot, indicating that TRF2 is not phosphorylated on S368 in this setting and that αATM-P cannot detect TRF2 that is not phosphorylated on S368 by western blot, even when it is highly abundant (Fig. 3-2E). Taken together, these data indicate that the αATM-P antibody is detecting a veritable phosphorylation event on serine 368 of TRF2 overexpressed in 293T cells.

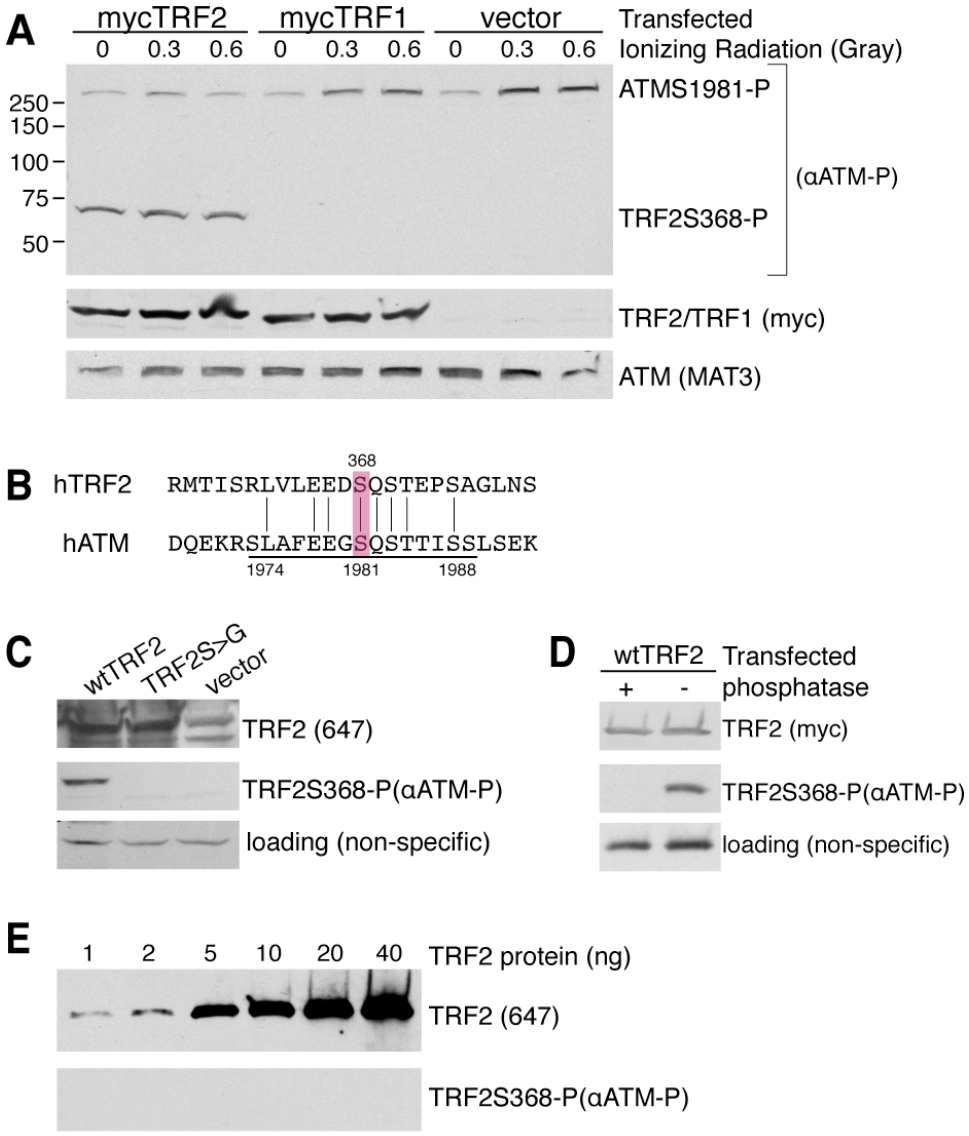

Figure 3-2: TRF2 expressed in 293T cells by transient transfection is phosphorylated on serine 368.
(A) αATM-P detects a band that co-migrates with TRF2 when TRF2 is expressed in 293T cells by transient transfection. Myc-tagged wildtype human TRF2 or TRF1, or the plasmid vector were expressed in 293T cells by transient transfection. 48 hrs. after transfection, cells were treated with low doses of IR, allowed to recover for 1 hr., and harvested.
(B) The peptide used to generate αATM-P (underlined) is highly similar to amino acids 361-375 of human TRF2. Identical amino acids are indicated.
(C) αATM-P does not detect TRF2 transiently expressed in 293T cells when S368 has been mutated to a neutral residue. Wildtype TRF2 (wtTRF2), TRF2 containing glycine at position 368 instead of serine (TRF2S>G) or the empty vector were expressed in 293T cells by transient transfection. A non-specific band detected by αATM-P serves as a loading control.
(D) Myc-tagged wildtype TRF2 expressed in 293T cells by transient transfection was immunoprecipitated using a polyclonal rabbit antibody against TRF2 (647) and treated with lambda phosphatase. A non-specific band detected by αATM-P serves as a loading control.
(E) TRF2 protein produced in insect cells using baculovirus is not detectable by αATM-P. Increasing amounts of TRF2 protein were analyzed by western blotting with antibody 647 to detect TRF2 and αATM-P to detect TRF2 phosphorylated on S368.

TRF2 S368 phosphorylation is positively regulated by ATR, and negatively regulated by mTOR

Because TRF2 S368 precedes a glutamine (Q), it represents a potential PIKK target. Furthermore, because the region surrounding TRF2 S368 so closely resembles the region surrounding ATM S1981, a site of autophosphorylation, it seemed likely that the kinase(s) responsible for TRF2 S368 phosphorylation were members of the PIKK family. Because ATM activation is inhibited in the context of TRF2 overexpression in 293T cells (Fig. 2-1), ATM seemed an unlikely candidate for positively regulating S368 phosphorylation in this setting.

In order to determine whether members of the PIKK family promoted phosphorylation of TRF2 on S368, 293T cells transfected with wildtype TRF2 were treated with the PIKK inhibitors caffeine and wortmannin. TRF2 S368 phosphorylation levels were monitored by western blot with the αATM-P antibody (Fig. 3-3A). Caffeine and wortmannin both severely reduced TRF2 phosphorylation on S368 when used at concentrations shown to inhibit ATM, ATR, and DNA-PK. Notably, when wortmannin was used at a lower concentration, 0.3 μM, known to inhibit ATM and DNA-PK but not ATR[210], it did not affect the level of S368 phosphorylation (Fig. 3-3A).

To help pinpoint the identity of the PIKK kinase(s) involved in TRF2 S368 phosphorylation, 293T cells transfected with wildtype TRF2 were treated with either IR to activate ATM or UV radiation to activate ATR, and allowed to recover

for 1 hr. before harvesting. TRF2 S368 phosphorylation levels were again monitored by western blot with the αATM-P antibody. While 5 Gy IR strongly induced ATM S1981 phosphorylation, visible in the same blot, TRF2 S368 phosphorylation was not affected (Fig. 3-3B). In contrast, UV radiation increased TRF2 S368 phosphorylation (Fig. 3-3B). UV-induced upregulation of TRF2 S368-P was evident as soon as 30 min. after UV (Fig. 3-3C), making it less likely that ATM activation by UV is playing a role in the phosphorylation[154]. Induction of TRF2 phosphorylation on S368 by UV radiation is repressed by caffeine treatment (Fig. 3-3D) consistent with positive regulation by a PIKK. HU treatment, which induces replication stress by depleting the deoxynucleotide triphosphate pool, also increased TRF2 S368 phosphorylation (Fig. 3-3E).

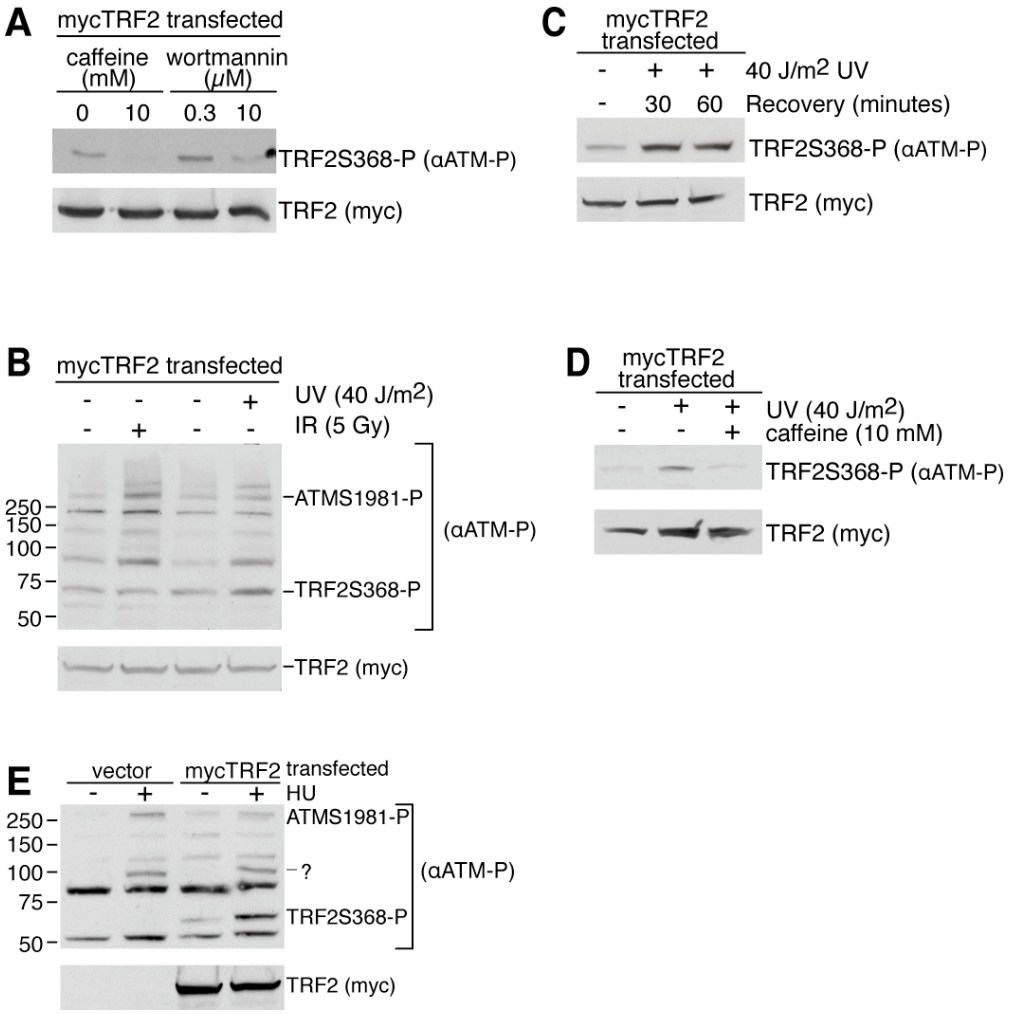

Figure 3-3: Phosphorylation of S368 on TRF2 expressed in 293T cells by transient transfection is diminished by PIKK inhibitors and induced by UV radiation and HU, but not IR.

(A) The phosphorylation of S368 on TRF2 expressed by transient transfection in 293T cells is diminished by the PIKK inhibitors caffeine and wortmannin. Myc-tagged wildtype TRF2 was expressed in 293T cells by transient transfection. 48 hrs. after transfection, cells were treated with 10 mM caffeine, 0.3 μM wortmannin, or 10 μM wortmannin for 4 hrs.

(B) Phosphorylation of S368 on TRF2 expressed in 293T cells by transient transfection is induced by UV radiation, but not IR. Myc-tagged wildtype TRF2 was expressed in 293T cells by transient transfection. 48 hrs. after transfection, cells were exposed to 5 Gy IR or 40 J/m^2 UV radiation. Cells were harvested 1 hr. after treatment.

(C) Induction of phosphorylation of S368 on transfected TRF2 by UV radiation is detectable 30 min. after treatment. Myc-tagged wildtype TRF2 was expressed in 293T cells by transient transfection. 48 hrs. after transfection, cells were exposed to 40 J/m^2 UV radiation, and allowed to recover for either 30 or 60 min. before harvesting.

(D) Induction of phosphorylation of S368 on transfected TRF2 by UV radiation is inhibited by caffeine. Myc-tagged wildtype TRF2 was expressed in 293T cells by transient transfection and exposed to 40 J/m^2 UV radiation. Cells were harvested 1 hr. after treatment. Indicated samples were preincubated with 10 mM caffeine for 4 hrs.

(E) HU treatment increases levels of S368 phosphorylation of transfected TRF2, but does not induce detectable levels of endogenous TRF2 phosphorylated on S368. 293T cells were transfected with myc-tagged wildtype TRF2 or an empty vector. 48 hrs. after transfection, cells were treated with 2 mM HU for 18 hrs.

To determine whether the ATR kinase is responsible for the phosphorylation of TRF2 on S368, an RNAi mediated knockdown approach was used in 293T cells. Dharmacon ON-TARGETplus™ SMARTpool siRNA against the ATR kinase was used to lower its expression. SMARTpool siRNA or control siRNA and TRF2 were cotransfected into 293T cells using DharmaFECT© Duo transfection reagent. Nearly complete knockdown of ATR was achieved using this strategy. ATR knockdown reproducibly led to diminished levels of TRF2 phosphorylated on S368 (Fig. 3-4A). shRNA-mediated knockdown of ATM (Fig. 3-4B) or DNA-PK (Fig. 3-4C) did not reduce levels of TRF2 phosphorylated on S368. Attempts to knock down SMG1, with three distinct shRNA constructs (Fig. 3-4D), two distinct siRNA duplexes, and Dharmacon ON-TARGETplus™ SMARTpool siRNA against SMG1, failed to achieve significantly reduced levels of SMG1 protein. Therefore, we cannot exclude involvement of SMG1 in the phosphorylation of TRF2 on S368.

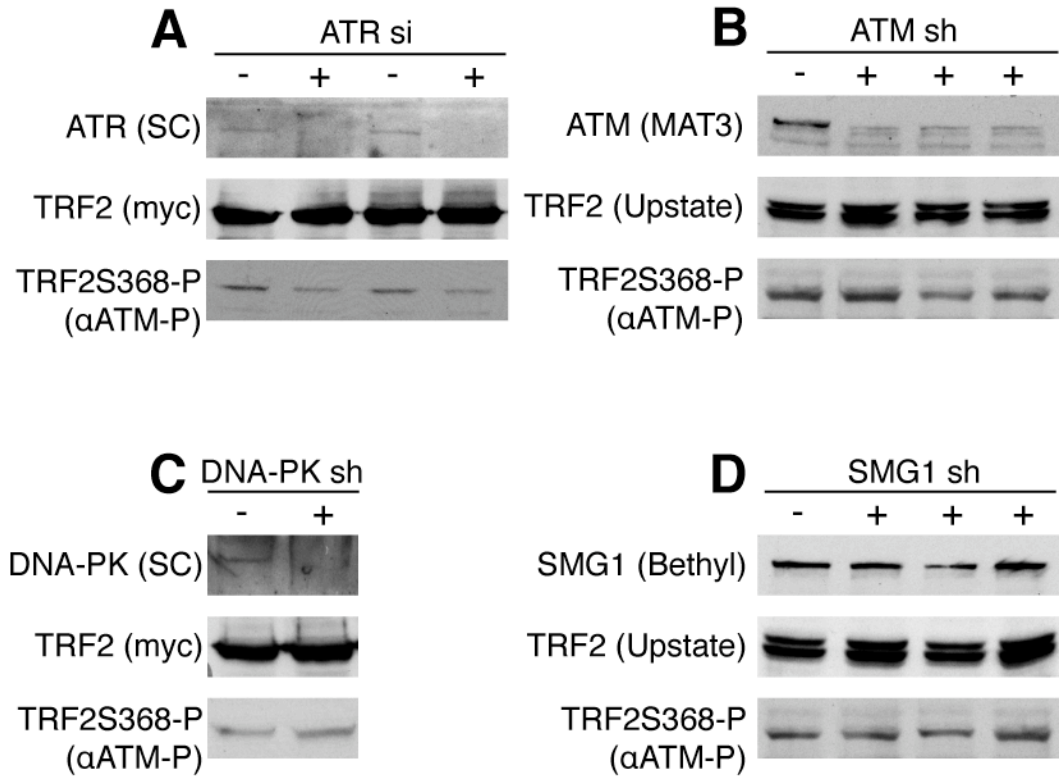

Figure 3-4: Knockdown of ATR, but not ATM or DNA-PK, reduces TRF2 phosphorylation on S368.
(A) siRNA-mediated knockdown of ATR reduces phosphorylation of transfected TRF2 on S368. 293T cells were co-transfected with myc-tagged wildtype TRF2 and Smart Pool siRNA targeting ATR or a control siRNA targeting luciferase. 48 hrs. after transfection, cells were harvested. Two independent transfections are shown.
(B) shRNA-mediated knockdown of ATM does not reduce phosphorylation of transfected TRF2 on S368. 293T cells were infected with 3 different shRNA constructs (1-3) targeting ATM or a control shRNA targeting luciferase. Subsequently, myc-tagged wildtype TRF2 was expressed by transient transfection. 48 hrs. after transfection, cells were harvested.
(C) shRNA-mediated knockdown of DNA-PK does not reduce phosphorylation of transfected TRF2 on S368. 293T cells were infected with an shRNA construct targeting DNA-PK (DNA-PK sh #2, DNA-PK sh #1 and sh#3 did not efficiently knockdown DNA-PK levels) or a control shRNA targeting luciferase. Subsequently, myc-tagged wildtype TRF2 was expressed by transient transfection. 48 hrs. after transfection, cells were harvested.
(D) shRNA mediated knockdown of SMG1 was not efficient. 293T cells were infected with 3 different shRNA constructs targeting SMG1 (1-3) or a control shRNA targeting luciferase. Subsequently, myc-tagged wildtype TRF2 was expressed by transient transfection. 48 hrs. after transfection, cells were harvested.

Effects of mTOR signaling on the phosphorylation of TRF2 on S368

In order to determine whether mTOR plays a role in the regulation of TRF2 phosphorylation on S368, wildtype mTOR was co-transfected into 293T cells with wildtype TRF2. Surprisingly, co-transfection of mTOR resulted in almost complete abolition of phosphorylation of TRF2 on S368, while total TRF2 levels were unaffected (Fig. 3-5A). Co-transfection of a second wildtype mTOR construct in a different vector also severely diminished TRF2 phosphorylation on S368, but a kinase-dead mTOR mutant did not (Fig. 3-5B).

If mTOR is a negative regulator of TRF2 phosphorylation on S368, TRF2 S368 phosphorylation should be inversely related to mTOR activity. The mTOR kinase activity should be high at the time of 293T transfection, which is done when cells are actively dividing. As the cells approach confluence, depletion of nutrients in the media will be sensed by mTOR and mTOR activity will be downregulated [211]. In order to test the effect of cell proliferation on the phosphorylation of TRF2 on S368, transfected 293T cells were monitored at 16 hr. intervals. mTOR activity was determined by phosphorylation of p70 S6 ribosomal kinase and p85 S6 ribosomal kinase, major mTOR targets. As expected, mTOR activity was high at the time of transfection and was diminished at later timepoints (Fig. 3-5C). Transfected TRF2 was already expressed at the 16 hr. timepoint, as determined by western blot with a myc antibody, but TRF2 phosphorylated on S368 was not detected until the 36 hr. time point, when

mTOR activity was low (Fig. 3-5C). These data are consistent with an inverse relationship between mTOR activity and TRF2 phosphorylation on S368.

To confirm that mTOR is a negative regulator of TRF2 phosphorylation on S368, we treated 293T cells transfected with TRF2 with the well-characterized mTOR inhibitor, rapamycin. Cells were subjected to rapamycin 12 hrs. after transfection when mTOR activity is still high. Although phosphorylation of p70 S6 ribosomal kinase and p85 S6 ribosomal kinase were reduced after treatment with 10 nM rapamycin for 30 min., no significant change in the phosphorylation of TRF2 on S368 occurred, even with concentrations as high as 50 nM (Fig. 3-5D). The interpretation of the lack of a rapamycin effect is confounded by recent data indicating that mammalian mTOR exists in two separate complexes, mTORC1 and mTORC2[212]. mTORC1 is rapamycin sensitive and performs the functions typically ascribed to mTOR, regulation of cell growth in response to nutrient availability. mTORC2 however, has a different set of binding partners, and is rapamycin insensitive. Its function is more elusive, and while it shares some functions of mTORC1, it positively regulates Akt/PKB while mTORC1 does not[213], [214] and may play a role in regulating the cytoskeleton[215] [216]. mTORC2 is generally rapamycin insensitive, however it has now been shown that treating cells for prolonged periods with rapamycin interferes with mTORC2 complex assembly and results in reduced functional mTORC2[217]. In order to determine whether mTORC2 plays a role in regulating TRF2 phosphorylation on S368, 293T cells transfected with TRF2 were treated with 20 nM rapamycin for 24 hrs. In

response to this treatment, a small but reproducible increase in TRF2 phosphorylation was observed, suggesting that mTORC2 may be a negative regulator of TRF2 phosphorylation on S368.

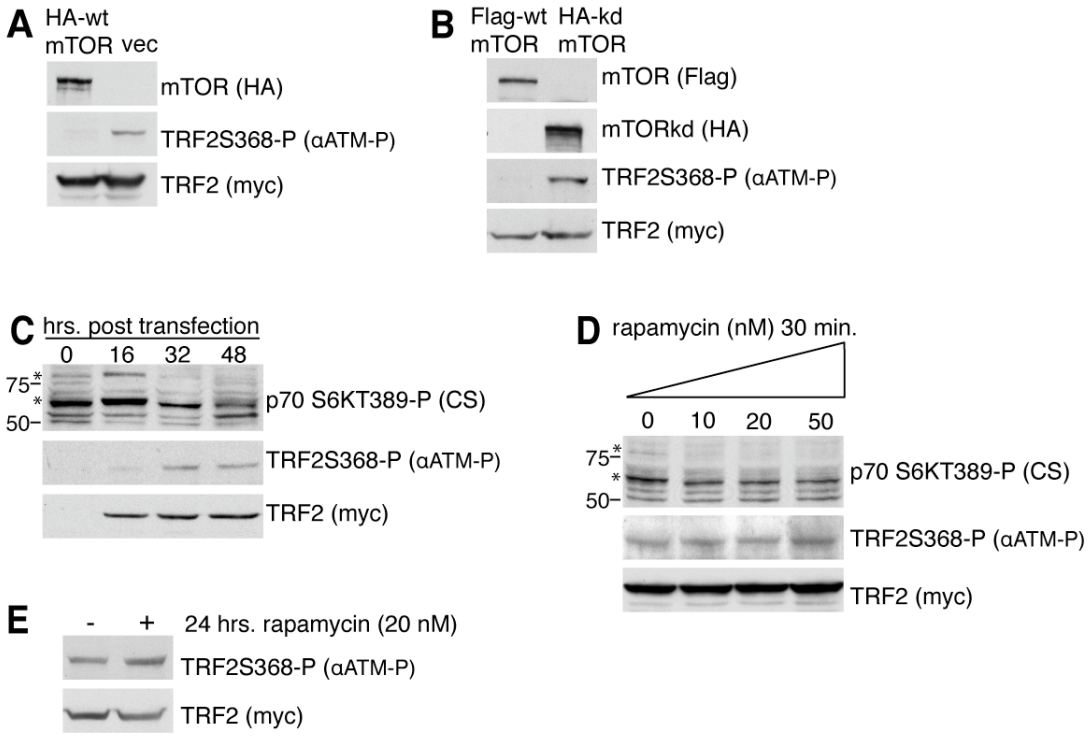

Figure 3-5: Effects of mTOR signaling on phosphorylation of TRF2 on S368.
(A) Overexpression of wildtype mTOR drastically reduces S368 phosphorylation of transfected TRF2. HA-tagged wildtype mTOR or an empty vector were co-transfected with myc-tagged wildtype TRF2 into 293T cells. 48 hrs. after transfection, cells were harvested.
(B) Overexpression of wildtype mTOR (different construct than in (A)) but not a kinase-dead allele, reduces S368 phosphorylation of transfected TRF2. Flag-tagged wildtype mTOR or HA-tagged kinase-dead mTOR were co-transfected with myc-tagged wildtype TRF2 into 293T cells. 48 hrs. after transfection, cells were harvested.
(C) Post-transfection, phosphorylation of TRF2 on S368 inversely correlates with mTOR activity. 293T cells were transfected with wildtype TRF2 and harvested at the indicated timepoints post-transfection. Lysates were analyzed by western blotting with phospho-p70 S6 Kinase antibody (Cell Signaling) which detects mTOR targets, p70 S6 kinase phosphorylated on T389 and p85 S6 kinase phosphorylated on T412 (asterisks).
(D) Rapamycin treatment for 30 min. does not affect S368 phosphorylation of transfected TRF2. Myc-tagged wildtype TRF2 was expressed in 293T cells by transient transfection. 48 hrs. after transfection, cells were treated with the indicated doses of rapamycin for 30 min.
(E) Rapamycin treatment for 24 hrs. increases S368 phosphorylation of transfected TRF2. Myc-tagged wildtype TRF2 was expressed in 293T cells by transient transfection. 24 hrs. after transfection, cells were treated with 20 nM rapamycin for 24 hrs.

Attempts to detect endogenous TRF2 phosphorylated on S368

Experiments described so far were performed in the setting of TRF2 expressed by transient transfection in 293T cells. Lysates from several different human cell types were analyzed by western blot with the αATM-P antibody to attempt to detect evidence of endogenous TRF2 phosphorylated on S368 (Fig. 3-6A). Endogenous TRF2 phosphorylated on S368 was not detected in the telomerase-positive transformed cell lines, HeLa or HT1080. The phosphorylation was likewise undetectable in BJ cells, non-telomerase expressing primary foreskin fibroblasts. Some telomerase-negative cells maintain their telomeres using the recombination-based ALT mechanism. Cells that employ the ALT mechanism contain ALT-associated PML bodies (APBs) that contain TRF1, TRF2, and a number of proteins involved in DNA replication and recombination[148]. ATR kinase activity may be high in APBs, potentially leading to detectable levels of TRF2 S368 phosphorylation. However, the modification was undetectable in the ALT cell line GM847 (Fig. 3-6A).

The region surrounding S368 is highly conserved in mammals (Fig. 3-1). In mouse TRF2 the phosphorylated residue predicted to be targeted by the αATM-P antibody is serine 366. Lysates from MEFs and various mouse tissues were analyzed by western blot with the αATM-P antibody for evidence of endogenous TRF2 phosphorylated on S366, but the modification was undetectable (Fig. 3-6B).

The inability to detect endogenous TRF2 phosphorylated on S368 by western blot with the αATM-P antibody suggests that the modification is present at low abundance, possibly only during specific phases of the cell cycle. In addition to being activated by DNA replication stress, the ATR pathway is involved in unperturbed DNA replication[218], and ATR has been detected at telomeres during S phase after aphidicolin block[20]. In light of our data indicating that ATR is a positive regular of TRF2 S368 phosphorylation, it seemed possible that the modification could be an S phase specific event.

To address the possibility that phosphorylation of TRF2 on S368 was an S-phase specific event, HeLa cells were blocked at the G1/S boundary by double thymidine block. After release from block, samples for FACs and western blot were taken at the indicated time points. TRF2 phosphorylated on S368 is not detectable throughout the cell cycle, including at the 2 hr. time point when the majority of cells are in S phase (Fig. 3-6C). We also employed centrifugal elutriation, which fractionates cell cycle populations based on their sedimentation rates. For each elutriation fraction, samples for western blot and FACs were taken. Although FACs analysis determined that the elutriation process efficiently fractionated cells according to cell cycle stage (Fig. 3-6D), TRF2 phosphorylated on S368 was not detectable in any of the fractions (Fig. 3-6E).

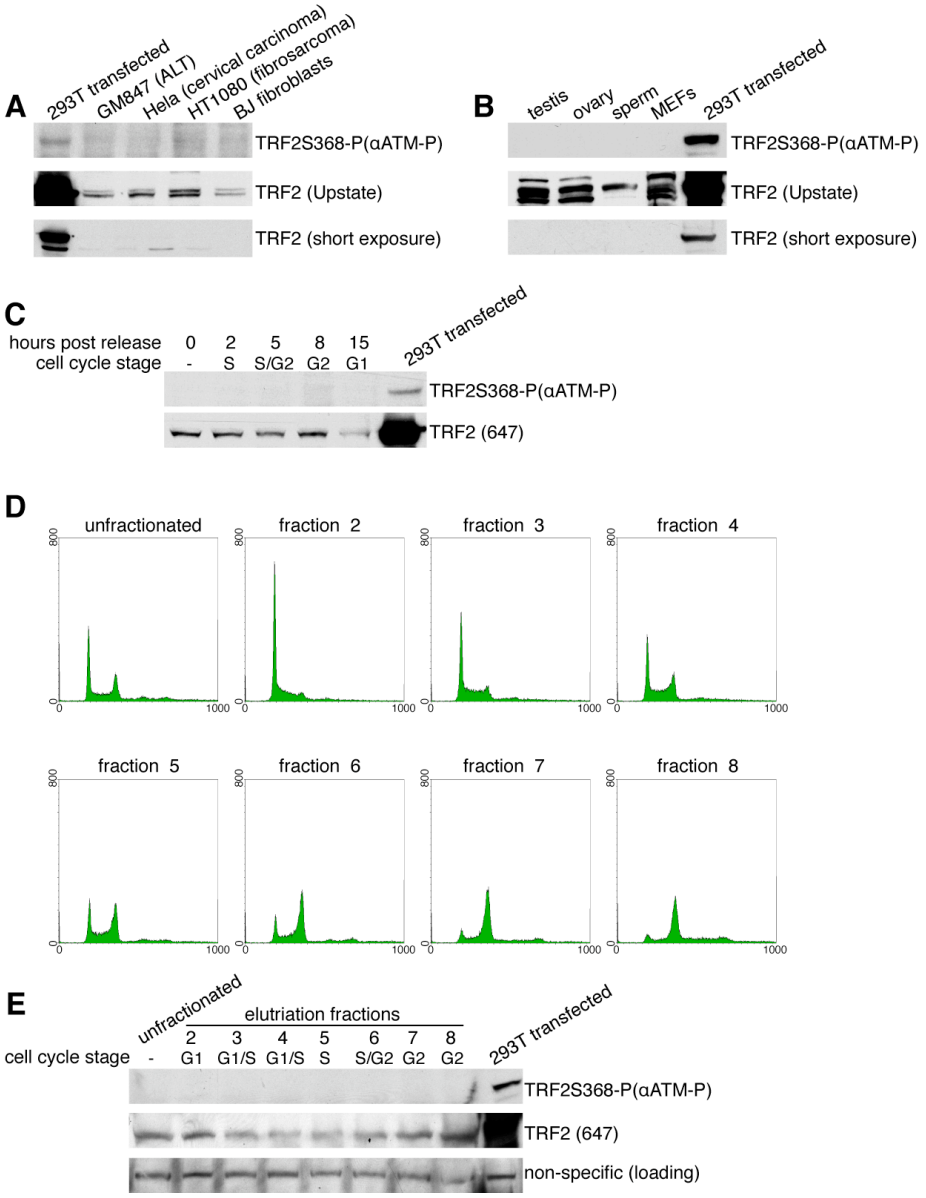

Figure 3-6: Attempts to detect endogenous TRF2 phosphorylated on S368 with αATM-P.
(A) Endogenous TRF2 phosphorylated on S368 is present at low or undetectable levels in several human cell types.
(B) Endogenous TRF2 phosphorylated on S368 in MEFs and mouse meiotic tissues is undetectable by western with αATM-P.
(C) Endogenous TRF2 phosphorylated on S368 is undetectable in cell-cycle specific samples from HeLa cells synchronized by double thymidine block. Cells were released from thymidine block and harvested at the indicated timepoints for western and FACs. FACs using PI determined the indicated phase of the cell cycle for each sample.
(D) FACs analysis of elutriated HeLa cells. HeLa S3 (suspension cells) were fractionated according to sedimentation properties using centrifugal elutriation. For each fraction, samples for western blot and FACs were taken. FACs using PI determined the indicated phase of the cell cycle for each sample. Y axis, cell numbers; x axis, relative DNA content on the basis of staining with propidium iodide.
(E) Endogenous TRF2 phosphorylated on S368 is undetectable in cell-cycle specific samples from HeLa cells fractionated by centrifugal elutriation. A non-specific band on the anti-TRF2 western blot serves as a loading control.

Because of the observed increase of the phosphorylation of transfected TRF2 in 293T cells after UV treatment and the finding that S368 phosphorylation is positively regulated by ATR, induction of DNA replication stress was employed in an attempt to increase S368 phosphorylation of endogenous TRF2 to detectable levels. Treatment of HeLa cells and untransfected 293T cells with UV did not result in detectable TRF2 S368 phosphorylation (Fig. 3-7A). As previously shown, HU treatment increased S368 phosphorylation of transfected TRF2, but did not induce detectable levels of endogenous TRF2 phosphorylated on S368 (Fig. 3-3E, vector transfected cells).

ATR activation can also be achieved by exposing cells to the alkylating agent methyl methanesulfonate [219] Untransfected 293T cells were treated with 0.02% MMS for four hrs. and subsequently analyzed by western blotting with the αATM-P antibody. The αATM-P antibody detected several bands where endogenous TRF2 is expected to run which were induced by MMS treatment (Fig. 3-7B). However, our attempts to immunoprecipitate TRF2 after MMS treatment to determine whether it was phosphorylated on S368 failed, so we were unable to confirm the identity of these bands.

We asked whether ATR activation at telomeres might induce phosphorylation of telomere bound TRF2 on S368. While removal of TRF2 from telomeres predominately activates checkpoint kinase ATM, inhibition of POT1 function activates ATR[97], possibly by exposing ssDNA which can be bound by RPA. In mouse, POT1 function is shared by two genes, Pot1a and Pot1b, which

have distinctive but overlapping roles in telomere end protection[118]. Cre was expressed in cells conditionally null for either Pot1a (Pot1a$^{F/-}$) or Pot1b (Pot1b$^{F/-}$) or both (Pot1a/b). Cells were harvested 96 hrs. after introduction of Cre, when ATR activation as determined by Chk1 phosphorylation is robust[97] and lysates were analyzed by western blot with the αATM-P antibody. Although Pot1a/b deletion induced a strong band of approximately 90 kDa on the αATM-P western blot, endogenous TRF2 phosphorylated on S368 was not detectable (Fig. 3-7C).

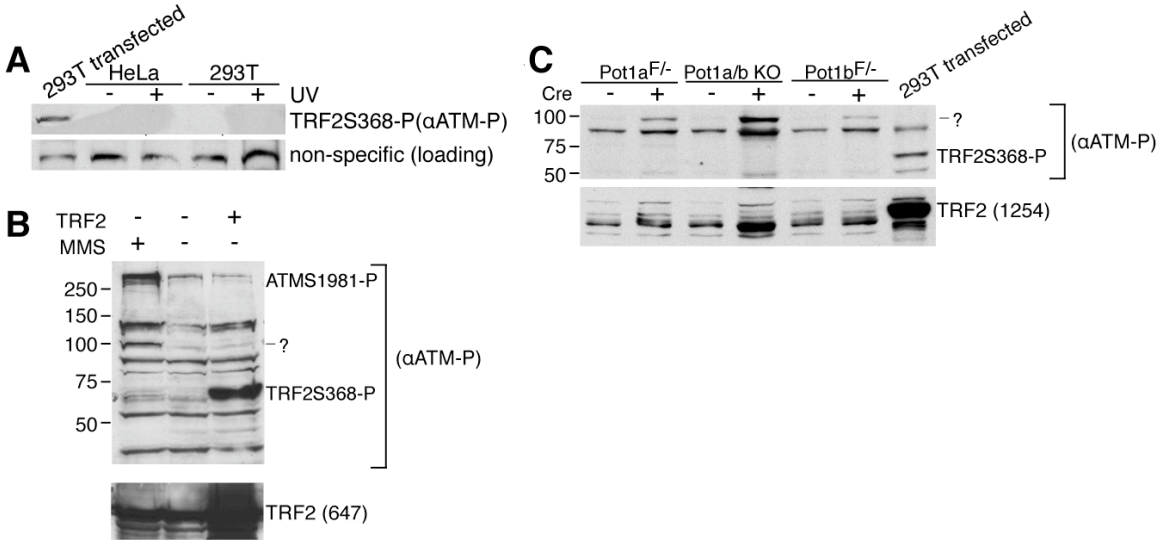

Figure 3-7: Attempts to detect endogenous TRF2 phosphorylated on S368 after induction of replication stress.
(A) UV radiation of HeLa cells and untransfected 293T cells does not induce detectable levels of S368 phosphorylation of endogenous TRF2. Cells were treated with 40 J/m^2 UV radiation and harvested 1 hr. after treatment. A non-specific band on the αATM-P western blot serves as a loading control. Lysate from 293T cells transfected with myc-tagged wildtype TRF2 is included as a positive control for detection of S368 phosphorylation.
(B) MMS treatment induces a band potentially representing endogenous TRF2 phosphorylated on S368. 293T cells transfected with myc-tagged wildtype TRF2 or a vector control were treated with 0.02% MMS for 4 hrs.
(C) Pot1a and Pot1b removal does not induce detectable levels of endogenous TRF2 phosphorylated on S368. MEFs conditionally null for either Pot1A (Pot1A$^{f/-}$), Pot1B (Pot1B$^{F/-}$) or both (Pot1a/b KO) were treated with Cre. 96 hrs. after Cre induction, cells were harvested. Lysate from 293T cells transfected with myc-tagged wildtype TRF2 is included as a positive control for detection of S368 phosphorylation.

We considered the possibility that the lack of detectable endogenous TRF2 phosphorylated on S368 was due to phosphatase activity. In order to test this, 293T cells transfected with wildtype TRF2 were treated with Okadaic Acid (OA), a potent inhibitor of protein phosphatases type I (PP1) and 2A (PP2A)[220]. As previously reported[221], OA treatment significantly increases ATM phosphorylation on S1981 (Fig. 3-8A). While OA did not increase total TRF2, a slight increase in S368 phosphorylation of transfected TRF2 was observed (Fig. 3-8A). Untransfected 293T cells were also treated with 100 nM OA. Upon long

exposure, the αATM-P antibody detects several bands that potentially co-migrate with TRF2 (Fig. 3-8A). However, we were unable to confirm the identity of these bands as our attempts to immunoprecipitate TRF2 after OA treatment to determine whether it was phosphorylated on S368 failed. HeLa 1.3 cells were also treated with increasing doses of OA. Although the αATM-P western blot shows a dose dependent increase in ATM S1981 phosphorylation, no bands potentially representing TRF2 phosphorylated on S368 were observed (Fig. 3-8A).

As discussed above, mTOR overexpression severely reduces S368 phosphorylation of TRF2 expressed in 293T cells by transient transfection, suggesting that mTOR is a negative regulator of TRF2 S368 phosphorylation. We postulated that inhibition of mTOR might increase the phosphorylation of endogenous TRF2 to detectable levels. MEFs over-expressing wildtype TRF2 from a lentiviral vector were incubated with increasing doses of rapamycin, however no bands potentially representing TRF2 phosphorylated on S368 were induced on the αATM-P western (Fig. 3-8B). In the same cells, inhibition of mTOR with rapamycin was combined with induction of replication stress by UV treatment, but endogenous TRF2 phosphorylated on S368 was not detected (Fig. 3-8B). In conclusion, our inability to detect endogenous TRF2 phosphorylated on S368 is most likely not due to inhibition of the phosphorylation by mTOR.

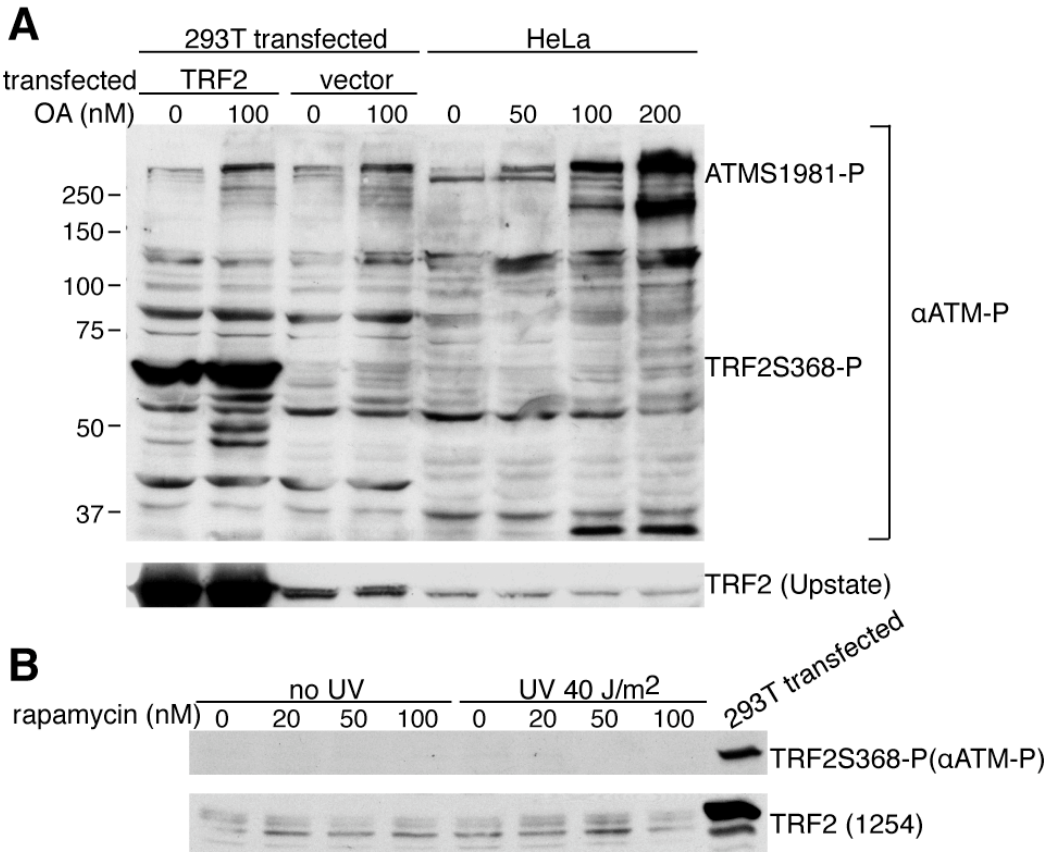

Figure 3-8: Attempts to induce detectable levels of phosphorylation of endogenous TRF2 on S368 by inhibiting phosphatases with Okadaic Acid and mTOR with rapamycin.
(A) OA treatment induces a band potentially representing endogenous TRF2 phosphorylated on S368. 293T cells transfected with either wildtype myc-tagged TRF2 or the empty vector were treated with 100 nM Okadaic Acid (OA) for 3 hrs. HeLa 1.3 cells were treated with the indicated doses of OA for 3 hrs. (B) MEFs expressing myc-tagged wildtype mouse TRF2 in a lentiviral vector were treated with 40 J/m^2 of UV radiation and allowed to recover for 1 hr. in the presence of the indicated dose of rapamycin.

Generating a specific antibody against TRF2 phosphorylated on S368

We argued that an antibody specific to TRF2 phosphorylated on S368 might improve our ability to detect the phosphorylation of endogenous TRF2. The peptide used to generate the αATM-P is remarkably similar to the corresponding region of TRF2, however they are not identical. Notably, TRF2 has the acidic residue aspartic acid (D) at S365 while ATM has the neutrally charged glycine (G) at the corresponding residue, 1980 (Fig. 3-9A). Using the

sequence surrounding TRF2 S368, we attempted to generate a phosphospecific antibody that could detect TRF2 phosphorylated on S368 with higher sensitivity and specificity than the αATM-P antibody. Amino acids 364-374 of human TRF2 are identical to the corresponding mouse residues (362-372) (Fig. 3-9A), so this phosphopeptide was selected for rabbit immunization by the company AnaSpec, San Jose, CA. The resulting antibody was affinity purified using the TRF2 phosphopeptide and affinity depleted with the non-phosphopeptide, to reduce cross-reaction with the non-phosphorylated target.

The purified antibody, designated αTRF2S368-P, was tested for ability to specifically detect TRF2 phosphorylated on S368 in western blots. Indicating incomplete phosphospecificity, αTRF2S368-P detected a mutant form of TRF2 containing S368 mutated to glycine, albeit at much lower levels than it detected wildtype TRF2 (Fig. 3-9B). As shown earlier, αATM-P does not cross-react with this mutant form of TRF2 (Fig. 3-9B). Furthermore, no significant difference in sensitivity between the two antibodies was observed. Because of its ability to distinguish between phosphorylated and non-phosphorylated TRF2, the αATM-P antibody was selected for future use detecting TRF2 phosphorylated on S368 by western blot.

αATM-P detects ATM phosphorylated on S1981 by immunofluorescence (IF)[194] precluding us from using it to detect TRF2 phosphorylated on S368 by IF. IF with αTRF2S368-P produced a nuclear granular staining pattern in HeLa cells, and an occasional large focus of signal was observed (Fig. 3-9C). The granular

staining pattern of αTRF2S368-P did not appear to be telomeric, and lack of colocalization with TRF1 confirmed this (Fig. 3-9C). IF with αTRF2S368-P was also performed in the cell line GM847, to determine if cells that maintain their telomeres using ALT have detectable TRF2 phosphorylated on S368. In these cells, αTRF2S368-P detected several large foci per cell that also stained positively for PML, indicating that they are ALT-associated PML Bodies (APBs) (Fig. 3-9D).

Because many SQ/TQ containing proteins involved in the DNA damage response localize to APBs, it was possible that αTRF2S368-P could be cross-reacting with another protein present in these structures. IR induced DNA damage foci also contain many DNA damage response proteins that are phosphorylated on SQ/TQ residues. However, it has previously been shown that TRF2 does not localize to these foci (Fig. 2-1C,[107]) so αTRF2S368-P should not be able to detect them. 53BP1 staining of HeLa cells subjected to 5 Gy IR revealed the expected induction of foci. Surprisingly, co-staining with αTRF2S368-P also revealed a strong induction of foci in response to IR that colocalized with 53BP1 almost completely (Fig. 3-9E). Even in untreated cells, αTRF2S368-P signal colocalizes with the occasional 53BP1 focus (Fig. 3-9E).

Figure 3-9: Generation of an antibody to detect TRF2 phosphorylated on S368, αTRF2S368-P.
(A) Peptide used to generate an antibody to detect TRF2 phosphorylated on S368, αTRF2S368-P. Alignment of the peptide used to generate αATM-P with amino acids 361-375 of human TRF2 and amino acids 359-373 of mouse TRF2. Peptide used to generate αTRF2S368-P is underlined.
(B) αTRF2S368-P is incompletely phosphospecific for TRF2 phosphorylated on S368. Lysates of 293T cells transiently transfected with either myc-tagged wildtype human TRF2 (wtTRF2), TRF2 containing glycine at position S368 instead of serine (TRF2S>G), or the empty vector were analyzed by western blot with αTRF2S368-P, αATM-P, and anti-TRF2 antibody (647). A non-specific band detected by αATM-P serves as a loading control.
(C) αTRF2S368-P produces a nuclear granular pattern by IF which is not telomere specific. IF on HeLa 1.3 cells with the αTRF2S368-P and a mouse antibody against human TRF1.
(D) αTRF2S368-P detects ALT-associated PML bodies in GM847 ALT cells. IF was performed on GM847 cells with αTRF2S368-P and an anti-PML antibody (Santa Cruz) to detect ALT-associated PML bodies.
(E) αTRF2S368-P signal colocalizes with 53BP1 at IR induced DNA damage foci. HeLa 1.3 cells were either untreated or subjected to 5 Gy IR. Cells were allowed to recover 1 hr. and fixed for IF. IF was performed with αTRF2S368-P and an antibody for 53BP1 (gift of T. Halazonetis).

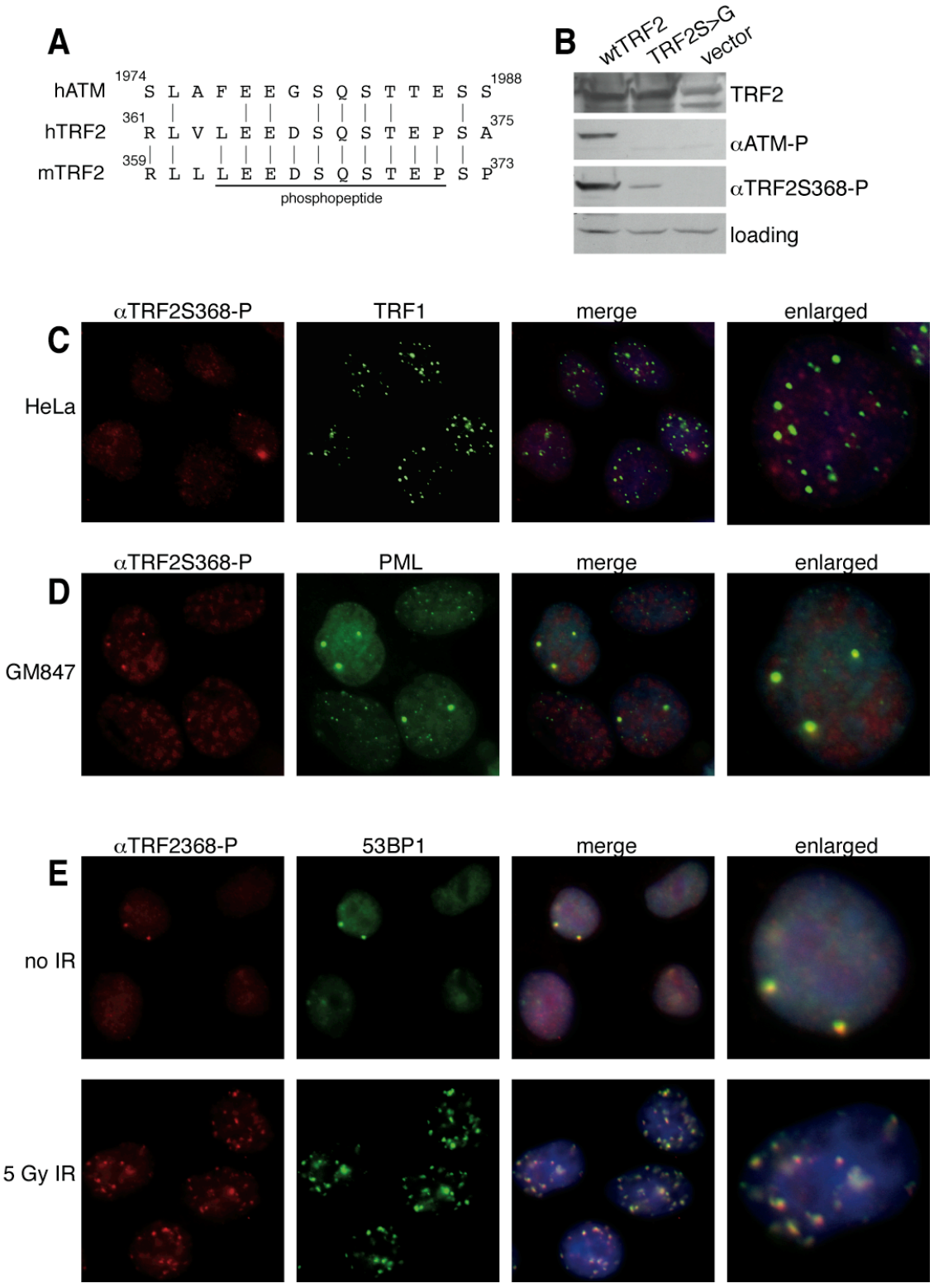
A
hATM 1974 S L A F E E G S Q S T T E S S 1988
hTRF2 361 R L V L E E D S Q S T E P S A 375
mTRF2 359 R L L L E E D S Q S T E P S P 373
phosphopeptide
B
wtTRF2
TRF2S>G
vector
TRF2
αATM-P
αTRF2S368-P
loading
C
αTRF2S368-P
TRF1
merge
enlarged
HeLa
D
αTRF2S368-P
PML
merge
enlarged
GM847
E
αTRF2368-P
53BP1
merge
enlarged
no IR
5 Gy IR

To definitively determine that αTRF2S368-P detects a protein in DNA damage foci other than TRF2, MEFs were employed in which one allele of TRF2 is deleted and the second allele is floxed, $TRF2^{F/-}$ [79]. In $TRF2^{F/-}$ MEFs not exposed to Cre, staining with αTRF2S368-P revealed a granular pattern, similar to the staining pattern observed in HeLa cells (Fig. 3-10A). As we observed in HeLa cells, the αTRF2S368-P signal occasionally showed foci in untreated cells and these colocalized with γH2AX foci (Fig. 3-10A). Foci containing DNA damage response proteins in cells that have not been subjected to DNA damage have been observed previously and their function is unknown.

Cre treatment efficiently abrogated TRF2 protein (Fig. 3-10B). As expected, Cre-mediated deletion of TRF2 results in robust TIF formation (Fig. 3-10C). As was observed after IR, αTRF2S368-P signal strongly colocalizes with these DNA damage foci, even though these cells no longer contain detectable levels of TRF2, indicating that this antibody detects a protein other than TRF2.

The extensive colocalization between the αTRF2S368-P signal and the 53BP1 signal observed in HeLa cells suggests that αTRF2S368-P may be detecting 53BP1 itself, which contains many SQ/TQ motifs. Examination of the amino acid sequence of 53BP1 revealed that the region surrounding Serine 25 was very similar to the peptide used to generate the αTRF2S368-P antibody (Fig. 3-10D). 53BP1 is phosphorylated on this residue in response to IR[222]. The high degree of similarity between the region surrounding TRF2 S368 and the region surrounding 53BP1 S25, and the extensive colocalization of signals, makes it

likely that the αTRF2S368-P signal observed in IF is at least partly due to cross-reaction with 53BP1 phosphorylated on S25.

However, signal resulting from αTRF2S368-P may be due to cross-reaction with more than one protein. αATM-P detects a band of approximately 100 kDa, which is conspicuously up-regulated by HU and MMS treatment, as well as Pot1a and Pot1b removal (Fig. 3-3E; 3-7B,C). This band represents another interesting candidate for cross-reaction with αTRF2S368-P. To determine the identity of this band, the amino acid sequences of proteins known to be involved in the DNA damage response with MWs between 80 and 120 kDa were examined. The 113 kDa protein MMS19 contains a region of striking similarity to the peptide used to generate αTRF2S368-P (Fig. 3-10E). MMS19 is the human homolog of *S. cerevisiae* Mms19, a protein involved in NER and RNA polymerase II transcription[223]. 293T cells were treated with 0.02% MMS and analyzed by western blot with αTRF2S368-P. As was seen with the αATM-P, MMS treatment induced a band of approximately 100 kDa (Fig. 3-10F). An antibody against hMMS19 (gift of J. Hoeijmakers) also detected a band of about 100 kDa. However, side by side comparison of western blots for MMS19 and αTRF2S368-P show that the candidate band detected by αTRF2S368-P exhibits a distinct electrophoretic mobility than the band detected by the MMS19 antibody (Fig. 3-10F), suggesting that MMS19 is not the target of the antibody cross-reactivity.

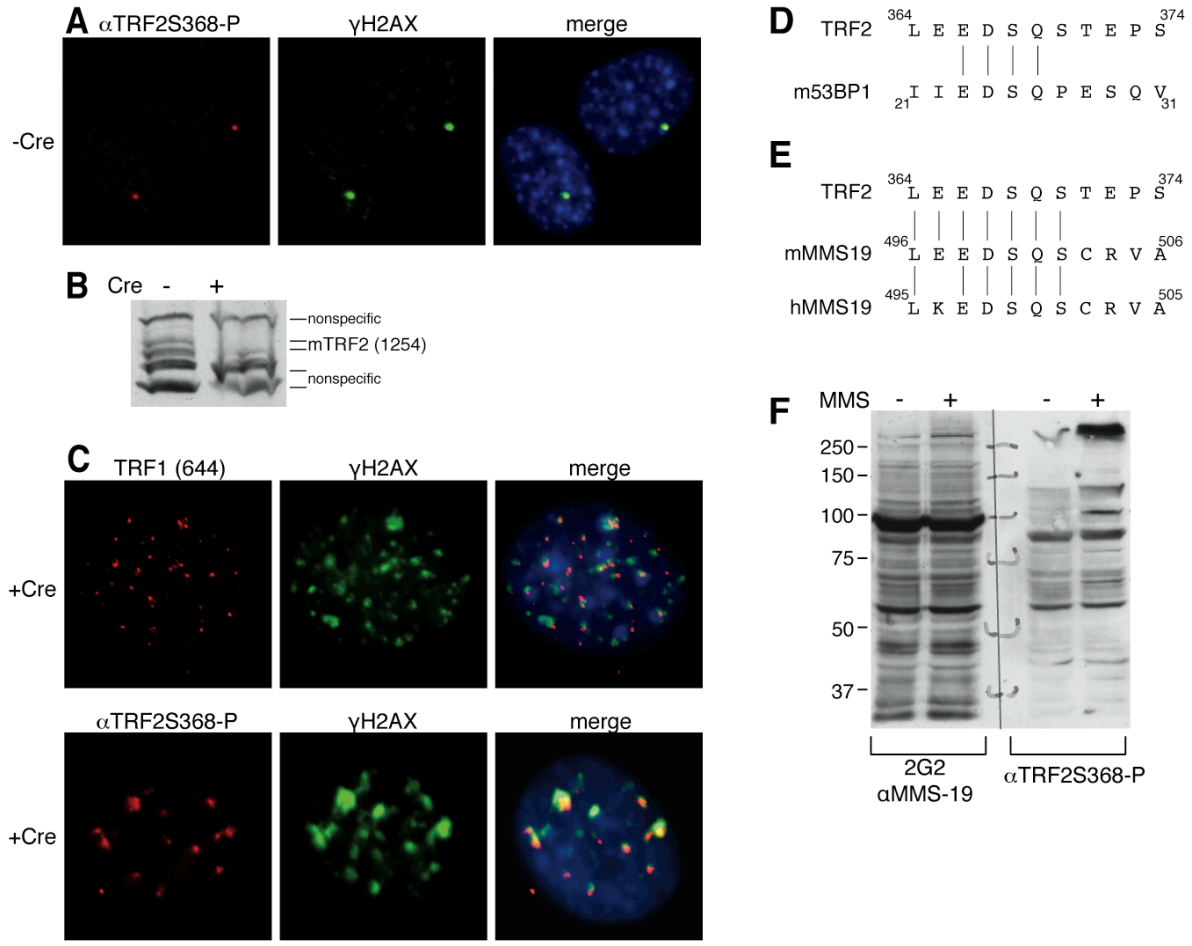

Figure 3-10: αTRF2S368-P cross-reacts with another protein present in DNA damage foci.
(A) αTRF2S368-P produces a nuclear granular pattern in MEFs and colocalizes with occasional γH2AX foci. $TRF2^{F/-}$ $p53^{-/-}$ MEFs (not exposed to Cre) were subjected to IF with αTRF2S368-P and an antibody against Phospho-H2A.X (Ser139, γH2AX) (Upstate).
(B) Expression of Cre in $TRF2^{F/-}$ $p53^{-/-}$ MEFs depletes TRF2 protein. 120 hrs. after the introduction of Cre, cells were harvested. Lysates were analyzed by western blot with an anti-TRF2 antibody (1254). Non-specific bands detected by the antibody are indicated.
(C) αTRF2S368-P detects TIFs after TRF2 has been removed. $TRF2^{F/-}$ $p53^{-/-}$ MEFs were exposed to Cre. 120 hrs. after the introduction of Cre, cells were harvested. IF was performed with an antibody for γH2AX and either an antibody for mouse TRF1 (644) or αTRF2S368-P.
(D) The peptide used to generate αTRF2S368-P is similar to 53BP1 amino acids 21-31.
(E) The peptide used to generate αTRF2S368-P is similar to a region of MMS19. Alignment of the peptide used to generate αTRF2S368-P with amino acids 496-506 of mouse MMS19 and 495-505 of human MMS19.
(F) αTRF2S368-P may cross-react with MMS19 on western blot. Untransfected 293T cells were treated with 0.02% MMS for four hrs. After transfer of protein to the nitrocellulose membrane, the blot was cut in half so that it could be individually probed with αMMS-19 (2G2, gift of J. Hoeijmakers) and αTRF2S368-P. Before exposure to film, blots were re-aligned, so that co-migration of MMS19 and band on the αTRF2S368-P blot could be determined.

The finding that αTRF2S368-P was capable of strongly cross-reacting with at least one other protein raised the possibility that a similar cross-reactivity might explain recent data regarding the phosphorylation of another SQ/TQ site within TRF2, Threonine 188 (T188). A phosphospecific antibody to TRF2 phosphorylated on T188 was used to show that TRF2 is phosphorylated on this residue in response to IR, and that this form of phosphorylated TRF2 localizes to dysfunctional telomeres, ALT-associated PML bodies, and unexpectedly, DNA damage induced by laser micro-irradiation and IR[209]. The same company that generated αTRF2S368-P, Anaspec, was used to generate the antibody in this study, which was designated anti-TRF2 Thr188P.

To determine whether anti-TRF2 Thr188P could cross-react with another protein present in DNA damage foci, $TRF2^{F/-}$ MEFs infected with a lentiviral vector were treated with Cre to remove all TRF2 protein (Fig. 3-11A). In MEFs not exposed to Cre, anti-TRF2 Thr188P staining was weak and occasionally formed small foci. In cells treated with Cre, TIF formation was monitored by IF for γH2AX. As was the case for αTRF2S368-P, anti-TRF2 Thr188P signal colocalized with TIFs after TRF2 depletion (Fig. 3-11B), showing that this antibody detects a non-TRF2 protein.

To confirm that anti-TRF2 Thr188P was capable of cross-reacting with another protein present in DNA damage foci, an allele of mouse TRF2 with both T188 and S366 mutated to alanines was expressed in $TRF2^{F/-}$ MEFs. Since these are the only two SQ/TQ motifs present in mouse TRF2, the mutant allele is

completely free of PIKK targets. Cre expression removed endogenous TRF2 (Fig. 3-11A). In cells infected with vector only, Cre expression caused TIF formation and the anti-TRF2 Thr188P signal strongly colocalized with these DNA damage foci (Fig. 3-11B). Because these cells no longer contain detectable TRF2, this indicates that anti-TRF2 Thr188P detects a protein other than TRF2. Cre was also expressed in cells containing the double phosphorylation mutant of TRF2 (Fig. 3-11A). This form of TRF2 localized to telomeres as shown by its colocalization with TRF1 (Fig. 3-11C). TIFs were not observed after Cre expression in these cells, indicating that the double phosphorylation mutant of TRF2 prevents telomeres from being recognized as DNA damage (Fig. 3-11D, No IR). After the introduction of Cre, MEFs were exposed to 5 Gy IR. γH2AX staining showed the expected IR induced foci, which were also strongly detected by anti-TRF2 Thr188P (Fig. 3-11D, 5 Gy). The findings that anti-TRF2 Thr188P detects IR induced DNA damage foci in cells in which the only form of TRF2 no longer contains a phosphorylatable residue at position 188, and that this antibody detects TIFs in cells that do not contain TRF2, clearly show that anti-TRF2 Thr188P is capable of cross-reacting with another protein present at sites of DNA damage.

Figure 3-11: The anti-TRF2 Thr188P antibody (Tanaka et al., 2005) is not specific for TRF2.
(A) Expression of Cre in $TRF2^{F/-}$ $p53^{-/-}$ MEFs depletes TRF2 protein. $TRF2^{F/-}$ $p53^{-/-}$ MEFs were infected with an allele of TRF2 with T188 and S368 mutated to alanines (mutant) or a vector control (vector). 120 hrs. after introduction of Cre, cells were harvested and lysates were analyzed by western blot with an anti-TRF2 antibody (1254). Non-specific bands detected by the antibody are indicated.
(B) The anti-TRF2 Thr188P (αTRF2T188-P) antibody detects TIFs after TRF2 has been removed. $TRF2^{F/-}$ $p53^{-/-}$ MEFs infected with vector only were exposed to Cre or left untreated. 120 hrs. after the introduction of Cre, cells were harvested and IF was performed with a γH2AX antibody and the anti-TRF2 Thr188P antibody. Merged image shows colocalization of the two signals after Cre treatment.
(C) The TRF2 double phospho-mutant allele localizes to telomeres. $TRF2^{F/-}$ $p53^{-/-}$ MEFs were infected with an allele of TRF2 with T188 and S366 mutated to alanines and exposed to Cre. 120 hrs. after introduction of Cre, cells were fixed and IF was performed with anti-c-myc to detect the introduced allele of TRF2 and an anti-TRF1 antibody (644) to detect telomeres.
(D) The anti-TRF2 Thr188P antibody detects IR induced DNA damage foci in cells in which endogenous TRF2 has been replaced with a mutant allele which contains an unphosphorylatable residue at position 188. 120 hrs. after introduction of Cre, $TRF2^{F/-}$ $p53^{-/-}$ MEFs expressing the mutant allele were subjected to 5 Gy IR or left untreated. After a one hr. recovery, cells were fixed and IF was performed with a γH2AX antibody and the anti-TRF2 Thr188P antibody (αTRF2T188-P). Merged image shows colocalization of the two signals.

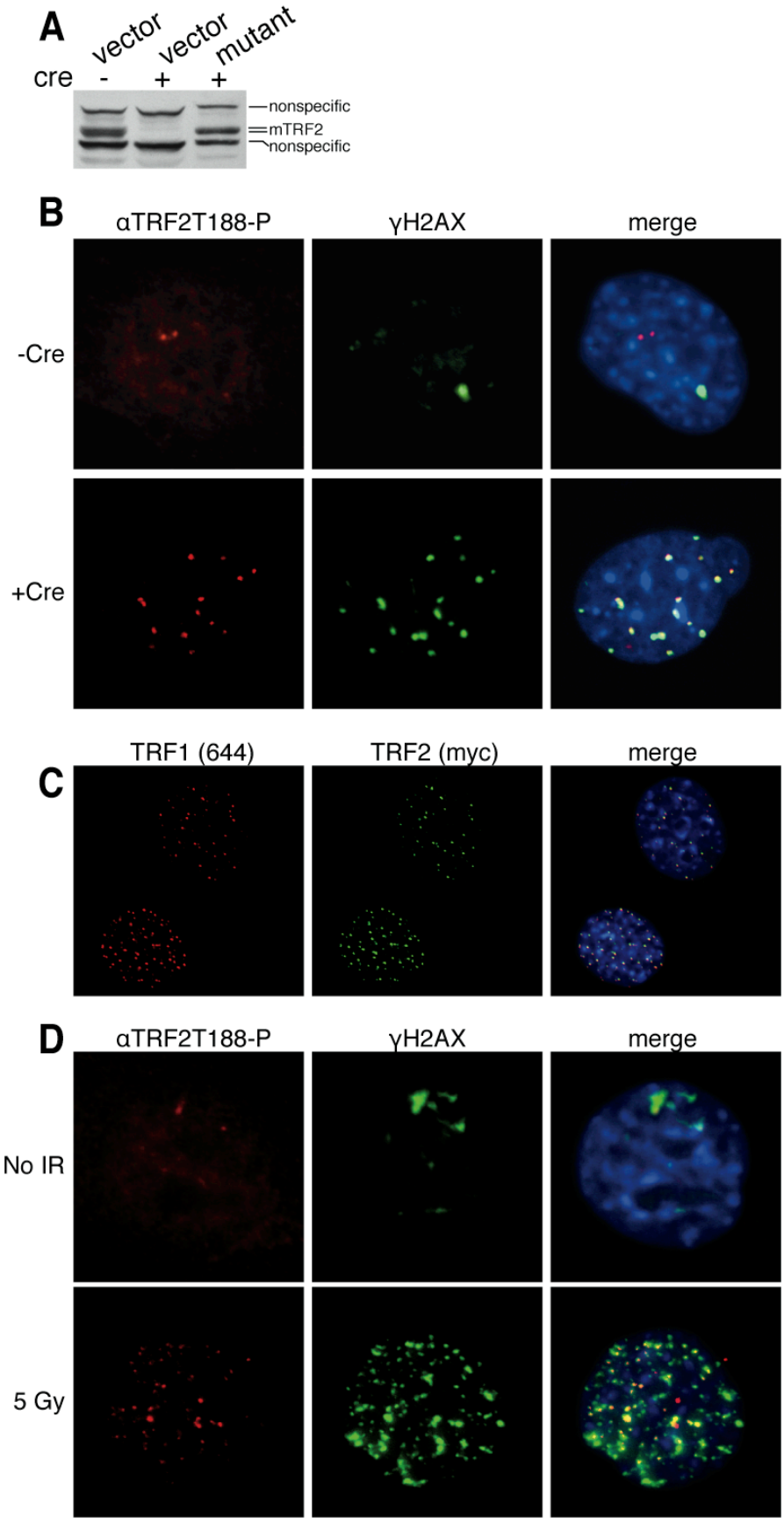
A
vector
vector
mutant
cre
-
+
+
nonspecific
mTRF2
nonspecific
B
αTRF2T188-P
γH2AX
merge
-Cre
+Cre
C
TRF1 (644)
TRF2 (myc)
merge
D
αTRF2T188-P
γH2AX
merge
No IR
5 Gy

DISCUSSION

We have shown that an antibody designed to detect ATM phosphorylated on S1981 also detects TRF2 phosphorylated on S368, when TRF2 is expressed by transient transfection in 293T cells. TRF2 phosphorylation was diminished when cells were treated with the PIKK inhibitors caffeine and wortmannin, and augmented by treatment with UV radiation but not IR. Knockdown experiments show that ATR is a positive regulator of TRF2 phosphorylation on S368, while reduction of ATM and DNA-PK protein had no effect on TRF2 phosphorylation levels. Surprisingly, co-transfection of mTOR strongly diminished phosphorylation of S368 of TRF2.

Because members of the PIKK family, including the ATR orthologs, are required for telomere length maintenance in yeast, the consequence of mutation of serine 368 of TRF2 for telomere length maintenance will be explored in the following chapter. Additionally, the positive regulation of TRF2 phosphorylation by ATR, but not DNA-PK or ATM, suggests that this modification may be functionally important during replication of telomeric DNA, an idea that will also be investigated in the next chapter.

To our knowledge, the finding that co-expression of mTOR had an inhibitory effect on the phosphorylation of TRF2 on S368 is the first report of a connection between the mTOR pathway and telomeres. Such a connection could be utilized in cases when mTOR signaling causes a population of cells to expand rapidly in response to favorable growth conditions. In many cell types,

proliferation can be limited by low levels of telomerase activity [224]. Perhaps mTOR, by regulating phosphorylation of shelterin components, can alter the accessibility of the telomere to telomerase, to prevent telomere length from limiting cell division. This model has the advantage of providing a rapid way for mTOR to affect telomere length that does not involve the slower processes of transcription and translation.

Ironclad evidence of endogenous TRF2 phosphorylated on S368 has been elusive. However, a recent report confirms that endogenous TRF2 can be phosphorylated on this residue *in vivo* in response to IR[225]. Matsuoka et al. performed immunoprecipitates using various SQ/TQ specific antibodies on 293T cells untreated and treated with 10 Gy IR. Mass spectrometry was performed on the immunoprecipitates to determine the identity of proteins phosphorylated specifically in response to IR. In immunoprecipitates with both an antibody specific to ATM S1981 (Rockland) and with αTRF2S368-P described here, a fragment of TRF2 phosphorylated on S368 and S380 (a second SQ in human TRF2 which is not conserved in mouse) was recovered. The data presented indicate only that TRF2 phosphorylation is enriched after IR treatment, it is unknown whether TRF2 is phosphorylated on S368 in untreated cells.

In our hands, IR treatment did not increase the phosphorylation of TRF2 overexpressed in 293T cells on S368 (Fig. 3-3B) and we did not see an induction of TRF2 phosphorylation of endogenous TRF2 with low doses of IR (Fig. 3-2A, vector). Matsuoka et al. were probably able to detect TRF2 phosphorylated on

S368 in response to IR because immunoprecipitation with phospho-specific antibodies, followed by mass spectrometric analysis, allowed for higher sensitivity than western blot on whole cell lysates. Additionally, much greater levels of IR (10 Gy) were employed, while in the experiments described here, 293T cells were analyzed after IR treatment of only 0.6 Gy. Nonetheless, ATM activation, as determined by autophosphorylation on S1981, is maximal after 0.4 Gy IR[194]. It is likely that the high levels of IR employed by Mastsuoka et al. activated ATR in addition to ATM, because even 5 Gy IR leads to ATR activation, as determined by Chk1 phosphorylation[158].

In spite of difficulties detecting endogenous TRF2 phosphorylated on S368 by western blot, the striking degree of evolutionary conservation of this residue and the findings of Matsuoka et al. suggest that S368 is a physiologically relevant phosphorylation site. Endogenous TRF2 phosphorylated on S368 is probably difficult to detect because it is present at very low levels. 293T transfection results in TRF2 expression levels several fold higher than endogenous (See Fig. 3-2C) and this may be the simple reason why S368 phosphorylation was only detected in this setting. Normally TRF2 is present only at the telomere, but when TRF2 was overexpressed in fibroblasts using a retrovirus, it was observed to saturate its telomere binding sites and distribute throughout the nucleus[115]. Since our data indicate that TRF2 S368 phosphorylation is induced by replication stress and positively regulated by ATR, it is likely that only a small percentage of TRF2,

perhaps only TRF2 in the immediate vicinity of a stalled replication fork, will be phosphorylated on S368.

These studies have highlighted the tendency of antibodies generated against SQ/TQ phosphorylation events on specific proteins to cross-react with proteins other than their desired target. By western, the αATM-P antibody detects TRF2 phosphorylated on S368 as well as at least one other protein whose phosphorylation is induced by DNA damage. Furthermore, two antibodies targeting different SQ/TQ motifs in TRF2 (anti-TRF2 Thr188 and αTRF2S368-P) are capable of detecting a protein other than TRF2 present in DNA damage foci.

The high concentration of SQ/TQ phosphorylated proteins present in DNA damage foci increases the likelihood of antibody cross-reaction in the IF setting. In order to use such antibodies for IF, stringent controls must be performed to rule out the possibility of cross-reaction. The danger of cross-reaction in western blot applications is mitigated somewhat by the aid of MW information about the detected protein. Nonetheless, controls are required to confirm the identity of the detected protein. The study by Matsuoka et al. clearly demonstrates the ability of SQ/TQ specific antibodies to immunoprecipitate proteins other than their intended targets. For example, αATM-P immunoprecipitated 15 distinct proteins which were phosphorylated in response to IR. Interestingly, one study used ChIP with αATM-P to show that phosphorylated ATM is present at telomeres during late S and G2 after cell cycle synchronization with thymidine and aphidicolin [226]. However, the authors did not test whether total ATM was detectable at telomeres

by ChIP during these cell cycle stages, allowing the possibility that the ChIP signal obtained αATM-P represents TRF2 phosphorylated on S368 rather than ATM phosphorylated on S1981.

Chapter 4: Functional Studies of TRF2 S368 Mutation

INTRODUCTION

The studies described in Chapter 3 shed light on the regulation of the phosphorylation of TRF2 on S368. The checkpoint kinase ATR, which responds primarily to DNA damage caused by replication stress[153] directly or indirectly, promotes this phosphorylation event. Phosphorylation of TRF2 on S368 is increased by HU treatment and UV radiation and diminished by siRNA mediated knockdown of ATR. These findings informed our study of the influence of S368 phosphorylation on TRF2 function.

TRF2 plays a major role in telomere protection and is also implicated in telomere length regulation. The phenotype of TRF2 loss was first studied using a dominant negative allele of TRF2 which lacks the N-terminal Basic domain and the Myb domain, required for DNA binding. Expression of this mutant, TRF2$^{\Delta B \Delta M}$, removes TRF2 from telomeres and leads to telomere fusion and growth arrest[63]. The double-stranded part of the telomere remains largely intact and is detectable at the sites of fusion, however the single stranded telomeric overhang is degraded[63]. Telomere fusions resulting from TRF2 inhibition are dependent on DNA Ligase IV and Ku indicating that they are generated by NHEJ[105 79 106]. Preceding telomeric fusion, many DNA damage response factors localize to telomeres including 53BP1, γH2AX, ATM phosphorylated on S1981, Mre11, Nbs1, and phosphorylated Rad17[95 96]. Consistent with the induction of a DNA

damage response, TRF2 loss leads to p53-mediated senescence or apoptosis, depending on cell type[63 102].

The phenotypes of TRF2 inhibition, first observed with the dominant negative allele, were recapitulated in mouse cells[79]. Celli and de Lange generated $TRF2^{F/-}$ MEFs by deleting one allele of TRF2 and flanking the second TRF2 allele with LoxP sites. By exposing $TRF2^{F/-}$ MEFs to Cre recombinase, the remaining allele of TRF2 is removed. As was observed with the dominant negative allele of TRF2, genetic removal of TRF2 results in degradation of the telomeric 3' overhang, telomeric fusions, and cell cycle arrest[79]. Additionally, Celli and de Lange observed that deletion of TRF2 causes destabilization of TRF2's binding partner Rap1. Confirming that the cause of these phenotypes is the loss of TRF2, each can be repressed by expression of TRF2 from an exogenous cDNA.

In mouse, the pertinent serine is located at position 366 (Fig. 3-1). By expressing TRF2 containing a mutation at S366 in $TRF2^{F/-}$ MEFs and removing endogenous TRF2 by introducing Cre recombinase, the effect of mutation of S366 on the ability of TRF2 to protect the telomere can be analyzed. Deletion of TRF2 results in a senescence-like arrest, preventing the procurement of mitotic samples, so $TRF2^{F/-}$ MEFs that were also deficient for p53 ($p53^{-/-}$) were used in these studies. Because the crucial ATM S1981 phosphorylation site closely resembles the region surrounding TRF2S366, we predicted that S366 could be involved in preventing the activation of ATM at telomeres.

In addition to examining its role in telomere protection, we also considered that phosphorylation of TRF2 on S368 may be involved in regulation of telomere length by TRF2. In human cells, TRF2 overexpression causes rapid telomere shortening[76 104] and shRNA mediated knockdown of TRF2 leads to telomere elongation (Takai, K. and de Lange, unpublished). Telomere shortening induced by TRF2 can occur in the absence of telomerase[104,109]. It is likely that the shortening observed upon overexpression of TRF2 is due to a process known as t-loop homologous recombination (t-loop HR), in which the telomeric t-loop is thought to serve as a substrate for Holliday Junction resolvases, resulting in drastic stochastic telomere shortening and the formation of extrachromosomal telomeric circles[21]. We investigate whether TRF2 mutated at position 368 can carry out t-loop HR, by overexpressing these alleles in human cells in which endogenous TRF2 has been knocked down with shRNA.

A potential role of ATR-mediated phosphorylation of TRF2 on S368 would be of interest given that *S. cerevisiae* Tel1 and Mec1 (homologs of the ATM and ATR kinases, respectively) are required for maintenance of telomere length[169 164 227]. Similarly, in the fission yeast, *S. pombe*, absence of Tel1 or Rad3 (the Mec1 homolog), causes telomere shortening[171 170]. In mammals, some evidence suggests that ATM and DNA-PK are involved in telomere length regulation, but this has not been thoroughly investigated[179 180 181]. Telomere length changes in the context of ATR deficiency have not been studied, owing primarily to the essential nature of ATR in mammalian cells[228].

The response of the ATR kinase to DNA replication stress might be particularly significant in the context of telomeres. In addition to imposing a cell cycle arrest and preventing late origin firing, a primary function of the ATR kinase in response to replication stress is to stabilize stalled replication forks[229]. The ATR pathway uses at least two parallel strategies to prevent the collapse of stalled forks and facilitate the restart of DNA replication. First, the ATR kinase acts to prevent components of the replisome from dissociating from stalled forks. The *S. cerevisiae* ATR ortholog, Mec1, and downstream components of the Mec1 pathway, are required to prevent loss of DNA polymerases from the replication fork when cells are treated with HU[230-232] and chicken DT40 cells that lack Chk1, the primary mediator of ATR activity, do not retain PCNA at stalled forks induced by aphidicolin[233]. Stalled forks can be restarted using recombination based or non-recombination based mechanisms[234](Fig. 4-0). While most models of replication fork restart involve the formation of a four–way Holliday Junction "chickenfoot" structure, resolution of these structures by Holliday Junction endonucleases can result in pathological genome rearrangements. The ATR pathway appears to have an anti-recombinogenic effect at stalled forks. Treatment of budding yeast which are deficient for Mec1 with HU results in the formation of foci of the recombination protein Rad52[235]. Similarly, HU treatment of fission yeast deficient in the ATR ortholog, Rad3, or the downstream Cds1 kinase, results in persistent foci of Rad22 (the Rad52 homolog) as well as formation of aberrant structures resembling recombination

intermediates[236]. Deletion of the fission yeast Rad51 homolog, Rhp51, reduces the formation of these structures and increases the proportion of Cds1 mutants which complete S phase[236] consistent with the ATR pathway negatively regulating deleterious recombination events at stalled forks. The ATR pathway may prevent recombination at stalled forks by negatively regulating Rad60[237] or the Holliday Junction specific endonuclease component Mus81[238,239]. There is also evidence that RecQ helicases promote non-recombinogenic fork-restart pathways at stalled forks[240,241] possibly by facilitating the reverse branch migration of regressed (chickenfoot) forks, by-passing the fork-stalling lesion and avoiding resolution by a Holliday Junction-specific nuclease[242].

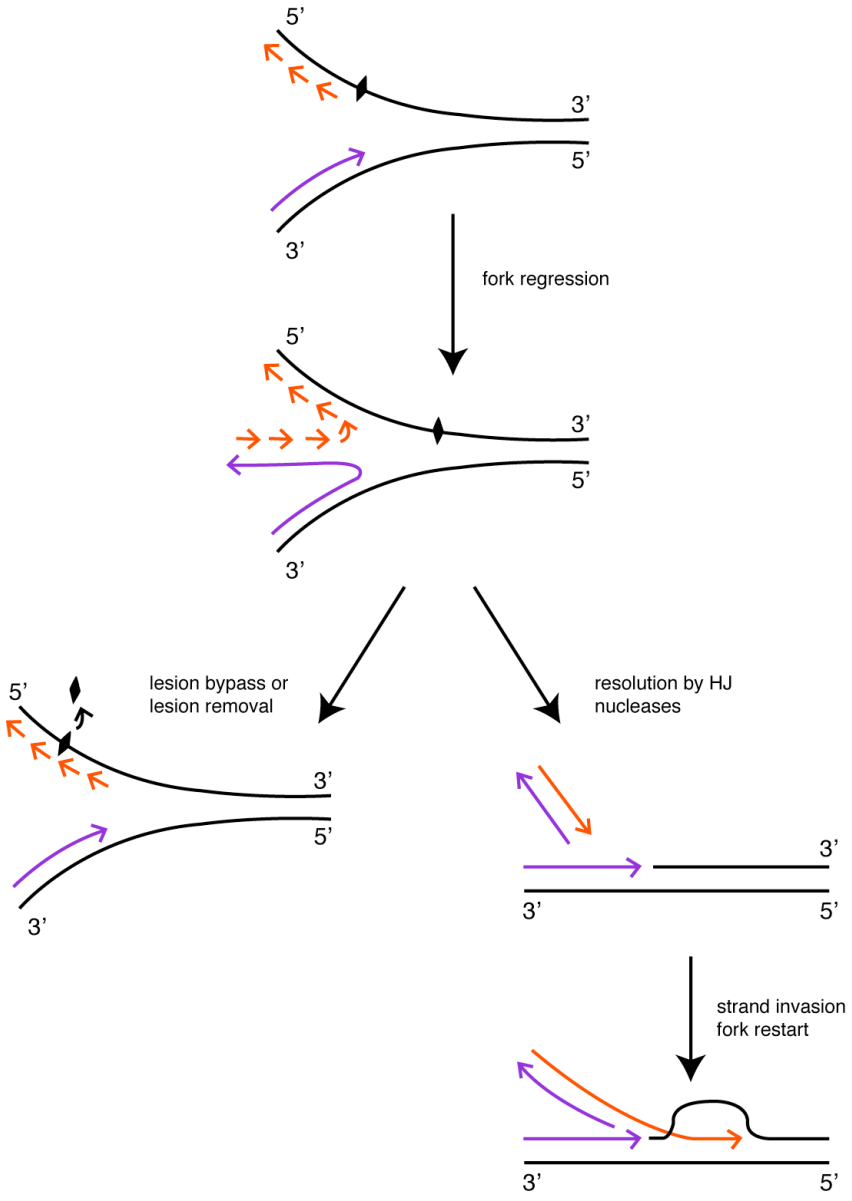

Fig. 4-0: Stalled replication forks can be restarted by recombination-dependent and non-recombination dependent mechanisms.
Replication forks stall when encountering certain types of lesions, here shown as a ♦ on the lagging strand template. When forks encounter such a lesion, the newly formed strands regress to form a four-way Holliday junction "chickenfoot" structure. In non-recombination based models of fork restart, the nascent lagging strand is extended using the nascent leading strand as a template. This allows the lesion to be bypassed or allows time for it to be removed. When the regressed fork is reversed, replication can restart directly. In recombination-based models of fork restart the "chicken-foot" is resolved by Holliday junction specific nucleases. After the lesion is removed, a strand invasion event takes place between the broken chromosome and the intact duplex. Replication restart can take place, but genome rearrangement may have occurred. This figure was adapted from Heller and Marians, 2007[234].

Single-stranded DNA is thought to be the major structure which signals replication stress and activates the ATR pathway[243]. Single-stranded DNA is coated with RPA, which binds and recruits the ATR/ATRIP complex[119] a replication fork stalls, single-stranded DNA may be generated in several different ways. Depending on where the fork-blocking lesion is located, dissociation of the replisome could leave either the single-stranded leading or lagging strand template uncovered. Another possibility is that the replicative helicases become "uncoupled" from the polymerases and continue unwinding duplex DNA even though the fork has stalled. This has been observed when forks are stalled by treatment with aphidicolin which inhibits DNA polymerases[244] UV and *cis*-platinum[245].

Replication forks may also stall without creating large amounts of ssDNA. This is the case when the replication fork encounters the protein-DNA complexes which form the rRNA Replication Fork Barriers (RFBs) of *S. cerevisiae*[246]. When a similar RFB was inserted ectopically into the *S. pombe* genome, Rad3 status did not affect viability, indicating that fork stabilization mediated by the ATR pathway is not required when replication forks encounter this type of barrier[247].

In theory, telomeric DNA presents several obstacles to the efficient passage of the replication fork. The G-rich strand of telomeric DNA can form quadruplex structures under certain conditions[186] which could prevent the passage of the replication fork[187]. Repeats can also lead to the formation of other unusual structures, such as H-DNA and "sticky" DNA, and may cause

polymerase slippage[188]. Furthermore, telomere-specific DNA binding proteins might hinder the passage of the replication fork, as is the case with the well-studied *E. coli* Tus protein[189].

Several lines of evidence indicate that the passage of the DNA replication fork through telomeric DNA is hindered. Telomeric DNA is a poor substrate in the *in vitro* replication system of linear SV40 DNA[190] and EM analysis of synthetic model replication forks consisting of telomeric DNA show frequent fork regression, often resulting in four-stranded chickenfoot structures[191]. *In vivo*, replication forks proceed slowly through telomeric DNA in *S. cerevisiae*[192 193]. High levels of TRF1 and TRF2 cause replication forks to stall at telomeric DNA both *in vitro*[190]. Interestingly, studies in *Xenopus* egg extracts showed that TRF1 dissociates from telomeric chromatin in a cell cycle dependent manner, possibly corresponding to the time when telomeres are replicated[248].

Replication fork progression through telomeric DNA could be facilitated by the recruitment of shelterin-associated factors. For example, TRF2 physically interacts with the RecQ helicases WRN and BLM and can stimulate their helicase activity on substrates resembling telomeric DNA[137 138]. RecQ helicases are believed to facilitate replication fork progression by disrupting obstructing DNA structures, including G quadruplex DNA, and may also play a role in the reinitiation of replication after fork collapse[139]. Impaired WRN function has deleterious consequences for telomeres that may be related to problems during telomere replication. Overexpression of a dominant negative WRN allele results

in the loss of lagging strand telomeres[52 249]. Late passage MEFs which are doubly deficient for WRN and telomerase exhibit frequent sister telomere exchanges, one possible outcome of replication fork collapse within a telomere[140]. Additionally, primary fibroblasts which lack WRN function undergo senescence which can be reversed by expression of telomerase[49]. A potential role for TRF2 in the replication of telomeric DNA is also suggested by the recent finding that in the absence of the *S. pombe* TRF1/TRF2 ortholog Taz1, replication forks stall as they approach telomeric DNA[250].

TRF2 S368 is conserved immediately adjacent to the TIN2 binding site in both human and mouse TRF2 (Fig. 3-1). This is especially notable because the hinge domain is the region of TRF2 least conserved between human and mouse, with only 70% amino acid identity[60]. This positioning raises the possibility that phosphorylation of TRF2 on S368 could influence the interaction between TRF2 and TIN2. A mechanism to modulate the interaction between TRF2 and TIN2 could be significant because the stable presence at the telomere of all shelterin components is influenced by TIN2. TIN2 can bind TRF1 and TRF2 simultaneously, and disruption of this interaction results in decreased telomeric TRF1 and TRF2, and a DNA damage response at telomeres[64 65]. TIN2 also binds TPP1 and is required for its localization to the telomere, and TPP1, in turn recruits POT1, and in mice, Pot1a and Pot1b[66 67 68].

This chapter describes experiments designed to test the role of phosphorylation on S368 in the function of TRF2. The effect of mutation at S368

on the protective function of TRF2 is examined. Additionally, telomere length homeostasis and the telomeric response to replication stress in cells expressing TRF2 phosphorylation mutants are analyzed. In search of a potential mechanism to explain the observed phenotypes of expression of the TRF2 phosphorylation mutants, the influence of phosphorylation status on the interaction between TRF2 and its binding partners is explored.

RESULTS

Isolation of MEF cell lines expressing TRF2 S366 mutants

Two different mouse TRF2 phosphorylation mutants were introduced into conditional $TRF2^{F/-}$ $p53^{-/-}$ MEFs. S366 was replaced with either an alanine (S366A) to mimic the unphosphorylated residue or a glutamate (S366E) to mimic constituitive phosphorylation. Wildtype TRF2 (wtTRF2) or the empty lentiviral vector were introduced into the same cells as controls.

Western blotting showed that the introduced alleles were expressed at higher levels than endogenous TRF2 (Fig. 4-1A). Since such supra-physiologic expression levels might compensate for subtle defects of the mutants, clonal populations with lower levels of TRF2 were isolated. Such clones also circumvent a second problem, cell to cell variation in expression level of the introduced allele (Fig. 4-1B). Clones were chosen for further use if their TRF2 expression was homogenous and comparable to endogenous TRF2 (Fig. 4-2).

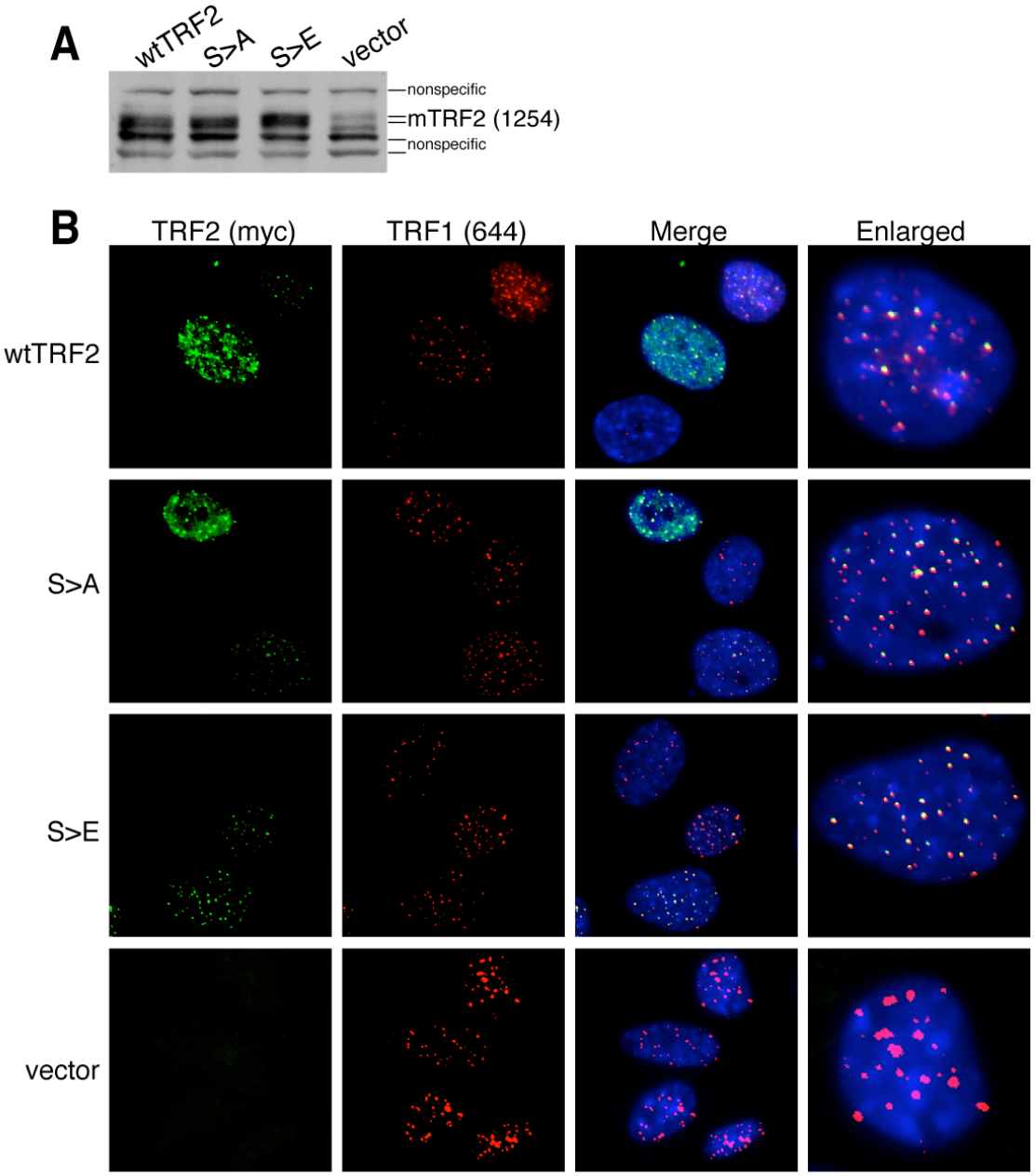

Figure 4-1: Introduction of TRF2 S366 mutant alleles into TRF2$^{F/-}$ p53$^{-/-}$ MEFs.
(A) TRF2$^{F/-}$ p53$^{-/-}$ MEFs were infected with either myc tagged wildtype TRF2 (wtTRF2), TRF2 with S366 mutated to alanine (S>A), TRF2 with S366 mutated to glutamate (S>E), or the empty lentiviral vector. MEFs were not treated with Cre. Cell lysates from infected MEFs were analyzed by western blot with antibody 1254 against mouse TRF2. Non-specific bands detected by the antibody are indicated.
(B) Infected MEFs, not treated with Cre, were analyzed by IF with anti-c-myc and an antibody against mouse TRF1 (644).

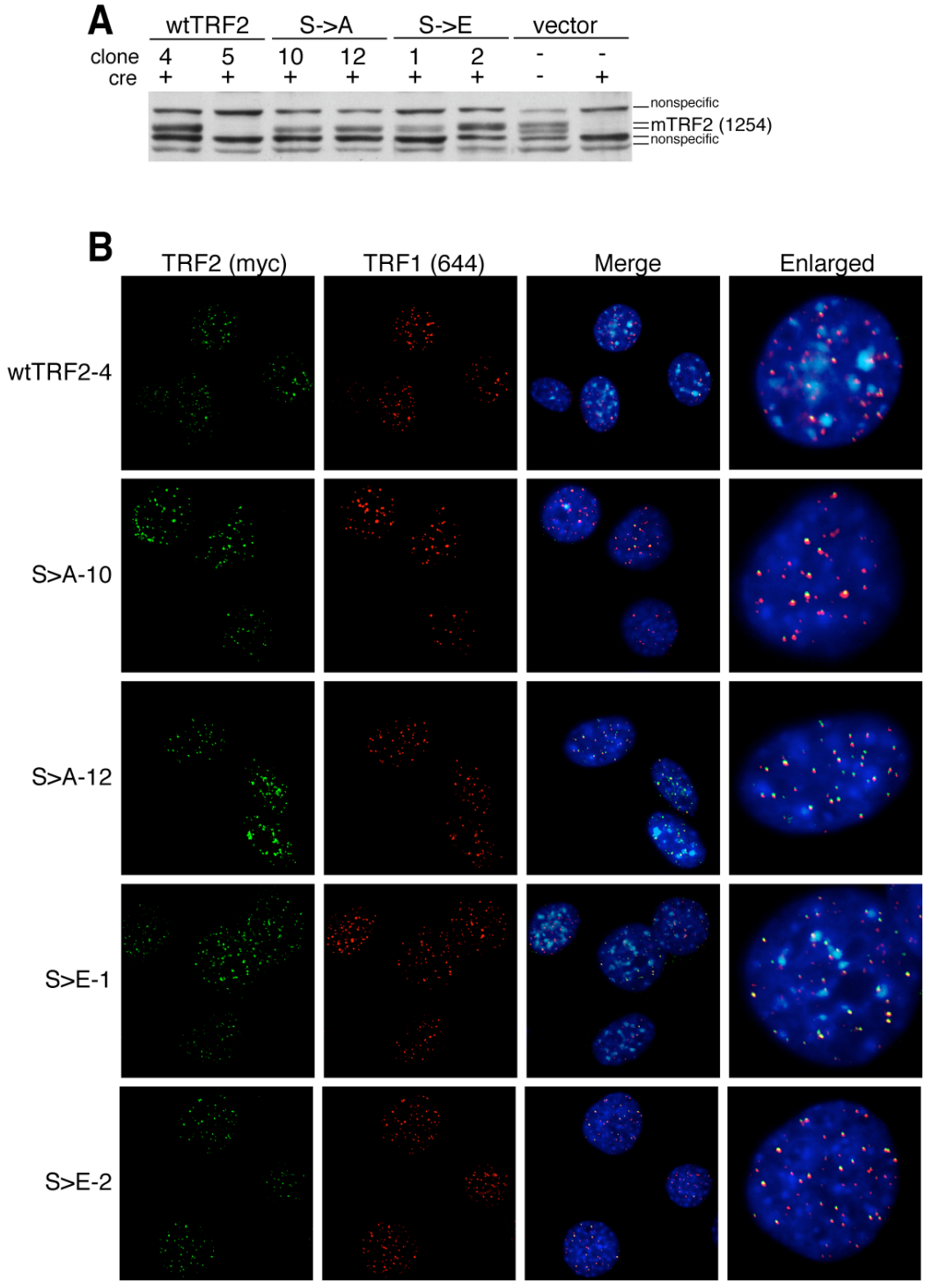

Figure 4-2: TRF2$^{F/-}$ p53$^{-/-}$ clonal cell lines expressing TRF2 S366 mutant alleles.
(A) Clonal cell lines were derived from TRF2$^{F/-}$ p53$^{-/-}$ MEFs infected with myc-tagged TRF2 alleles. 120 hrs. after Cre exposure, cells were harvested. Cell lysates were analyzed by western blot with antibody 1254 against mouse TRF2. Non-specific bands detected by the antibody are indicated.
(B). IF was performed with anti-c-myc and an antibody against mouse TRF1 (644).

TRF2 S366 mutants localize to telomeres, stabilize Rap1, and prevent telomeres from activating the DNA damage response

To determine whether the TRF2 S366A and TRF2 S366E mutants are positioned at telomeres, their cellular localization was analyzed by IF 120 hrs. after Cre was introduced to remove endogenous TRF2. The efficiency of Cre-mediated deletion of TRF2 was determined by loss of endogenous TRF2 expression in the vector expressing cells. Both mutants colocalized extensively with the telomeric protein TRF1, indicating that they localize to telomeres (Fig. 4-2B). Telomeric localization of TRF2 S366A and TRF2 S366E was confirmed by ChIP (Fig. 4-3A,B). Additionally, ChIP showed that the telomeric localization of the other shelterin components were not perturbed in the presence of TRF2 S366A and TRF2 S366E (Fig. 4-3A,B).

Differential salt extraction on MEFs expressing TRF2 S366A and TRF2 S366E was performed to determine if mutation at S366 affects the chromatin association of TRF2. Cells were lysed in buffer containing 150 mM KCl and subsequently extracted with buffer containing 420 mM KCl to release chromatin-bound proteins. As expected, γ-tubulin localized primarily to the 150 mM soluble fraction while the majority of wildtype TRF2 was present in the chromatin bound 420 mM fraction, as has been reported previously [251]. Mutation at S366 did not significantly affect the distribution of TRF2 between the soluble and chromatin-bound fractions (Fig. 4-3C).

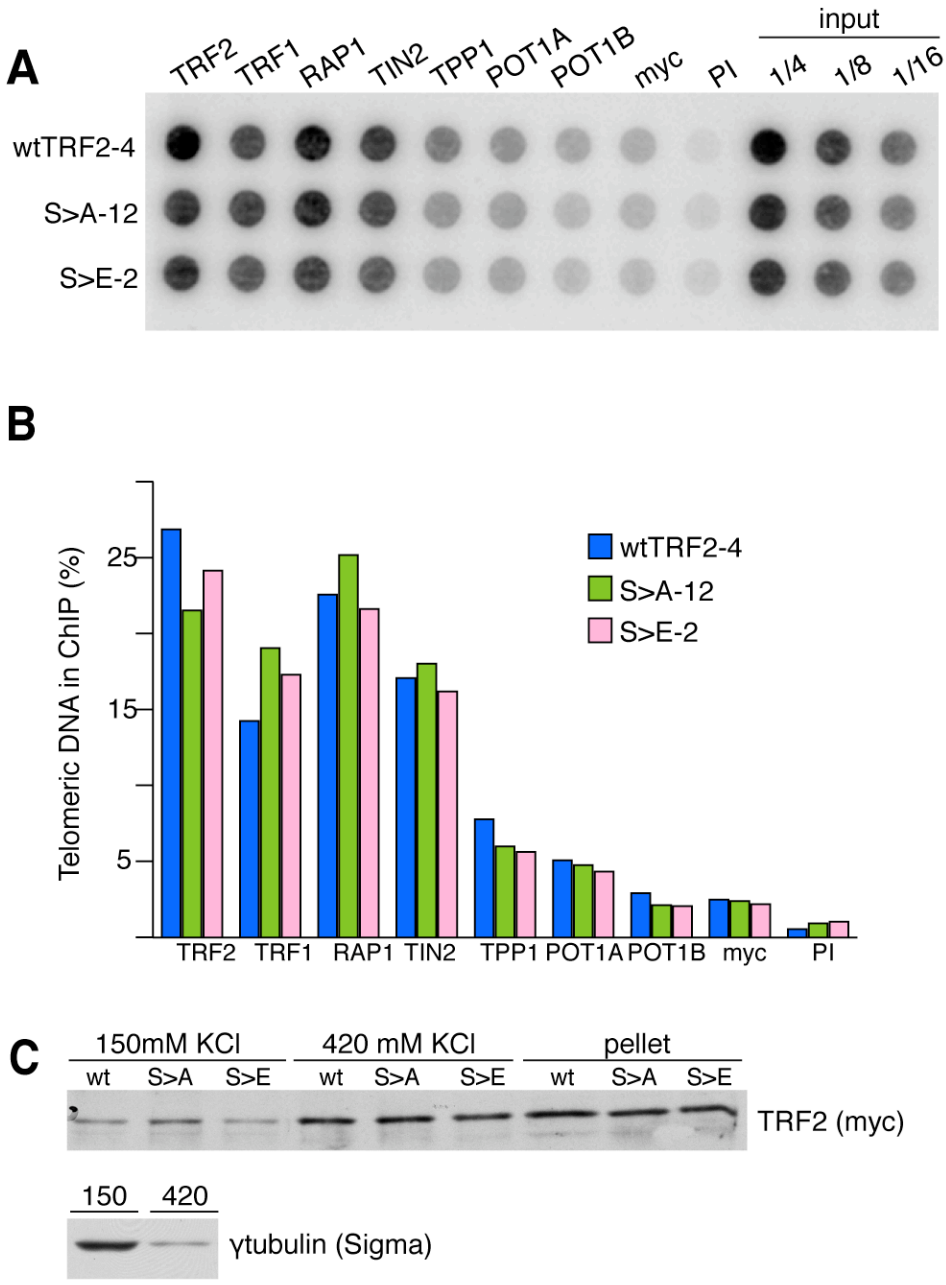

Figure 4-3: TRF2 S366 mutation does not affect shelterin localization.
(A) ChIP was performed on the indicated cell lines 120 hrs. after introduction of Cre. Immunoprecipitated DNA was blotted onto a membrane and probed with the telomere specific γ^{32}-P end-labeled oligonucleotide probe $(CCCTAA)_4$. Antibodies used were TRF2: 1254, TRF1: 644, Rap1: 1252. TIN2: 1447, TPP1: 1151, POT1A: 1220, POT1B: 1223, myc: anti-c-myc, 9E10 (Calbiochem). PI stands for Pre-Immune serum (from animal used to generate Rap1 antibody 1252).
(B) Quantitation of signals in (A).
(C) TRF2 S366 mutation does not affect the chromatin association of TRF2. 120 hrs. after the introduction of Cre, uncloned cell populations expressing the indicated alleles of TRF2 were lysed in buffer containing 150 mM KCl. Chromatin bound proteins were subsequently extracted using 420 mM KCl. The remaining pellet was lysed in Laemmli buffer and sonicated. Lysates were analyzed by western blot with anti-c-myc and anti-γtubulin.

In order to assess the function of TRF2 S366A and TRF2 S366E, the ability of these alleles to stabilize Rap1 was examined after introduction of Cre to remove endogenous TRF2. Western blotting and IF analysis showed that both mutant alleles stabilized Rap1 as efficiently as wildtype TRF2 (Fig. 4-4).

Figure 4-4: TRF2 S366 mutants stabilize Rap1.
(A) MEFs infected with wildtype TRF2, TRF2 S366 mutants, or an empty lentiviral vector were exposed to Cre. 120 hrs. after Cre introduction, cells were harvested and western blot was performed with antibodies against mouse TRF2 (1254) and mouse Rap1 (1252). MEFs infected with vector but not exposed to Cre are included for comparison.
(B) IF was performed on indicated cell lines harvested 120 hrs. after Cre exposure, with anti-c-myc and an antibody against mouse Rap1 (1252).

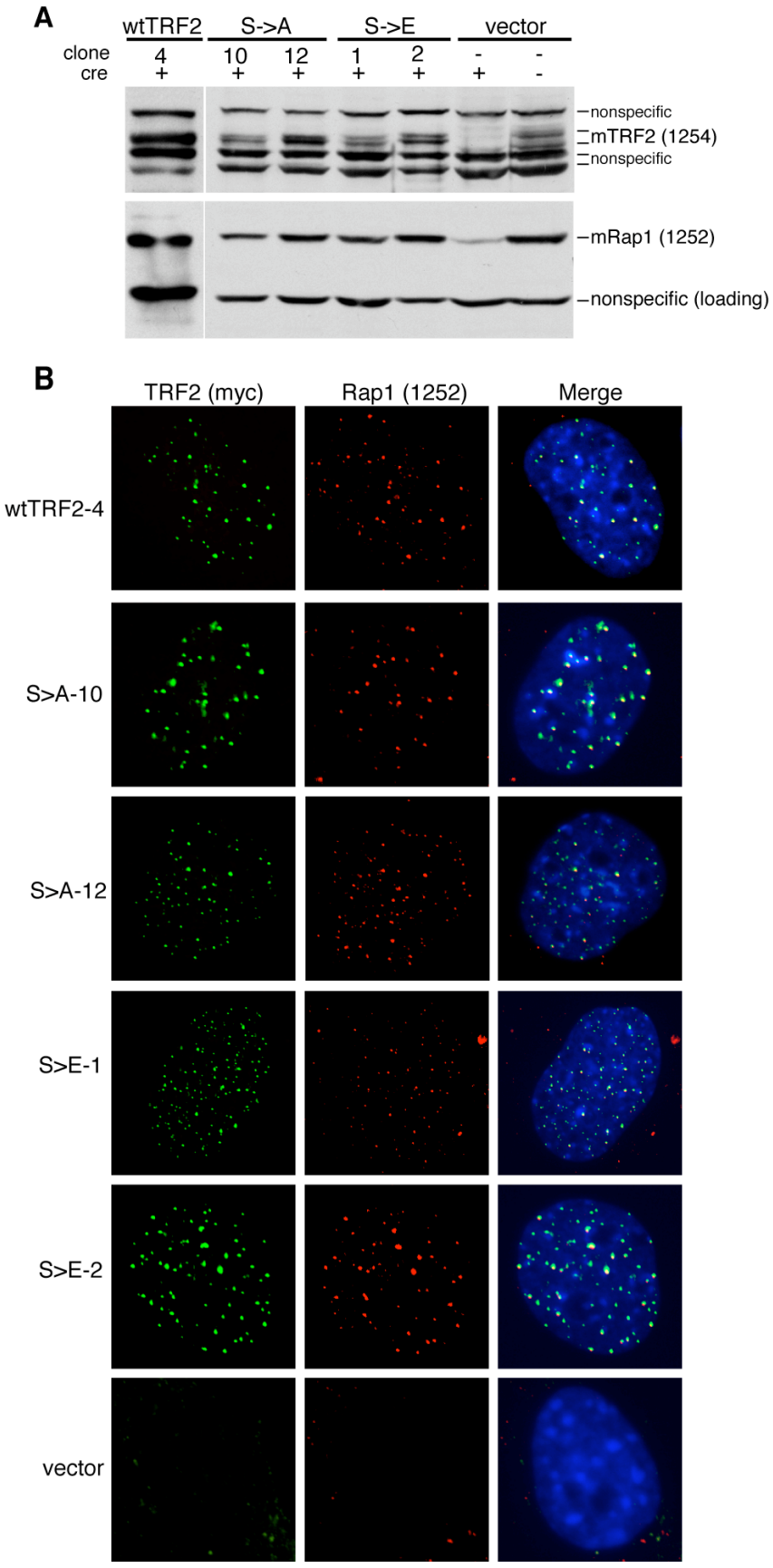
A
wtTRF2
S->A
S->E
vector
clone
cre
4
+
10
+
12
+
1
+
2
+
-
+
-
-
nonspecific
mTRF2 (1254)
nonspecific
mRap1 (1252)
nonspecific (loading)
B
TRF2 (myc)
Rap1 (1252)
Merge
wtTRF2-4
S>A-10
S>A-12
S>E-1
S>E-2
vector

TRF2 S366A and TRF2 S366E prevented telomeres from activating the DNA damage response. Whereas vector-infected cells showed the expected induction of 53BP1 TIFs after exposure to Cre, TIFs did not form in the clones containing TRF2 S366A or TRF2 S366E, as was the case for cells expressing wildtype TRF2 (Fig. 4-5). Cre-treated cells of each of the clonal lines often exhibited several (usually 1-4) 53BP1 foci, but in less 2% of cells did more than two of these foci colocalize with telomeric DNA. Consistent with their lack of a DNA damage response, cells containing mutant versions of TRF2 did not arrest, but grew at a similar rate to cells infected with wildtype TRF2 (Fig. 4-6). There was no evidence for positive selection of cells which had not been exposed to Cre, as expression of mutant alleles was maintained at the same level over time.

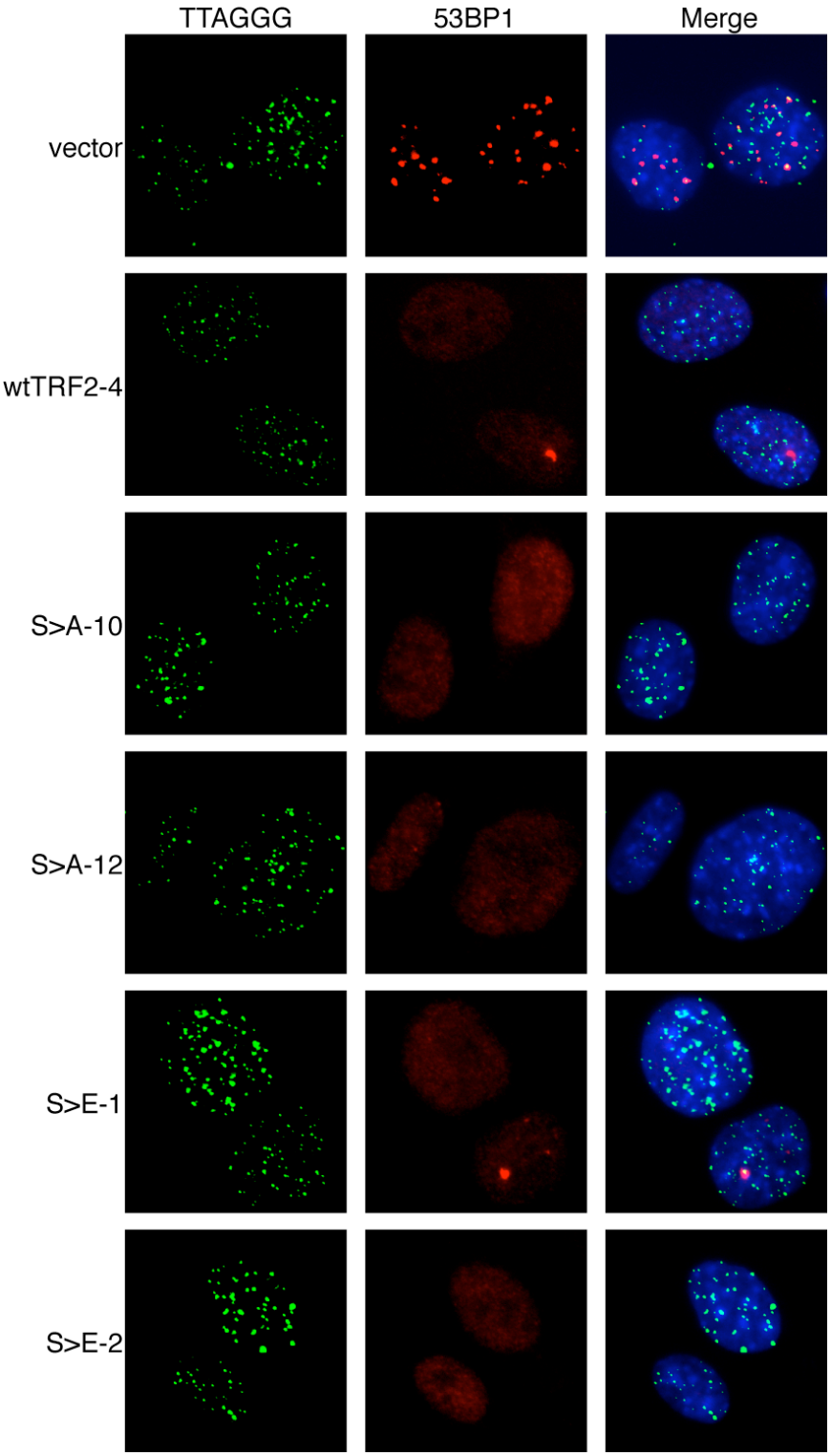

Figure 4-5: TRF2 S366 mutants prevent TIF formation.
120 hrs. after the introduction of Cre, the indicated cells lines were fixed. IF was performed for 53BP1 (Novus) in conjunction with FISH with a PNA probe specific for telomeric repeats. Colocalization of 53BP1 with telomeres in vector cells indicates the presence of TIFs.

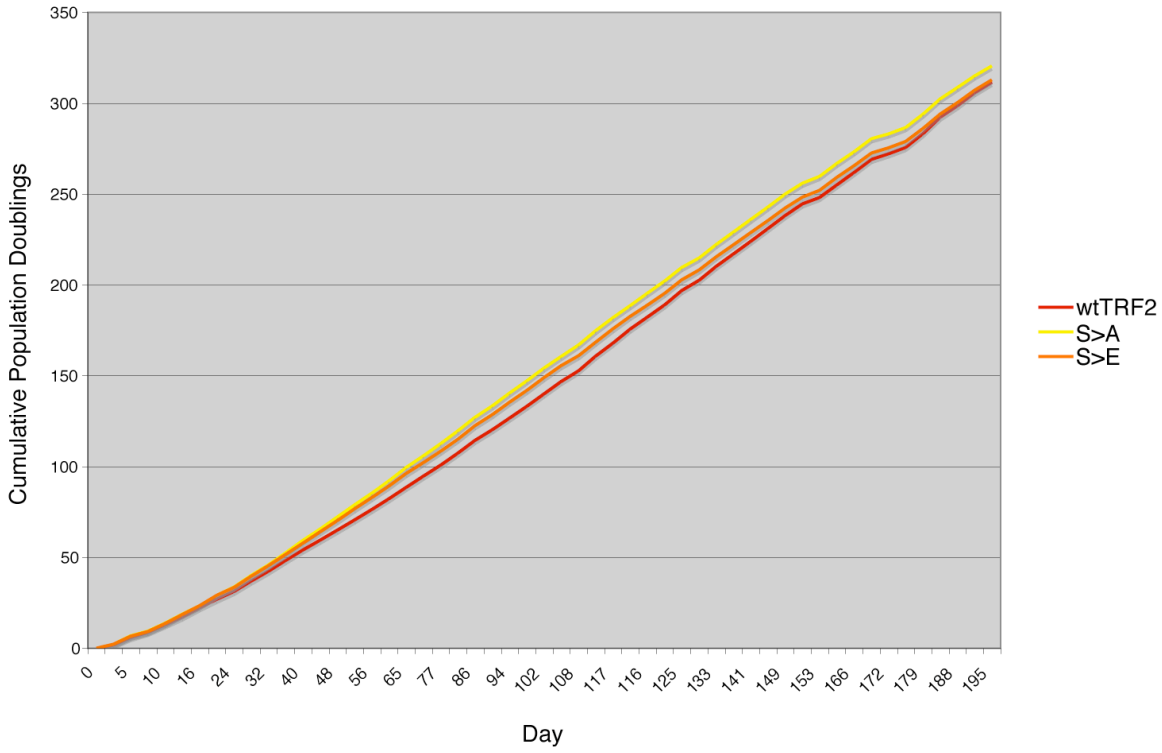

Figure 4-6: MEFs expressing TRF2 S366 mutants grow at a normal rate.
Growth curve of uncloned populations of cells expressing wildtype TRF2 or S366 mutant alleles. Growth curve begins 120 hrs. after the introduction of Cre.

In addition to being proficient in repressing a DNA damage response at telomeres, the TRF2 S366A and S366E alleles prevented unscheduled DNA repair at chromosome ends. Whereas single-stranded telomeric DNA was degraded in vector control cells lacking TRF2, cells containing wildtype TRF2 or the phosphorylation mutants showed no reproducible decrease in the amount of single-stranded DNA signal (Fig. 4-7). Furthermore, telomere fusions were not observed in cells expressing either wildtype TRF2 or either of the phosphorylation mutants. Telomere fusions were readily detected in the vector controls cells by telomeric DNA in-gel hybridization (Fig. 4-7) and on metaphase spreads (Fig. 4-8).

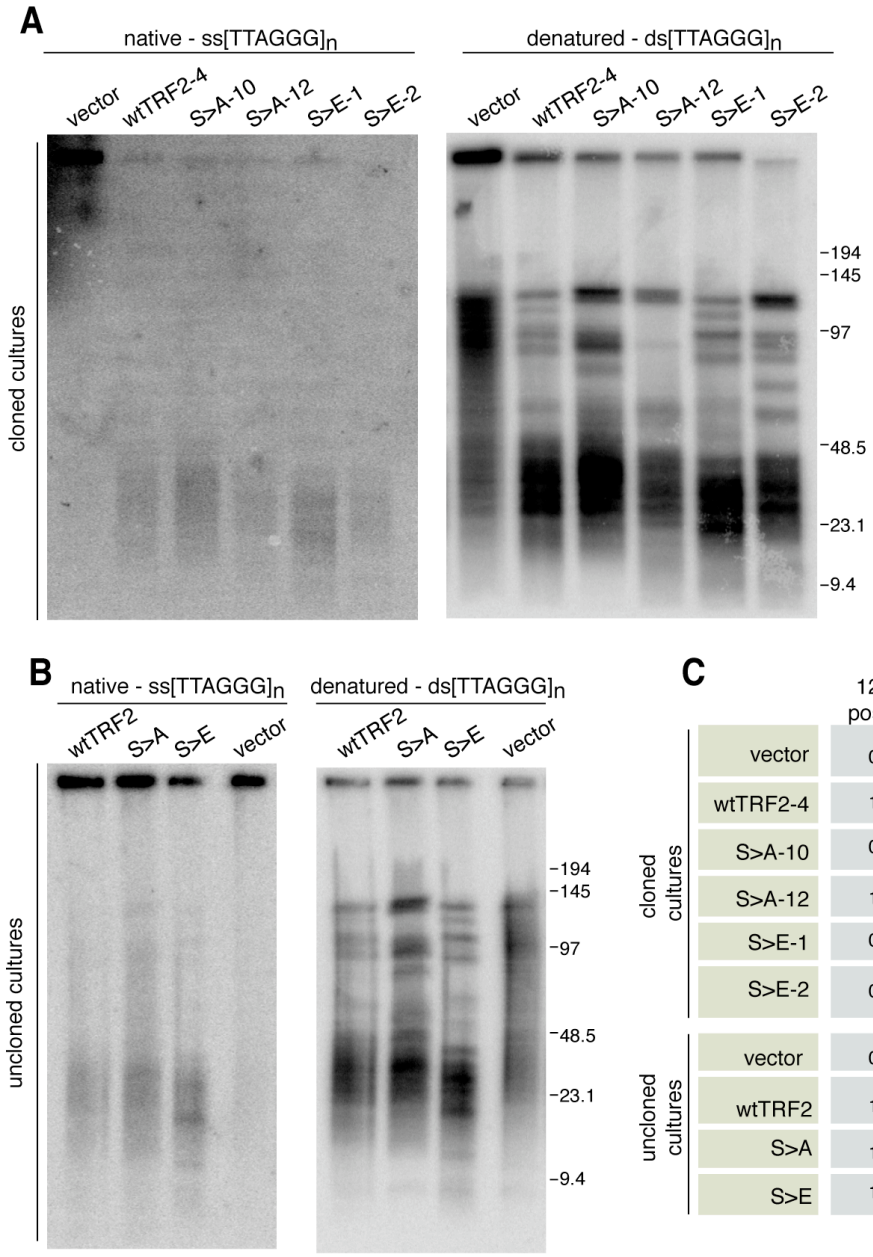

Figure 4-7: TRF2 S366 mutants prevent telomeric overhang loss and fusions.
(A) 120 hrs. after the introduction of Cre, cells were harvested from the indicated clonal cell lines. DNA was digested with MboI restriction endonuclease and subjected to PFGE. In-gel hybridization was performed under native conditions and the telomeric overhang was detected by probing with the γ-^{32}P end labeled oligonucleotide probe $(CCCTAA)_4$ (Left). DNA was denatured *in situ* and reprobed (Right).
(B) 120 hrs. after the introduction of Cre, cells were harvested from the indicated uncloned cell populations and treated as in (A).
(C) Overhang signal was quantitated using ImageQuant software and normalized to the total telomeric signal obtained after denaturation. For each experiment, the normalized value for overhang signal was set to one for cells expressing wildtype TRF2 and relative values for other samples are shown.

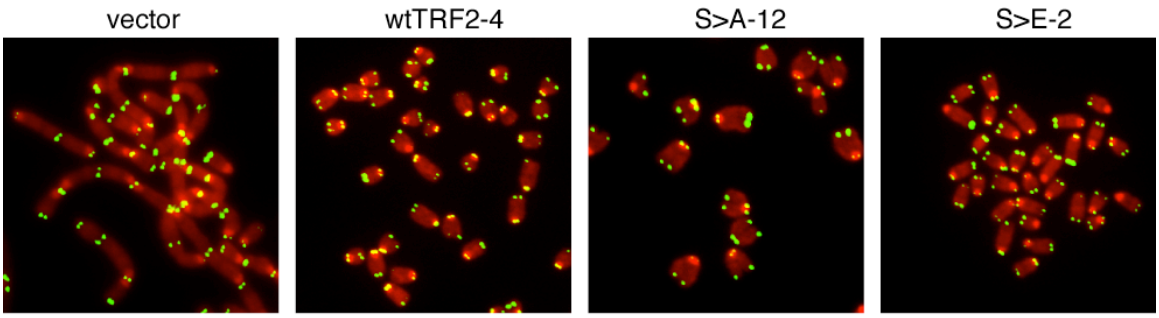

	chromosome ends analyzed	telomere fusions	fraction of telomeres fused (percentage)
vector	300	210	70
wtTRF2-4	2148	0	<0.1
S>A-10	2958	8	0.27
S>A-12	2458	2	<0.1
S>E-1	2250	2	<0.1
S>E-2	2894	0	<0.1

Figure 4-8: TRF2 S366 mutants prevent telomere fusions.
Metaphase spreads of the indicated cell lines were obtained 120 hrs. after the introduction of Cre. FISH was performed with a telomere-specific probe (green) and DNA was counterstained with DAPI (red). Chromosomal fusions containing telomeric DNA at the site of fusion were counted for the indicated cell lines.

The effect of TRF2 S366 mutation on Sister Telomere Exchange

To determine whether phosphorylation of TRF2 on S366 plays a role in the repression of homologous recombination at telomeres, MEFs expressing TRF2 S366A and TRF2 S366E were subjected to chromosome-orientation fluorescent *in situ* hybridization (CO-FISH). CO-FISH, by differentially labeling the parental TTAGGG and CCCTAA strands of sister telomeres in metaphase spreads, allows the detection of telomere sister-chromatid exchanges (T-SCE).

The frequency of sister telomere exchange was found to be between 0.02 and 0.04 exchanges per chromosome end, consistent with what has previously been reported[106]. However, no significant difference was found between the Cre-treated clonal lines expressing wildtype TRF2 and those expressing the phosphorylation mutants (Fig. 4-9).

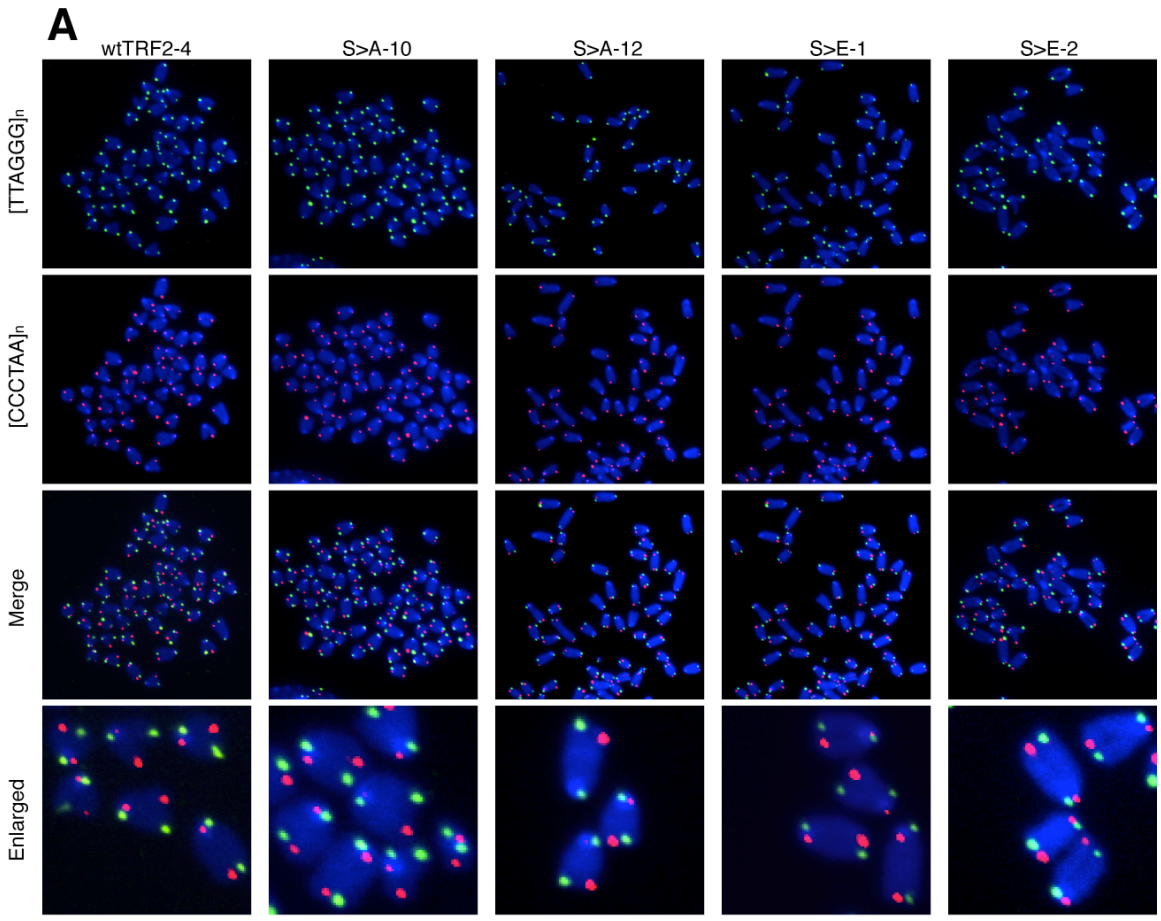

B

Clone	Ends Counted	Exchanges	Exchanges/End
wtTRF2-4	2148	62	0.03
S>A-10	2958	101	0.03
S>A-12	2458	92	0.04
S>E-1	2250	40	0.02
S>E-2	2894	83	0.03

Figure 4-9: S366 mutation does not affect frequency of Telomere Sister Chromatid Exchange.
(A) 120 hrs. after the introduction of Cre, the indicated cell lines were incubated for 14 hrs. in the presence of BrdU and BrdC and metaphase spreads were prepared. Spreads were subjected to CO-FISH with a G-rich telomere specific probe (green) and a C-rich specific probe (red), and stained with DAPI (blue).
(B) Quantification of frequency of Telomere Sister Chromatid Exchange

The effect of TRF2 S366 mutation on telomere length control in mouse cells

To study telomere length homeostasis in the presence of TRF2 S366 mutants, we returned to the uncloned cell populations for each allele of TRF2, thereby avoiding the complications of clonal variations in telomere length. The uncloned cell populations were treated with Cre, and their telomere length was monitored over time. No significant change in telomere length was observed over the first 150 PDs (Fig. 4-10A). Eventually, MEFS expressing TRF2 S366E began to exhibit dramatic telomere lengthening, while in wildtype TRF2 expressing cells, telomere length remained relatively constant (Fig. 4-10A). The telomere lengthening in the presence of TRF2 S366E was apparent both in bands representing individual longer telomeres (indicated by * in Fig 4-10A) and in the bulk population of telomeres between approximately 25 and 50 kb. In the presence of TRF2 S366A, subtle changes in telomere length were observed. Individual longer telomeres (represented by discrete bands of higher MW) slightly decreased in length, while the bulk telomere length population appeared to slightly elongate and become less heterogeneous. Western blotting showed that expression of the introduced alleles was maintained throughout the experiment (Fig. 4-10B). The experiment was repeated and the changes in telomere length observed in the initial experiment were not reproduced (Fig. 4-10C).

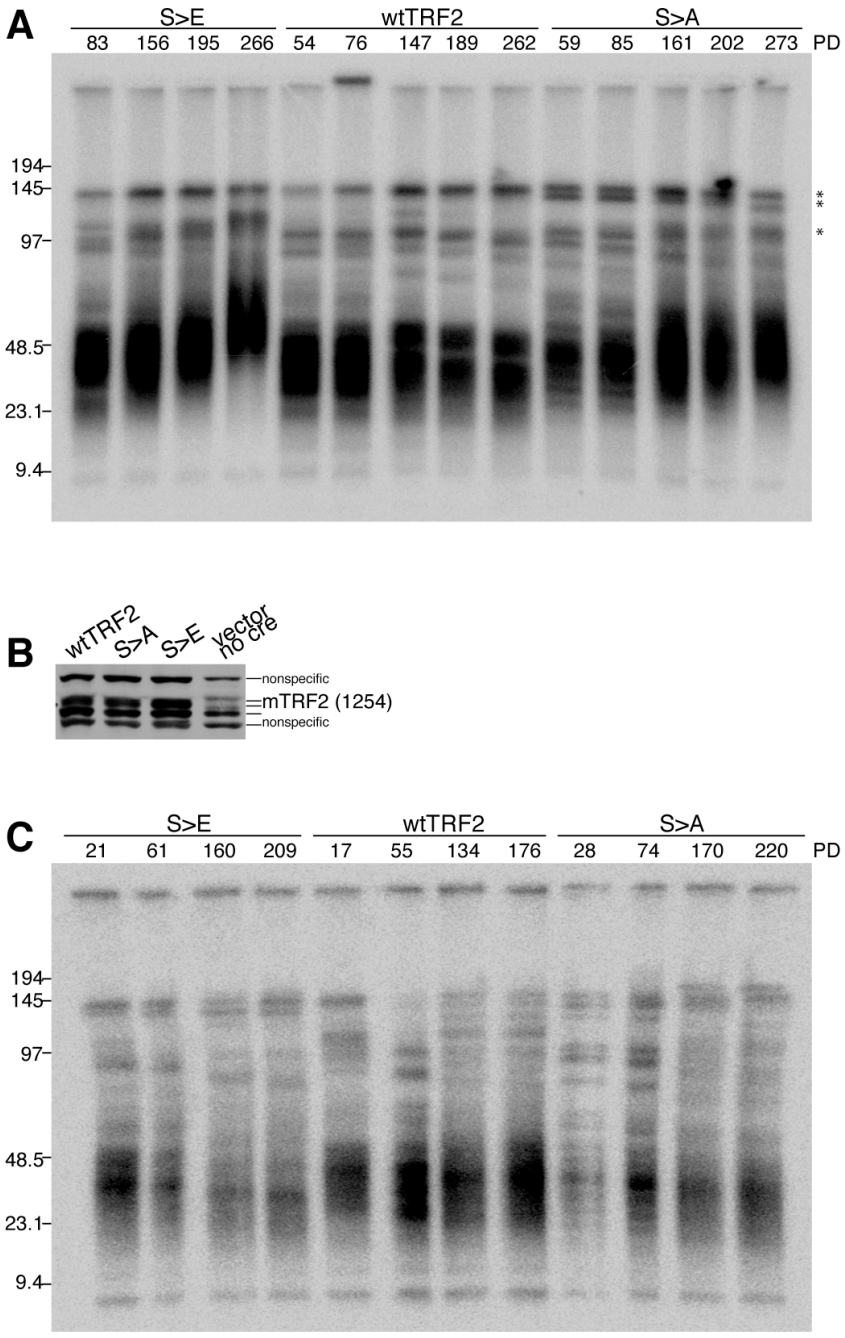

Figure 4-10: Telomere length changes in uncloned populations of cells expressing wildtype TRF2 or S366 phosphorylation mutants.

(A) Uncloned populations of cells expressing wildtype TRF2 or phosphorylation mutants were exposed to Cre (see Fig 4-6 for growth curve) and DNA samples were taken periodically. DNA was subjected to PFGE and telomeres were detected by in-gel hybridization under denaturing conditions with a telomeric probe. Asterisks indicate bands representing individiual high MW telomeres.

(B) Expression of TRF2 alleles is maintained throughout the experiment. Cells were harvested at the termination of the experiment and lysates were analyzed by western blotting with an antibody against mouse TRF2 (1254). Cells infected with vector and not exposed to Cre are included to show levels of endogenous TRF2.

(C) Uncloned populations of cells were again exposed to Cre and telomere length was followed as in (A).

The effect of TRF2 S368 mutation on telomere length control in human cells

The effect of TRF2 S368 mutation on telomere length was also analyzed in human cells, which are a more established system for the study of telomere length regulation than mouse cells. For this purpose, a HeLa subclone (Hela 204) was used with short and stable telomeres, so that telomere length changes could be easily monitored. An shRNA targeting the 5' UTR of TRF2 was used to stably knockdown TRF2 levels to nearly undetectable levels (Fig. 4-11A), and cells were subsequently infected with either wildtype TRF2, TRF2 S368A, TRF2 S368E, or the empty vector. However, after the experiment was finished it was discovered that the construct used to express TRF2 S368E contained a cloning abnormality resulting in the duplication of amino acids 362-374. Cells grew similarly (Fig. 4-11B) and telomere length changes were measured over approximately 80 PDs. As previously observed (Takai and de Lange, unpublished), reduced levels of TRF2 lead to telomere lengthening (Fig. 4-11C). Also as expected, overexpression of wildtype TRF2 shortened telomeres, potentially due to t-loop HR. Interestingly S368A expressing cells and cells expressing the abnormal TRF2 S368E construct did not shorten, suggesting that these mutants are incapable of facilitating t-loop HR. This experiment must be repeated to confirm these findings and also to ensure that all alleles of TRF2 are still expressed at the end of the experiment.

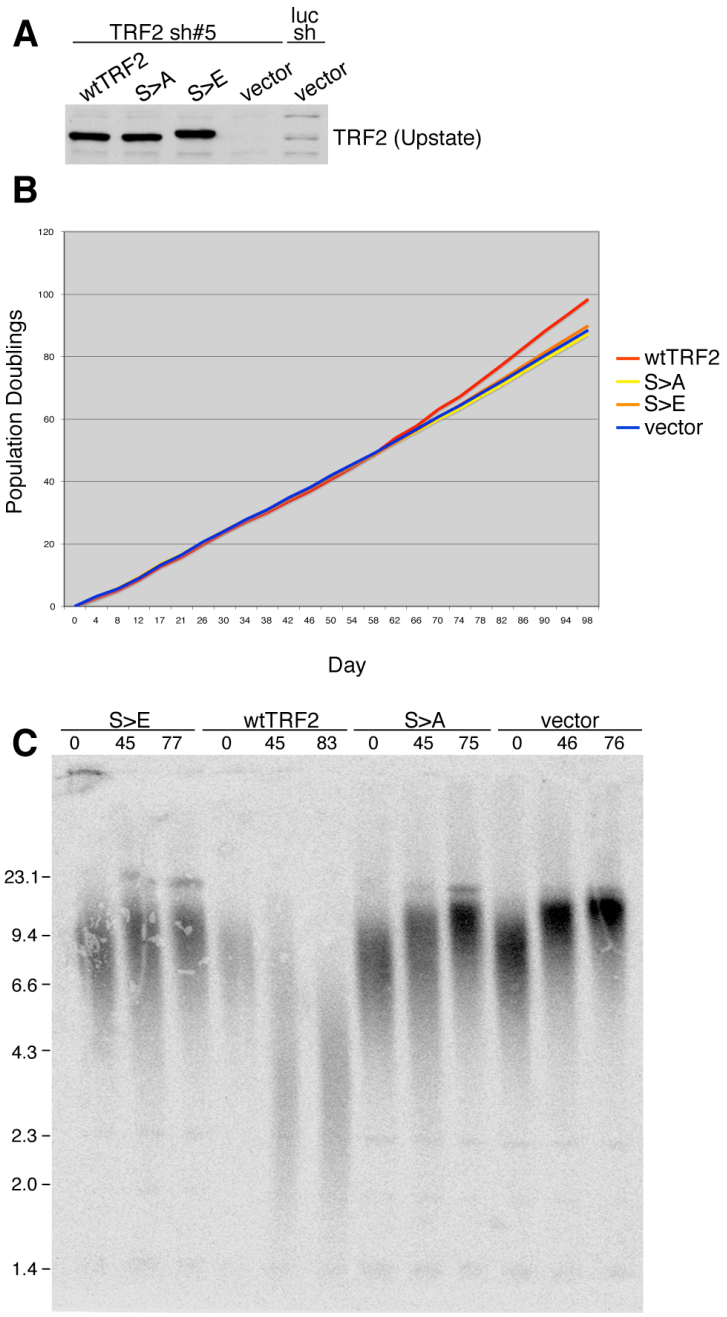

Figure 4-11: Telomere length changes in human cells overexpressing wildtype TRF2 and TRF2 S368 mutants.
(A) HeLa clonal cell line 204 was treated with an shRNA targeting the 5' UTR of TRF2 (sh#5) or an shRNA targeting luciferase (luc sh). Subsequently, cells were infected with wildtype TRF2, phosphorylation mutant alleles, or the pWZL retroviral vector. After 10 days hygromycin selection, cells were harvested and western blot was performed with an anti-TRF2 antibody (Upstate).
(B) Growth curve of Hela 204 cells infected with TRF2 alleles or vector. Growth curve starts 10 days after beginning hygromycin selection.
(C) After hygromycin selection, cells were grown for over 70 PDs and samples were taken periodically. DNA was digested with MboI and AluI and separated on a 0.7% gel. Southern Blot was performed using a telomere-specific probe.

The effect of TRF2 S366 mutation on the telomeric response to replication stress

To determine whether the presence of TRF2 mutated at S366 affected cellular survival under conditions of DNA replication stress, cells expressing wildtype TRF2, TRF2 S366A, or TRF2 S366E, and wildtype MEFs immortalized with SV40 Large T antigen ("Control MEFs") were exposed for 24 hrs. to a low dose (0.3 μM) of the DNA polymerase inhibitor aphidicolin. After the drug was removed, cells were grown in fresh media and survival was determined by colony formation 3-4 days later. Both clonal cell lines expressing TRF2 S366E were much less sensitive to aphidicolin than the control MEFs or the clonal cell lines expressing wildtype TRF2 or TRF2 S366A (Fig. 4-12).

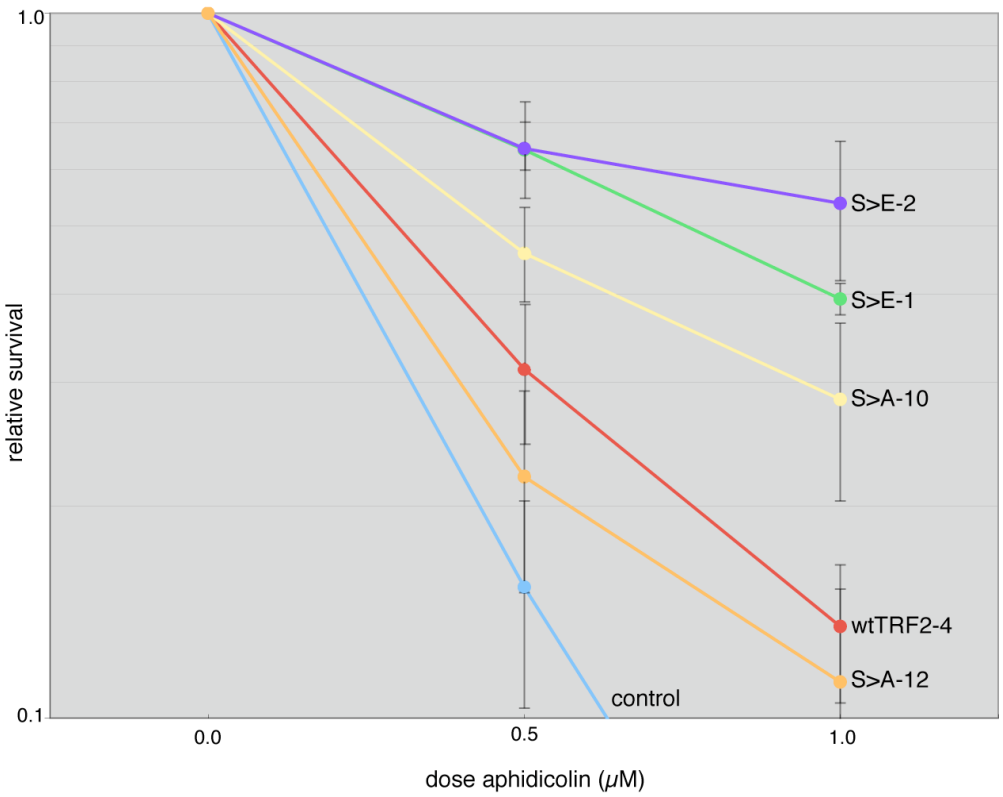

Figure 4-12: Expression of TRF2 with a phosphomimetic mutation at position 366 enhances survival after aphidicolin.
MEFs expressing the indicated TRF2 alleles were infected with the pWZL-Cre retrovirus and selected with hygromycin for seven days. Control cells are MEFs wildtype at the TRF2 locus immortalized with the SV40 Large T antigen. Cells were either untreated or exposed to 0.5 μM or 1 μM aphidicolin. For each experiment, 500 cells per well were plated in triplicate in 6 well dishes, for each dose. After 24 hrs., media containing aphidicolin was removed and cells were grown in fresh media until colony formation was apparent, about 3-4 days. Cells were fixed, stained with Coomassie, and colonies were counted. The average of three wells for each dose was taken. For each experiment, the mean number of surviving colonies at each aphidicolin dose was normalized to mean number of colonies present in the untreated wells. For each cell type, the mean of three independent experiments is shown. Error bars represent standard deviation.

Metaphase spreads were obtained from the control MEFs and the cell lines expressing wildtype TRF2 or the phosphorylation mutants, which had been untreated or treated with 0.3 μM aphidicolin for 24 hrs. As a measure of global genome damage as a result of aphidicolin treatment, chromatid breaks were quantified. Consistent with the survival data, both clonal cell lines expressing

TRF2 S366E exhibited a much smaller induction of chromatid breaks after treatment with aphidicolin, than the control MEFS or the clonal cell lines expressing wildtype TRF2 or TRF2 S366A (Fig. 4-13).

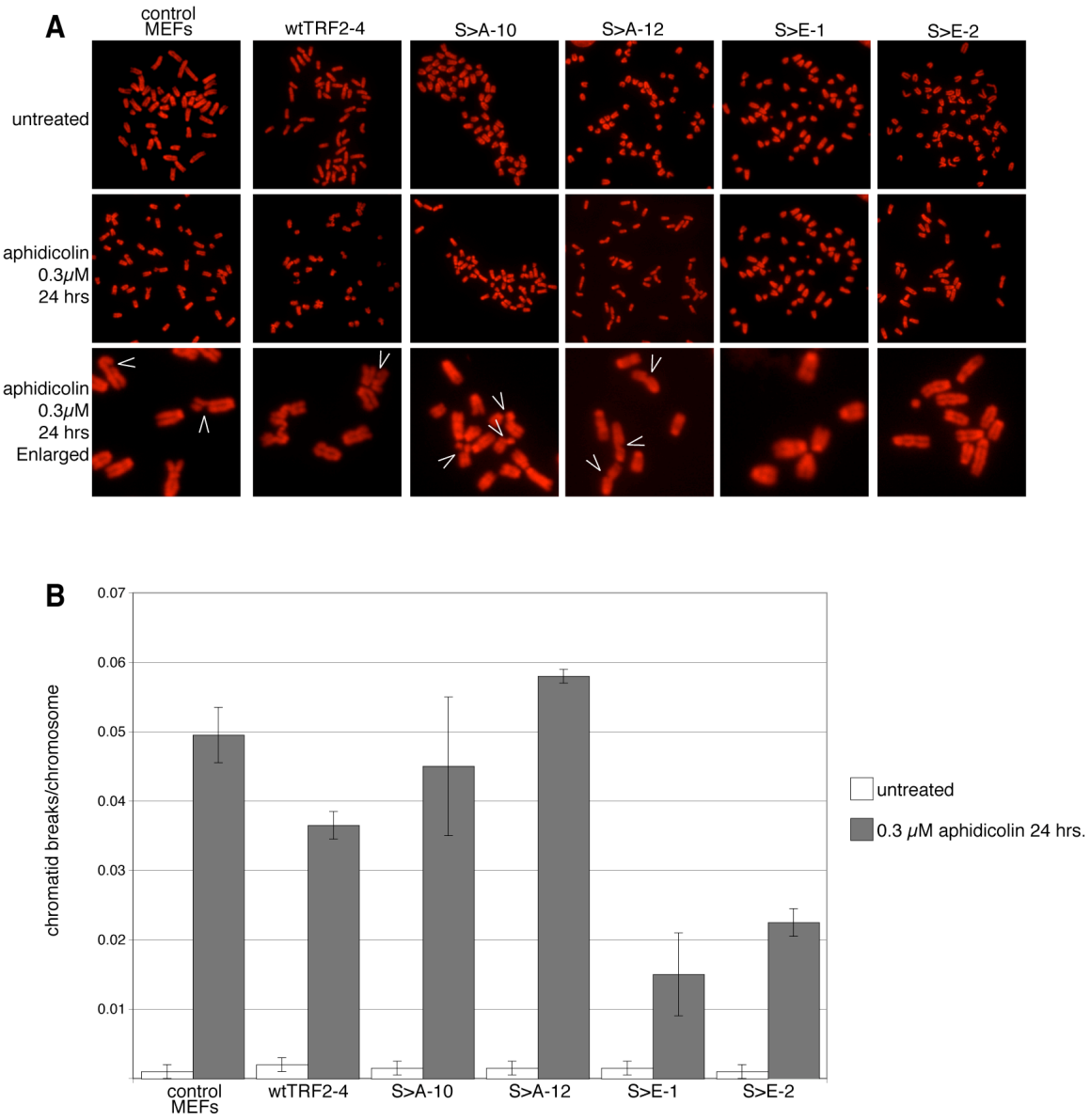

Figure 4-13: TRF2 S366 mutants affect the magnitude of chromatid breakage induced by aphidicolin.
(A) MEFs expressing the indicated TRF2 alleles were infected with the pWZL-Cre retrovirus and selected with hygromycin for seven days. Control cells are MEFs wildtype at the TRF2 locus immortalized with the SV40 Large T antigen. Cells were either untreated or treated with 0.3 μM aphidicolin for 24 hrs. Metaphase spreads were obtained and stained with DAPI (red). White arrows indicate chromatid breaks. (B) Over 1000 chromosomes of each cell type were analyzed for the presence of chromatid breaks in two independent experiments. Error bars represent standard deviation.

Induction of 53BP1 foci was observed in control MEFs and in MEFs expressing TRF2 S366 mutants and co-staining with a telomeric probe revealed that many of the induced foci colocalized with telomeres (Fig. 4-14).

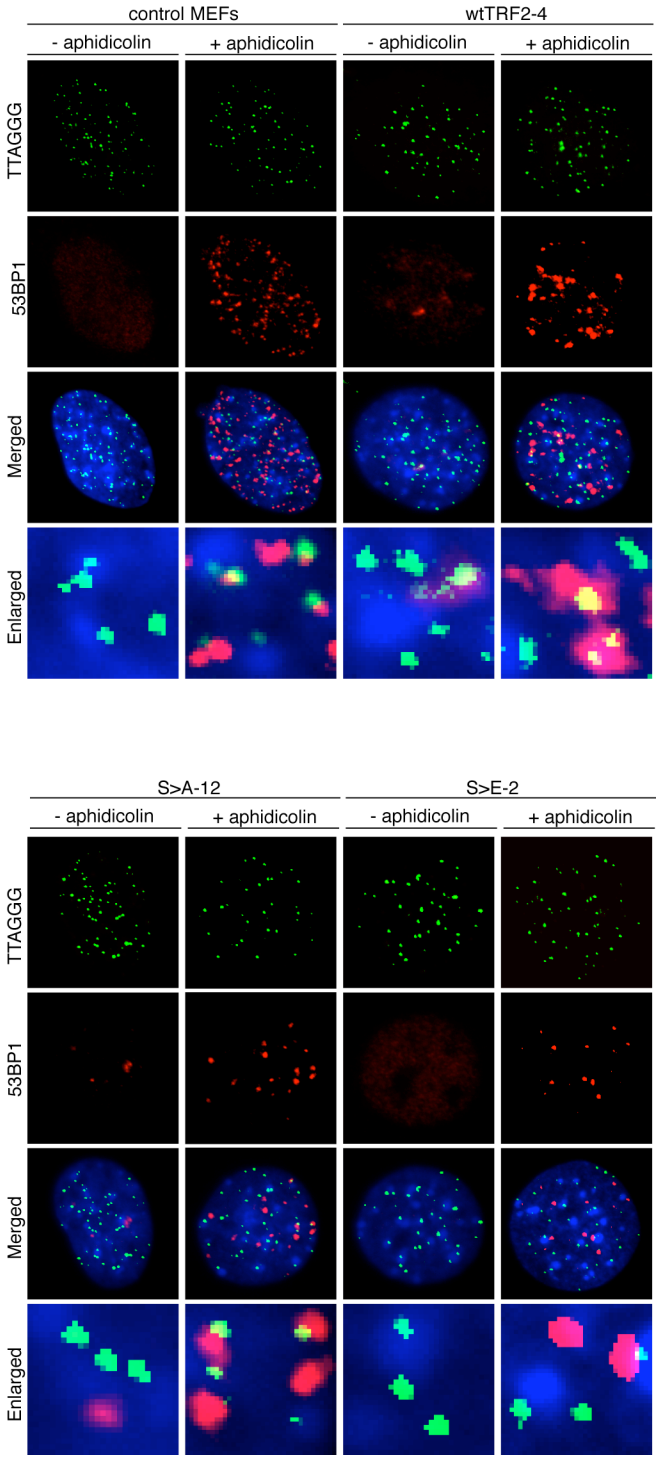

Figure 4-14: Many 53BP1 foci induced by aphidicolin treatment localize to telomeres.
MEFs expressing the indicated TRF2 alleles were infected with the pWZL-Cre retrovirus and selected with hygromycin for seven days. Control cells are MEFs wildtype at the TRF2 locus immortalized with the SV40 Large T antigen. Cells were either untreated or treated with 0.3 μM aphidicolin for 24 hrs. IF was performed with an antibody for 53BP1 (Novus) in conjunction with FISH with a PNA probe specific for telomeric repeats.

However while aphidicolin treatment resulted in approximately 33 53BP1 foci per cell in control MEFs, the same treatment resulted in an average of only 7 53BP1 foci per cell in MEFs expressing S366E (Fig. 4-15A). In control MEFs and MEFs expressing wildtype TRF2 and S366A, a startling percentage, 25-28%, of the induced foci colocalized with telomeres (Fig. 4-15B). A similar result has been observed in human cells (van Overbeek and de Lange, unpublished). Similarly, in MEFs expressing TRF2 S366E, a large fraction of the induced foci colocalized with telomeres, however there was a small but significant reduction in the fraction of 53BP1 foci that localized to telomeres ($p < 0.05$, Student's T test comparing wtTRF2-4 and S>E-2) (Fig. 4-15B).

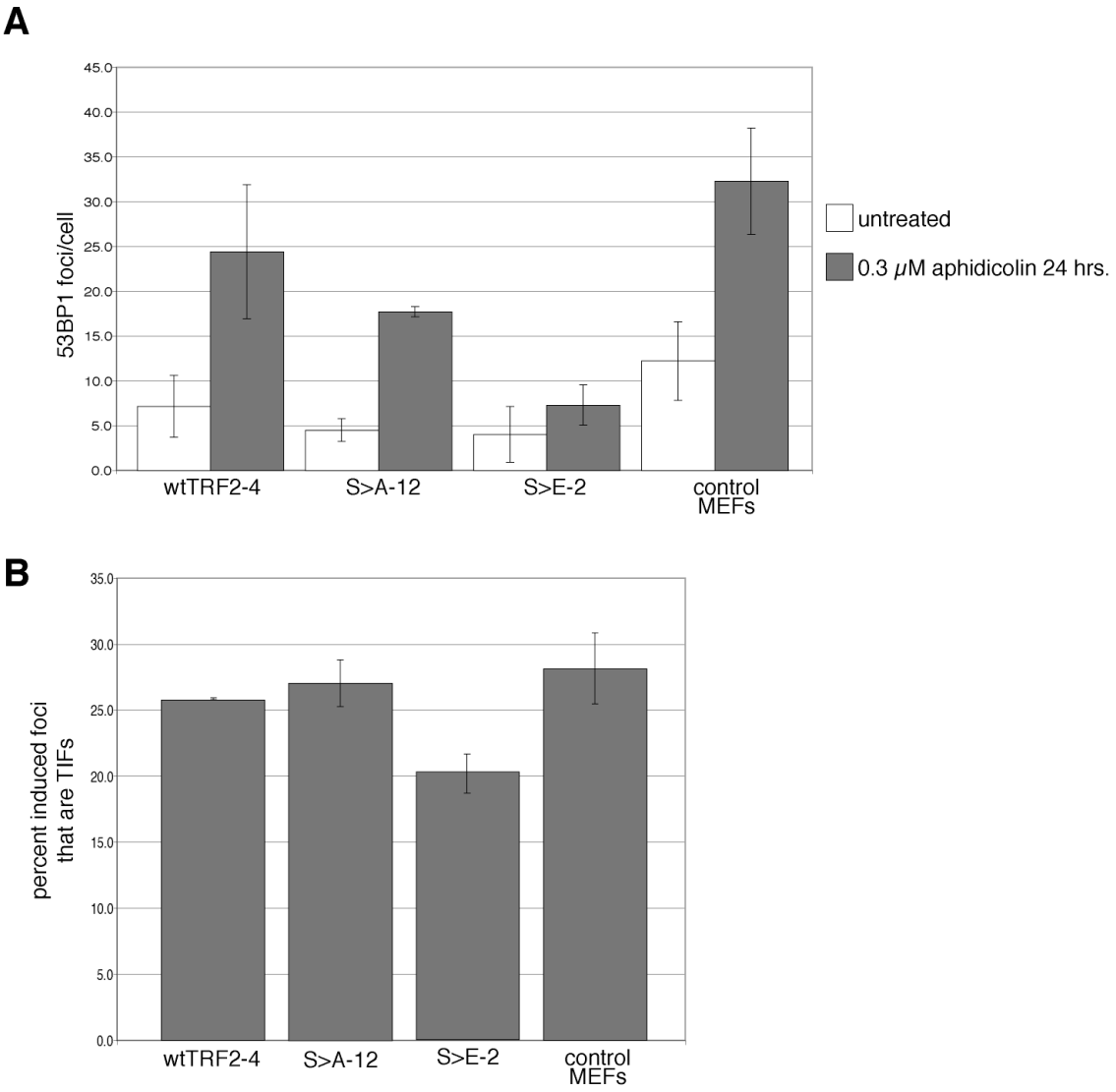

Figure 4-15: MEFs expressing TRF2 containing a phosphomimetic mutation at S366 exhibit fewer 53BP1 foci after aphidicolin treatment, and a smaller percentage of the induced 53BP1 foci colocalize with telomeres.

(A) MEFs expressing the indicated TRF2 alleles were infected with the pWZL-Cre retrovirus and selected with hygromycin for seven days. Control cells are MEFs wildtype at the TRF2 locus immortalized with the SV40 Large T antigen. Cells were either untreated or treated with 0.3 μM aphidicolin for 24 hrs. IF was performed with an antibody for 53BP1 (Novus) in conjunction with FISH with a PNA probe specific for telomeric repeats. For each cell type, over 60 random cells were imaged in two independent experiments. Errors bars indicate standard deviation.

(B) Quantification of 53BP1 foci induced by aphidicolin treatment in (A) which colocalize with telomeric signal. Error bars represent standard deviation.

TRF2 S368 phosphorylation affects the efficiency of the TRF2-TIN2 interaction

In order to determine whether TRF2 S368 phosphorylation status affected the interaction between TIN2 and TRF2, Flag-tagged TIN2 and several myc tagged TRF2 mutants were co-transfected into 293T cells. $TRF2^{\Delta T}$, a TRF2 mutant from which the residues required for *in vitro* TIN2 interaction have been deleted, was included as a negative control. Immunoprecipitation was performed with antibodies against TRF2 and TIN2, and their interaction was analyzed by western blotting with Flag and Myc antibodies. As predicted, $TRF2^{\Delta T}$ no longer interacted with TIN2 (Fig. 4-16A). Reproducibly, immunoprecipitations of TRF2 with a phosphomimetic mutation at S368 (aspartate) contained significantly less TIN2. Conversely, immunoprecipitations of TRF2 containing a glycine at S368 to mimic the constituitively unphosphorylated residue, contained slightly more TIN2. When TIN2 was immunoprecipitated, the same pattern was present but was less pronounced. An important caveat to this experiment is the presence of endogenous wildtype TRF2 in the cell lysates, which is not distinguished from the transfected TRF2 by the antibodies used for immunoprecipitation. Presence of endogenous TRF2 may cause these experiments to underestimate the magnitude of the impact of S368 mutation on the interaction between TIN2 and TRF2.

Because a phosphomimetic mutation at S368 resulted in reduced interaction with TIN2, we sought to determine whether the increased resistance to aphidicolin observed in cells expressing TRF2 S366E was due to decreased

association of TRF2 with TIN2. To this end, we tested the aphidicolin sensitivity of two clonal cell lines expressing mouse TRF2$^{\Delta T}$, a mutant missing the amino acids required for the interaction between TRF2 and TIN2. TRF2$^{\Delta T}$ expressing cells did not exhibit increased resistance to aphidicolin (Fig. 4-16B).

Figure 4-16: A phosphomimetic mutation at position S368 weakens the interaction between TRF2 and TIN2, but expression of a TRF2 mutant lacking the TIN2 interaction domain does not enhance survival in aphidicolin.
(A) Myc-tagged wildtype TRF2 (WT), TRF2 with S368 mutated to a glycine (S>G), TRF2 with S368 mutated to an aspartate (S>D), or TRF2 lacking the TIN2 interaction domain (ΔT) and alleles of TRF2 flag-tagged TIN2 were co-transfected into 293T cells. 48 hrs. after transfection, cells were harvested and TRF2 was immunoprecipitated using antibody 647 and TIN2 was immunoprecipitated using antibody 864. Immunoprecipitates were analyzed by western blot with anti-c-myc and anti-Flag.
(B) MEFs expressing the indicated TRF2 alleles were infected with the pWZL-Cre retrovirus and selected with hygromycin for 7 days. Control cells are MEFs wildtype at the TRF2 locus immortalized with the SV40 Large T antigen. Cells were either untreated or exposed to 0.5μM or 1μM aphidicolin. For each dose, 500 cells per well were plated in triplicate in 6 well dishes. After 24 hrs., media containing aphidicolin was removed and cells were grown in fresh media until colony formation was apparent, about 3-4 days. Cells were fixed and stained with Coomassie and colonies were counted. Mean number of surviving colonies at each aphidicolin dose was normalized to mean number of colonies present in the untreated wells.

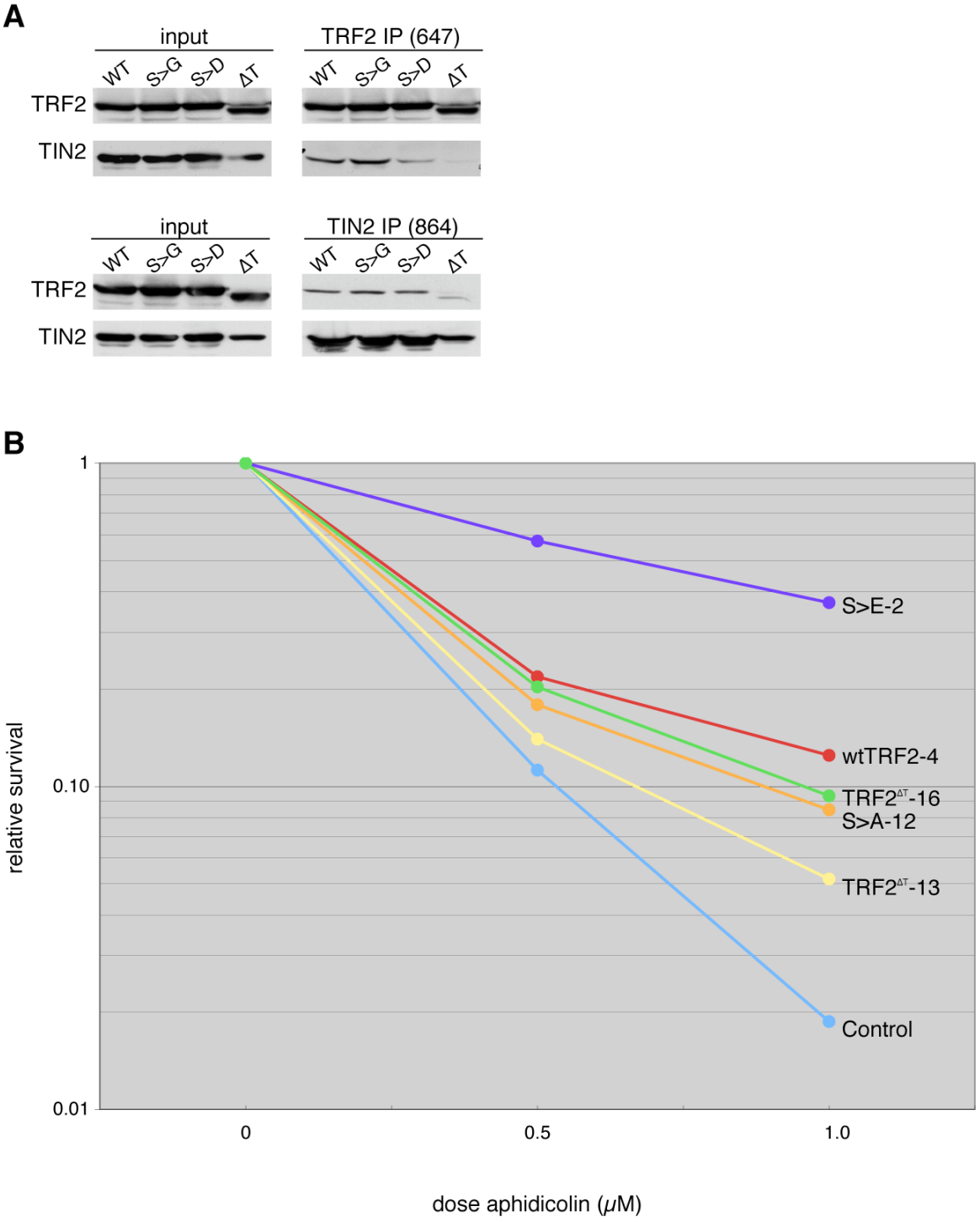
A
input
TRF2 IP (647)
WT
S>G
S>D
ΔT
TRF2
TIN2
input
TIN2 IP (864)
WT
S>G
S>D
ΔT
TRF2
TIN2
B
1
0.10
0.01
relative survival
0
0.5
1.0
dose aphidicolin (μM)
S>E-2
wtTRF2-4
TRF2ΔT-16
S>A-12
TRF2ΔT-13
Control

DISCUSSION

TRF2 containing mutations at the putative ATR phosphorylation site, S366, localized to telomeres and prevented telomeres from being recognized by the DNA damage response. Expression of TRF2 S366A and TRF2 S366E prevented TIF formation, overhang degradation, and telomere fusion. TRF2 S366A and TRF2 S366E expressing cells exhibited normal levels of T-SCE.

Mutation at position 368 seems to be able to affect telomere length regulation in some settings. Dramatic telomere lengthening occurred in MEFs expressing TRF2 S366E during the course of the first long-term telomere length study. However, when the experiment was repeated, the telomere length change was not reproduced. Because culture conditions such as serum composition can affect telomere length (Ye and de Lange, unpublished), it is possible that an unidentified idiosyncrasy in culture condition led to the observed lengthening in one experiment and not the other.

In human cells, initial experiments suggest that overexpression of TRF2 S368 mutants does not result in telomere shortening, as is observed when wildtype TRF2 is overexpressed. Because telomere shortening caused by overexpression of TRF2 is thought to result from t-loop HR[21], S368 mutants may be unable to influence this process.

We have shown that telomeres suffer a disproportionately large percentage of the damage caused when replication forks are stalled with aphidicolin. In wildtype cells, 25% of aphidicolin induced 53BP1 foci colocalized

with telomeres. Surprisingly we found that expression of TRF2 containing a phosphomimetic mutation at position 366 (TRF2 S366E) improved cellular survival after aphidicolin treatment. Expression of TRF2 S366E decreased the total amount of chromatid breaks and 53BP1 foci induced by aphidicolin.

In spite of having a genome-wide effect, several lines of evidence indicate that TRF2S366E is acting through a telomere based mechanism to improve the outcome to aphidicolin. Improved outcome was shown in two separate clonal cell lines where S366E is present at similar levels as endogenous TRF2 (Fig. 4-2A) and localizes primarily to telomeres (Fig. 4-2B). Even though S366E is not present at high levels and it localizes primarily to telomeres, it is still formally possible that its observed effects are due to its ability to titrate an unknown factor away from the rest of the genome. However, it is difficult to propose a factor whose titration away from stalled forks would improve their resolution. In fact, known TRF2 interacting proteins, WRN and BLM, if prevented from localizing to stalled replication forks by TRF2S366E, would be predicted to make the situation worse, not better.

Additionally, in the presence of TRF2 S366E, a small but significant decrease in the percentage of aphidicolin induced 53BP1 foci localized to telomeres. We believe that it is likely that by relieving replication stress specifically at the telomere, S366E improves the outcome of aphidicolin treatment for the whole genome. We propose that the high percentage of stalled forks observed at telomeres after aphidicolin act as a sink for replication fork

processivity factors. This telomeric sink would enhance the effect of aphidicolin on the rest of the genome, increasing the frequency of fork stalling, and also increasing the likelihood that stalled forks will not be reinitiated and form DSBs.

It is possible that TRF2 might facilitate the passage of the replication fork through telomeric DNA by recruiting and/or regulating the RecQ helicases BLM and WRN. TRF2 has been shown to interact with both of these helicases and to be able to stimulate their helicase activity on telomeric DNA substrates. Perhaps S366 phosphorylation regulates TRF2's interaction with these proteins. RecQ helicases may facilitate passage of the replication fork through telomeric DNA by unwinding G-quartet structures. Additionally, RecQ helicases can facilitate re-start of stalled forks by promoting the formation and branch migration of stalled forks (chickenfeet)[139].

Another non-mutually exclusive model for TRF2 S368 phosphorylation to be able to relieve replication stress at the telomere is through its effect on the TRF2-TIN2 interaction: a phosphomimetic mutation at S368 slightly diminished the ability of TRF2 to interact with TIN2. Replication stress at the telomere would locally activate ATR resulting in the phosphorylation of TRF2 on S368. Phosphorylation on S368 is expected to weaken the interaction between TRF2 and TIN2, which could change the stability of the entire shelterin complex, perhaps "loosening" its association with chromatin so that the replication fork can more easily pass. However, expression of an allele of TRF2 which no longer interacts with TIN2 ($TRF2^{\Delta T}$) did not lead to the increased resistance to

aphidicolin seen when TRF2 S366E is expressed, indicating that the increased resistance cannot be simply explained by loss of the TRF2/TIN2 interaction. It is likely that the effect of phosphorylation of S366 relieves replication stress at the telomere through a more subtle and complex mechanism. One possibility is that TRF2 S366 acts as a molecular switch at times of replication stress at the telomere, weakening TRF2's interaction with TIN2, while strengthening TRF2's interaction with WRN or additional protein(s) which facilitate replication fork processivity.

Chapter 5: Discussion

TRF2 CAN INHIBIT ATM ACTIVATION

TRF2 prevents telomeres from activating a DNA damage response that is dependent on the checkpoint kinase ATM. Here we explored one potential mechanism by which TRF2 performs this function. We showed that TRF2 can prevent ATM autophosphorylation on S1981 in response to IR, an event which is critical for the signaling function of ATM, at least in humans. Taken together with the finding that ATM and TRF2 directly interact, this suggests that TRF2 itself can inhibit the activation of ATM.

The mechanism by which TRF2 directly inhibits ATM is currently unknown. In the ATM activation model proposed by Bakkenist and Kastan, an as yet undetermined signal from damaged chromatin causes multimeric ATM to autophosphorylate and dissociate into its active, monomeric form. Bakkenist and Kastan showed that 0.5 Gy IR, which causes approximately 18 DSBs per nucleus, results in the phosphorylation of over 50% of ATM on S1981. To explain this, they propose that DSBs cause a topological change in chromatin which can be detected throughout the nucleus. Alternatively, activation and dissociation of ATM molecules in the immediate vicinity of DNA damage could magnify the signal by phosphorylating additional molecules of ATM, leading to a chain reaction of ATM activation that would ultimately result in a large portion of the nucleoplasmic pool of ATM being phosphorylated. Like ATM, TRF2 exists as

a dimer or higher order multimer, raising the possibility that TRF2 interaction with ATM could act as a clamp to prevent ATM that is activated at the telomere from dissociating and amplifying the DNA damage signal. We attempted to test this model, but were unable to detect multimeric ATM in unperturbed cells.

Another possibility is raised by the finding that a region within the flexible hinge domain of TRF2 strongly resembles the region surrounding S1981 of ATM. When ATM is in its inactive multimeric state, the kinase domain of one ATM molecule interacts with the autophosphorylation site of another molecule. Perhaps the TRF2 hinge domain blocks the phosphorylation of ATM at the telomere by acting as a decoy for the ATM S1981 phosphorylation site. Several lines of evidence argue against this model. TRF2 was shown to interact with amino acids 1439-2138 of ATM, which do not contain its kinase domain. Furthermore, this model predicts that activated ATM would phosphorylate TRF2 on the site which resembles the ATM autophosphorylation site, and it does not appear to do so.

Activation of ATM at telomeres when TRF2 is removed may not only be due to loss of the direct inhibition of TRF2 by ATM. The concomitant removal of the shelterin binding partners of TRF2, Rap1, and TIN2, may also be responsible. So far, siRNA mediated knockdown of Rap1 has not yielded conclusive information regarding the protective function of this protein, and definitive identification of the contribution of Rap1 to telomeric protection awaits the generation of a genetic knockout. However, expression of a TRF2 mutant,

TRF2$^{\Delta T}$, which does not interact with TIN2, results in TIF formation (Donigian et al., in prep.). If the DNA damage response observed when TRF2 is removed from telomeres is due to loss of TIN2, TIF formation induced by TRF2$^{\Delta T}$ expression should be dependent on ATM. Another possibility is that TRF2$^{\Delta T}$ causes a DNA damage response at telomeres because recruitment of TPP1 and Pot1 is diminished in this setting. In this case, the DNA damage response induced by TRF2$^{\Delta T}$ should be dependent on the ATR kinase. Experiments are currently underway to distinguish between these two possibilities.

TRF2 may also prevent ATM activation at the telomere by modifying the chromosome terminus so that it does not resemble a DSB, perhaps by promoting the formation of t-loops. Because TRF2 removal causes degradation of the 3' overhang, it is predicted to disrupt t-loops, making it difficult to discern whether loss of t-loops upon TRF2 inhibition is a cause or a consequence of the resulting DNA damage response. However, when TRF2 is removed in MEFs which also lack the NHEJ component DNA Ligase IV, telomeres activate an ATM dependent damage response, although the 3' overhang is not removed[79]. Whether t-loops still form in this setting would inform on their relative importance in preventing the activation of ATM at telomeres.

The relative importance of the direct inhibition by TRF2 in preventing the activation of ATM at the telomere could be addressed by construction of a mutant of ATM which no longer interacts with TRF2. Fine mapping of the region of ATM which interacts with TRF2 may allow the identification of point mutations

which disrupt the ATM-TRF2 interaction without interfering with the function of ATM in the DNA damage response. Expression of such a separation of function mutant of ATM in AT cells would be expected to rescue the checkpoint functions of ATM in response to IR, but would cause ATM to be activated specifically at telomeres, if direct inhibition of ATM by TRF2 is required. If the DNA damage response at telomeres is absent or not as robust in this setting, as when TRF2 is removed completely, this would suggest that direct inhibition of ATM by TRF2 is not the only mechanism by which TRF2 prevents ATM activation at telomeres.

A NOVEL PHOSPHORYLATION SITE IN TRF2, S368, IS POSITIVELY AND NEGATIVELY REGULATED BY PIKKS

A novel phosphorylation site was detected in TRF2 with an antibody against ATM phosphorylated on S1981, αATM-P. αATM-P detects TRF2 phosphorylated on S368 by western blot when TRF2 is overexpressed by transient transfection in 293T cells. S368 is located in the flexible hinge domain of TRF2, and is conserved immediately adjacent to the TIN2 binding site in both human and mouse, raising the possibility that phosphorylation of TRF2 on S368 may influence the interaction between TRF2 and TIN2. S368 is conserved in all known TRF2 proteins, including chicken and zebrafish, suggesting that it is important for TRF2 function.

The regulation of TRF2 phosphorylated on S368 was studied by overexpressing TRF2 by transient transfection in 293T cells. Because S368

precedes a glutamine (Q) it represents a potential PIKK target. The PIKK inhibitors, caffeine and wortmannin, both diminished TRF2 phosphorylation on S368, indicating that S368 is positively regulated by (a) PIKK(s). Phosphorylation of S368 was increased by UV radiation and HU treatment but not IR, implicating the ATR kinase, the primary PIKK which responds to DNA damage related to replication stress, as a positive regulator of the phosphorylation. This was confirmed by siRNA mediated knockdown of ATR, which reduced TRF2 phosphorylation on S368. Knockdown of ATM and DNA-PK did not affect levels of TRF2 phosphorylated on S368. Unexpectedly, overexpression of mTOR severely abrogated TRF2 S368 phosphorylation, suggesting that mTOR may negatively regulate this phosphorylation event.

To our knowledge, the finding that mTOR may negatively regulate TRF2 phosphorylation on S368 is the only report of a connection between the mTOR pathway and telomere biology. Such a connection is not entirely unexpected, as telomeres are involved in regulating cell proliferation and mTOR controls cell growth and proliferation in response to nutrient availability. Our findings indicate that a systematic evaluation of the role of mTOR in telomere biology is called for. The effect of mTOR on telomere length homeostasis could be analyzed by inhibiting mTOR with rapamycin and following telomere length over time. Similarly, whether mTOR influences telomere protection should be investigated.

Our attempts to find evidence of endogenous TRF2 phosphorylated on S368 largely failed. Using the αATM-P antibody in western blot, we analyzed the

lysates from many cell types in both human and mouse cells for evidence of TRF2 phosphorylated on S368. Treatment of cells with a variety of DNA damaging agents did not induce detectable levels of TRF2 phosphorylated on S368. However, treatment of 293T cells with the alkylating agent MMS did induce a band on the αATM-P western which could potentially represent TRF2 phosphorylated on S368. Unfortunately our attempts to immunoprecipitate TRF2 after MMS treatment to determine whether it was phosphorylated failed. We were also unable to detect evidence of cell cycle specific phosphorylation of TRF2 on S368.

Our inability to detect phosphorylation of endogenous TRF2 on S368 suggests that this form of TRF2 is normally present at extremely low levels; our ability to detect the modification easily when TRF2 is expressed by transient transfection in 293T cells is probably due to the extremely high levels of TRF2 overexpression achieved in this setting. Since our data indicates that TRF2 S368 phosphorylation is induced by replication stress and is positively regulated by the ATR kinase, it is likely that only a small percentage of TRF2, perhaps only those molecules in the immediate vicinity of a stalled replication fork, will be phosphorylated on S368. Recently, a large scale study identified proteins which are phosphorylated in response to IR by immunoprecipitation with SQ/TQ phosphospecific antibodies followed by mass spectrometric analysis[225]. TRF2 was found to be phosphorylated on S368 in response to 10 Gy irradiation, the first instance of ironclad evidence that endogenous TRF2 can be phosphorylated

on S368. Contrarily, we were not able to detect phosphorylation of endogenous TRF2 after IR nor did we see an increase in the phosphorylation of TRF2 expressed by transient transfection in response to IR. In our hands, TRF2 phosphorylation on S368 could only be induced by agents which cause DNA replication stress. The discrepancy may be explained by the finding that IR can secondarily activate ATR at the dose used by Matsuoka et al.[158].

TRF2 S368 MUTANTS LOCALIZE TO TELOMERES AND FULFILL THE MAJOR PROTECTIVE FUNCTIONS OF TRF2

The effect of mutation of S366 on the ability of TRF2 to protect the telomere was analyzed by expressing TRF2 alleles with mutations at S366 in $TRF2^{F/-}$ MEFs and removing endogenous TRF2 with Cre recombinase. TRF2 S366 mutants localized to telomeres and did not grossly impact the telomeric localization of other shelterin components. The phosphorylation mutants suppressed the telomeric deprotection phenotypes of TRF2 loss: TIF formation, growth arrest, overhang removal, and telomere fusions. Furthermore, normal rates of T-SCE were observed in cells expressing TRF2 S366 mutants, indicating that the mutants protect telomeres from this form of homologous recombination. However, loss of TRF2 only causes increased rates of T-SCE when Ku is also deficient[106], so the effect of TRF2 S366 mutants on T-SCE should also be investigated in the Ku null setting.

TRF2 S368 PHOSPHORYLATION AND TELOMERE LENGTH CONTROL

To study telomere length homeostasis in the presence of TRF2 S366 mutants, uncloned cell populations of $TRF2^{F/-}$ MEFs expressing S366 mutants were exposed to Cre, and their telomere length was monitored over time. The first time this experiment was performed, striking telomere elongation was observed in the presence of TRF2 containing a phosphomimetic mutation at position 366 (S366E). However, when the experiment was repeated, the telomere length changes observed in the initial experiment were not reproduced and telomere length in each cell population was relatively stable. It is possible that an unidentified idiosyncrasy in cell culture conditions led to the observed telomere lengthening in one experiment and not the other. It should be noted that the role of TRF2 and other shelterin components in telomere length regulation in mouse cells has not been studied to date. Therefore, there is little knowledge on the behavior of MEF telomeres and effects of growth conditions on their dynamics.

The effect of S366 mutation on telomere length was also examined in human cells, which are a more established system for the study of telomere length regulation than mouse cells. While overexpression of wildtype TRF2 caused the expected rapid telomere shortening, surprisingly, expression of TRF2 S368 mutants did not. However, this experiment has only been performed once and it was also subsequently discovered that the construct used to express TRF2 S368E contained a cloning abnormality resulting in duplication of amino acids

362-375. Telomere shortening due to overexpression of wildtype TRF2 may occur by t-loop HR; our initial results suggest that TRF2 S368 mutants may be unable to influence this process. T-loop HR requires the Mre11 complex member Nbs1, raising the possibility that the observed inability of the S368 mutants to promote t-loop HR is due to an impaired interaction with the Mre11 complex. We have attempted to test the effect of mutation of S368 on the interaction between TRF2 and the Mre11 complex, however difficulties in detecting the interaction at all have prevented us from doing so. WRN and BLM are also TRF2 interacting partners which could potentially be involved in the promotion of t-loop HR by TRF2. However, it is unlikely that a decreased interaction between TRF2 and WRN is responsible for the inability of TRF2 S368 mutants to influence t-loop HR, because t-loop HR induced by TRF2$^{\Delta B}$ expression was unaffected by WRN deficiency (Wang and de Lange, unpublished).

Finally, the effect of ATR deficiency on telomere length homeostasis should be investigated. No data is currently available regarding telomere length in the absence of ATR, largely because loss of ATR function is incompatible with life[228]. However, the existence of Seckel Syndrome, a disease in which patients have low levels of functional ATR due to a mutation that affects splicing efficiency[252] indicates that it should be possible to severely deplete ATR protein by shRNA mediated knockdown without killing cells, and telomere length could be studied in this setting.

TELOMERES ARE UNUSUALLY SENSITIVE TO REPLICATION STRESS

Unexpectedly, telomeres suffer a disproportionately large fraction of the damage caused when replication forks are stalled with aphidicolin. In control MEFs, over 25% of the 53BP1 foci induced by aphidicolin treatment colocalize with telomeric DNA. Similar results have been obtained when human cells are treated with aphidicolin (van Overbeek and de Lange, unpublished). Impaired replication fork passage through the telomere could be due to several factors (Fig. 5-1). As the fork progresses through telomeric DNA, and single-stranded DNA forms, G quadruplex structures may form on the G rich strand. A replication block of this nature is expected to lead to uncoupling of replicative helicases and polymerases, exposure of large amounts of single-stranded DNA, and activation of the ATR checkpoint pathway. A second possibility is that shelterin itself acts as a barrier to the passage of the replication fork, and may need to be removed or modified in order for the fork to pass. If shelterin does hinder the passage of the replication fork, it may function in a similar manner to the RFBs formed within rDNA repeats of budding yeast by the binding of the Fob1 protein (discussed in the introduction to Chapter 4). This type of replication fork blockage does not lead to the generation of large amounts of single-stranded DNA[246] and does not appear to require the ATR pathway for fork stabilization[247]. Consistent with non-reliance on the ATR pathway, which acts to prevent recombination at stalled replication forks, introduction of a RFB into an ectopic site in the *S. pombe* genome led to increased rates of intrachromosomal recombination[247].

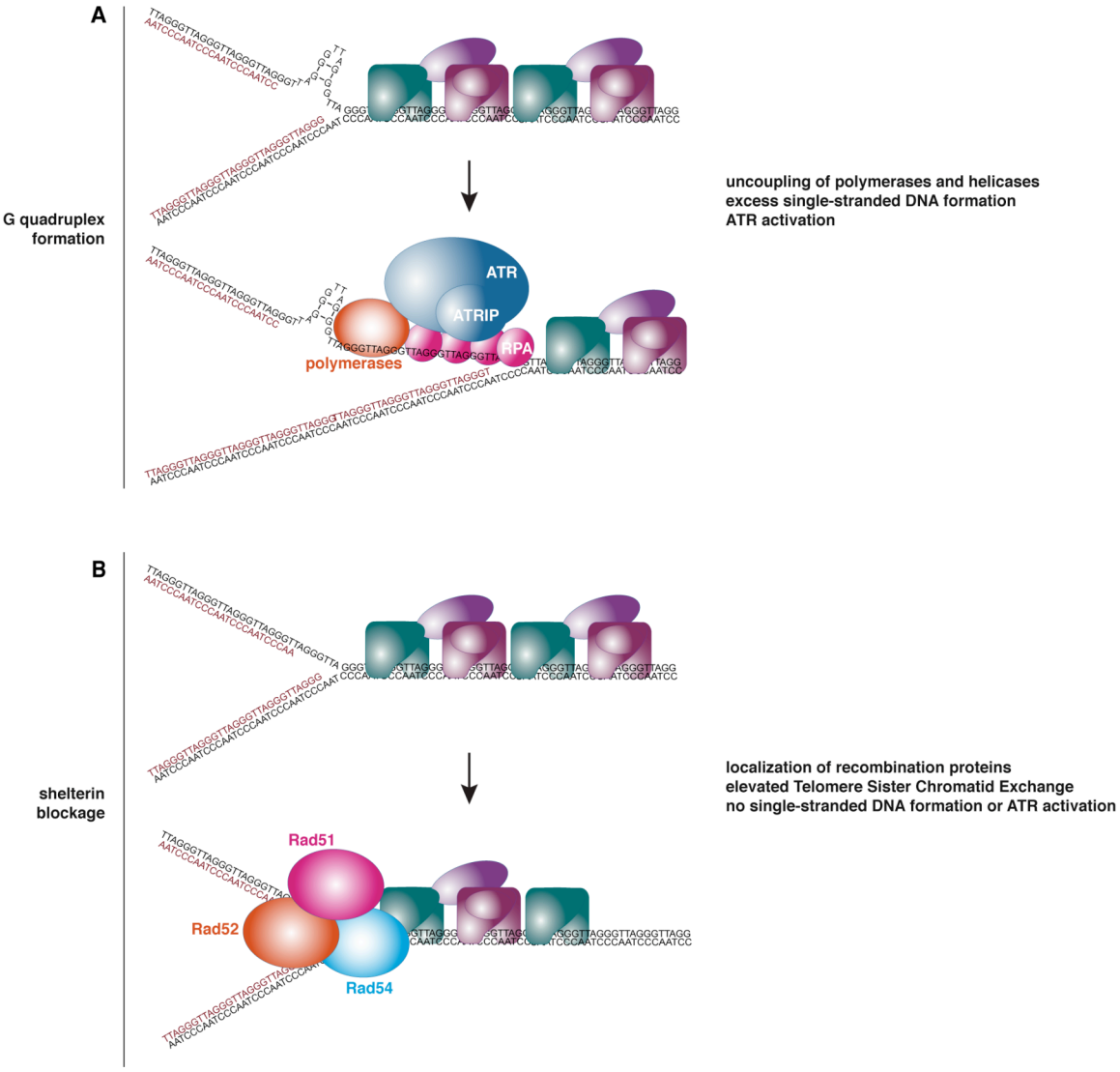

Fig. 5-1: Two models for replication fork hindrance in telomeric DNA
(A) G quadruplex formation on the G rich strand would be expected to cause stalling of the replicative polymerases on the lagging strand. Continued unwinding by the replicative helicases would lead to the creation of single-stranded DNA which can be bound by RPA and activate the ATR checkpoint pathway. (B) Blockage of the replication fork by shelterin is not expected to lead to the generation of single-stranded DNA and the activation of the ATR checkpoint pathway. In a poorly understood process, this type of proteinacious replication block leads to increased recombination at the stalled fork.

To distinguish between these two possibilities for the basis of the replication sensitivity of telomeres, recombination at telomeres after aphidicolin treatment could be examined. If the telomeric sensitivity to replication stress is due to Q quadruplexes leading to the uncoupling of replicative helicases and

polymerases, the ATR pathway would be activated and downregulate recombinogenic events at telomeres. If shelterin is the primary culprit, elevated levels of recombination at telomeres would be expected. Also in this case, overexpression of shelterin would be expected to increase the sensitivity of telomeres to aphidicolin and increase levels of telomeric recombination events.

In human cells, aphidicolin treatment leads to an increased frequency of T-SCE detected by CO-FISH (van Overbeek and de Lange, unpublished) indicating that collapsed forks within telomeres are repaired by HR between sister chromatids and suggesting that shelterin is at least partially responsible for the hindrance of replication forks in telomeric DNA. It remains to be determined whether a similar outcome occurs in mouse cells. However, even if the elevated levels are of HR also occur at mouse telomeres after exposure to aphidicolin, it is impossible to rule out a contribution of G quadruplex formation to the aphidicolin sensitivity of telomeres. This would need to be investigated more directly by examining single-stranded DNA formation and the activation of the ATR pathway specifically at telomeres after aphidicolin treatment. Furthermore, if the aphidicolin sensitivity is due to G quadruplex formation, overexpression of the RecQ helicases WRN and BLM would be predicted to ameliorate the sensitivity, while their genetic deletion would exacerbate it. We have shown that expression of an allele of TRF2 containing a phosphomimetic mutation at a site known to be positively regulated by ATR, partially relieves replication stress induced by aphidicolin at the telomere. This finding is strongly suggestive that the ATR

pathway is active at telomeres under conditions of replication stress, and that an ATR dependent pathway is at least partially responsible for the elevated sensitivity of telomeres to aphidicolin.

Our findings have shown that telomeres are exquisitely sensitive to replication stress induced by aphidicolin. However, aphidicolin has been used to synchronize cells and study telomeres during specific phases of the cell cycle. For example, it was shown in aphidicolin synchronized cells that several factors indicative of DNA repair activities and replication fork restart, including Rad1 and Rad17, localize to telomeres during S phase[20]. These findings should be interpreted with caution, as they may be a result of aphidicolin induced damage and not representative of normal replication of telomeres during S phase, as the authors have surmised. Alternative methods of cell synchronization that do not rely on drugs which cause replication stress, such as centrifugal elutriation and contact inhibition and release, should be employed when possible.

TRF2 PHOSPHORYLATION ON S366 MAY RELIEVE REPLICATION STRESS AT THE TELOMERE

Because phosphorylation of TRF2 on S368 is mediated by ATR and is induced by replication stress, we analyzed the effect of TRF2 S366 mutants on the telomeric response to replication stress. Surprisingly, we found that expression of TRF2 containing a phosphomimetic mutation at position 366, TRF2 S366E, improved cellular survival after aphidicolin treatment. We also found that

cells expressing TRF2 S366E had fewer chromatid breaks and 53BP1 foci after treatment with aphidicolin.

In spite of having a genome wide effect, several lines of evidence indicate that TRF2 S366E mitigates the deleterious effects of aphidicolin treatment by relieving replication stress at the telomere. Increased survival and decreased chromatid breaks and 53BP1 foci were demonstrated in two independent clonal cell lines. In both cell lines TRF2 S366E is expressed at similar levels as endogenous TRF2 and localizes primarily to telomeres. Additionally, in the presence of TRF2 S366E, the percentage of aphidicolin induced 53BP1 foci which localized to telomeres was decreased by a small but significant amount. We believe it is likely that by relieving replication stress specifically at the telomere, TRF2 S366E improves the outcome of aphidicolin treatment for the whole genome. We propose that the great number of stalled forks at telomeres caused by aphidicolin treatment acts as a sink for replication fork processing factors. This telomeric sink would enhance the effect of aphidicolin on the rest of the genome, increasing the frequency of fork stalling, and also increasing the likelihood that stalled forks will not be reinitiated, and so will form DSBs. If this is true, factors involved in sensing and processing stalled replication forks including ATR, ATRIP, Rad17, the 9-1-1 complex, WRN, and BLM, should be abundant at telomeres after aphidicolin treatment. Furthermore, cells with shorter telomeres should exhibit enhanced survival after aphidicolin treatment, compared with cells with longer telomeres.

At least two factors may contribute to poor replication fork processivity in telomeric DNA: the tendency of the G rich strand to form G quartets when single-stranded and the potential of shelterin binding to hinder the passage of the replication fork. Phosphorylation of TRF2 on S368 could potentially address both of these issues. For example, phosphorylation of S368 could allow TRF2 to bind and recruit a factor which resolves G quartets. Excellent candidates for such a factor are the RecQ helicases, WRN and BLM, known interacting partners of TRF2, which can resolve G quartets and also may play a role in the reinitiation of stalled replication forks. Secondly, phosphorylation of TRF2 on S368 could modify the conformation of shelterin so that the replication fork can more easily pass through telomeric DNA. We have demonstrated that a phosphomimetic mutation at position 368 decreases the TRF2-TIN2 interaction. Because TIN2 also interacts with TRF1, decreased interaction with TRF2 is not expected to result in loss of TIN2 at telomeres. Accordingly, ChIP data indicates that TIN2 is not significantly decreased at telomeres in the presence of TRF2 S366E. However, a weakened interaction between TRF2 and TIN2 has the potential to affect the conformation of the entire shelterin complex, because in addition to TRF2, TIN2 binds TRF1 and TPP1. Therefore, phosphorylation of TRF2 on S368, by weakening the interaction between TIN2 and TRF2, could “loosen” the conformation of the shelterin complex, allowing the replication fork to more easily pass.

If expression of TRF2 S366E relieves replication stress at the telomere, expression of TRF2 S366A is expected to heighten the sensitivity of telomeres to replication stress. For example, in the models discussed above, TRF2 S366A would be expected to exhibit reduced interaction with RecQ helicases and increased binding with TIN2. However, in general, we observed that expression of TRF2 S366A did not greatly alter telomeric sensitivity to replication stress. It is possible that under conditions of replication stress, several components of shelterin are phosphorylated by ATR and act in concert to relieve replication stress at the telomere. This would reduce the impact of mutation of any single site within shelterin. In fact, there are conserved potential PIKK targets (SQ/TQ motifs) in many shelterin componenets including TRF1, Rap1, and TIN2. Exploration of the regulation of the phosphorylation of these additional sites and their role in the replication of telomeric DNA is of immediate interest.

PHOSPHOSPECIFIC ANTIBODIES DIRECTED AGAINST SQ/TQ MOTIFS HAVE A TENDENCY TO CROSS-REACT WITH PHOSPHOPROTEINS OTHER THAN THEIR INTENDED TARGETS

In the course of our studies, we have documented several instances where antibodies targeting phosphorylated SQ/TQ motifs within specific proteins cross-react with phosphoproteins other than their intended targets. By western blot, the antibody targeting ATM phosphorylated on S1981, αATM-P, detects TRF2 phosphorylated on S368 and at least one other protein that is

phosphorylated in response to DNA damage. Furthermore, two antibodies targeting different SQ/TQ motifs in TRF2 detect a protein other than TRF2 in DNA damage foci. Recently it was shown that SQ/TQ specific antibodies readily immunoprecipitate phosphoproteins other than their intended targets[225]. These findings indicate that antibodies against phosphorylated SQ/TQ motifs should be used with caution and stringent controls are required to confirm the identity of the detected protein. Additionally, studies which have utilized this type of antibody need to be re-evaluated to consider the possibility of cross-reaction.

Materials and Methods

Cell culture

IMR90 primary lung fibroblasts (ATCC), HeLa subclones 1.3 and 204, $p53^{-/-}$ and SV40 transformed MEFs, 293T cells, Phoenix ecotropic and amphotrophic packaging cell lines, and GM847 cells were grown in DMEM supplemented with 100 U/ml penicillin (Sigma), 0.1 μg/ml of streptomycin (Sigma), 2.0 mM L-glutamine (Invitrogen), 0.1 mM non-essential amino acids (Invitrogen), and 10% Fetal Bovine Serum. BJ fibroblasts (Clontech) were grown in 4:1 DMEM/199 media supplemented with 15% fetal bovine serum, 100 U/ml penicillin (Sigma), 0.1 μg/ml of streptomycin (Sigma), 2.0 mM L-glutamine (Invitrogen), 0.1 mM non-essential amino acids (Invitrogen), and 1 mM sodium pyruvate (Sigma). All cells were grown at 37°C, 5% CO_2, and 95% relative humidity. Cells were passaged by pre-rinsing with room temperature Trypsin-EDTA (Gibco, 0.25%) followed by incubation in Trypsin-EDTA for 2-5 min. Cells were seeded as indicated in text. Cells were counted with a Counter Counter Z1 Particle counter. For growth curves, 300,000 cells were plated on a 10 cm dish and grown for 72 hrs. Cells were harvested using trypsin and recovered in 4 ml of media, and the total cell number was determined. 300,000 cells were plated in a new 10 cm dish. At specified times, extra cells were plated in order to obtain protein and DNA samples for analysis. Population doublings were determined by the following formula: PD = original PD + [ln(# cells at passage/#cells seeded)/ln(2)] using Excel.

Radiation and drug treatment of cells

For γ-irradiation, cells were seeded in 6 cm culture dishes and exposed to a Ce^{137} source. Cells were allowed to recover in the incubator for the indicated amount of time before harvesting. For UV radiation, media was removed and reserved. Cells were subjected to the indicated dose of UV radiation in a Stratalinker 1800 (Stratagene). Reserved media was added back to cells and cells were allowed to recover in the incubator for the indicated amount of time before harvesting. Cells were treated with the indicated amounts of aphidicolin (Sigma), caffeine (Sigma), wortmannin (Sigma), Okadaic Acid (Sigma), MMS (Sigma), hydroxyurea (Sigma), and rapamycin (Calbiochem) for the indicated amounts of time. After treatment, MMS was neutralized with an equal volume of 10% sodium thiosulfate for 5 min.

Calcium phosphate transfection of 293T cells

One day prior to transfection, 1 x 10^6 293T cells were plated in 10 cm dishes. Cells were transfected with 10 μg of the appropriate plasmid using $CaPO_4$ coprecipitation. For each plate, 428 μl H_20, 62 μl 2M $CaCl_2$, and 10 μg plasmid DNA was mixed with an equal amount of 2X HBS (50 mM HEPES pH 7.05, 10 mM KCl, 12 mM dextrose, 280 mM NaCl, 1.5 mM Na_2PO_4) while being mixed by blowing air through a 2 mL pipette with a Pipet-aid (Drummond). Media was refreshed 5-8 hrs. after transfection. 48 hrs. after transfection, cells were harvested in media, counted, washed with PBS, and resuspended in 200-500 μl of lysis buffer (50 mM Tris-HCl pH 7.4, 1% Triton X-100, 0.1% SDS, 150 mM

NaCl, 1 mM EDTA, 1 mM DTT, 1 mM PMSF, with a complete mini-protease inhibitor tablet [Roche] per 10 ml). The NaCl concentration was raised to 400 mM, and the lysate was incubated on ice for 20 min. The NaCl concentration was reduced to 200 mM with an equal volume of cold water, cell debris was removed by centrifugation at 13K for 10 min. at 4°C. 4X Laemmli buffer (0.24 mM Tris-HCl, 4% SDS, 20% glycerol, 10% beta-mercaptoethanol, 0.004% bromophenol blue) was added to the lysate at a ratio of 1:3. Samples were boiled for 5 min.

Immunoprecipitations

For immunoprecipitation of proteins expressed by transient transfection in 293T cells, transfection and harvesting was performed as above. 50 µL of 2X Laemmli buffer was added to 50 µL of lysate and set aside as the "Input." Antibody (2 µL of affinity purified and commercial antibodies, 10 µL of crude serum) was added to 400 µL of lysate. Samples were nutated at 4°C for 5 hrs. 60 µL of a Protein G sepharose slurry (50% [v/v] Protein-G sepharose [Amersham] in PBS in 1 mg/ml BSA) were added and samples were nutated at 4°C for an additional 60 min. Beads were washed 3 times at 4°C with lysis buffer, and immunoprecipitated protein was eluted with 60 µL 2X Laemmli buffer. For immunoprecipitation of endogenous ATM from IMR90 fibroblasts for the phosphorylation assay, cells were resuspended in lysis buffer (50 mM Hepes pH 7.5, 150 mM NaCl, 50 mM NaF, 1% Tween-20, 0.2% NP40, 1mM PMSF, with 1 complete mini-protease inhibitor tablet [Roche] per 10 mL) and centrifuged at 13K rpm for 10 min. 400 µl of lysate was incubated with 30 µl of blocked protein G beads and 100 µl of

D16.11 monoclonal supernatant. Beads were washed once in lysis buffer and twice in RIPA buffer and resuspended in 60 µl of 2X Laemmli buffer. To generate Protein G sepharose slurry, 3-4 mL of beads were centrifuged at 1K for 1 min. at 4°C, supernatant was removed, and beads were washed with PBS 3 times. Beads were resuspended with an equal volume of 5% BSA in PBS and nutated at 4°C for 1 hr. Sodium azide was added to 0.02% and beads were stored at 4°C.

Retroviral gene delivery

One day prior to transfection, 1 x 10^6 Phoenix packaging cells (293T derived cell lines) were plated in 10 cm dishes. For infection of mouse cells, Phoenix ecotropic cells were used. For infection of human cells, Phoenix amphotropic cells were used. Phoenix cells were transfected with 20 µg of the appropriate plasmid DNA by $CaPO_4$ coprecipitation (described above). The media was refreshed 5-8 hrs. later, and again 24 hrs. later. 36 hrs. after transfection, media was filtered through a 0.4 µm filter and polybrene was added to a final concentration of 4 µg/mL. Fresh media was added to the virus producing cells. This procedure was repeated 3 additional times at 12 hr. intervals. If appropriate, 12 hrs. after the final infection, fresh media was added containing antibiotics for selection (puromycin 2 µg/ml, hygromycin 90 µg/ml) for 4-5 days until uninfected control cells were completely dead.

Lentiviral gene delivery

293T cells were transfected using calcium phosphate with 3 µg each of helper plasmids (pMDLg/RRE, pRSV-rev, and pCMV-VSVG) and 7 µg of lentiviral vector (pLenti6/Ubc/V5, Invitrogen) carrying the appropriate transgene per 10 cm dish. Fresh media was added 5-8 hrs. after transfection. 72 hrs. after changing the media, virus-containing media was collected in a 50 ml conical tube and centrifuged for 5 min. at 1K rpm at 4°C. The virus was filtered through a 0.4 µm filter and polybrene was added to a final concentration of 4 µg/ml. $2x10^5$ MEFs were plated for each infection, the day before infection. Half of the filtered virus was used for the initial infection. Remaining virus was kept on ice and used for a second infection 12 hrs. later. 12 hrs. after the second infection, virus containing medium was replaced with fresh medium. The following day, media was replaced with media containing 6 µg/ml blasticidin. After four days of selection, blasticidin concentration was dropped to 2.5 µg/ml and cells were selected for an additional 7 days.

Isolation of clonal lines

$TRF2^{f/-}$ MEFs expressing TRF2 alleles (not exposed to Cre) were plated at low density (500-2000 cells/10 cm dish) and grown for approximately 2 weeks until clonal populations were visible under the light microscope. Clonal populations of cells were isolated by trypsinizing cells in cloning cylinders. Clonal populations were transferred to a well of a 96 well plate. When the cells reached confluence

in the well, the clonal population was expanded.

Expression of Cre Recombinase

Cre was introduced into MEFs using pMMP Hit & Run Cre-GFP retrovirus[253] or pWZL-Cre retrovirus (containing the hygromycin resistance gene) using the retroviral infection technique described above.

Whole cell lysates and western blots

For whole cell lysates, cells were harvested, washed with PBS, counted and resuspended in 2X Laemmli buffer at a concentration of 5000 cells/µl. Lysates were boiled for 5 min. and DNA was sheared through a 28 gauge insulin syringe. Protein samples were separated by SDS-PAGE and blotted onto nitrocellulose membranes. Membranes were blocked in 10% milk in PBST (0.5% Tween-20 in PBS) for 30 min. at RT and nutated with primary antibodies in 0.1% milk in PBST overnight at 4°C. Membranes were washed 3 times in PBST, nutated in secondary antibody in 0.1% milk in PBST for 45 min. at RT, and washed 3 times with PBST at RT. ECL (Amersham) was applied to membranes for 5 min. before exposure to film.

Synchronization of HeLa cells

0.5 x 10^6 HeLa cells were plated in a 10 cm culture dish and treated with 2 mM thymidine 24 hrs. later. After 14 hrs., cells were washed 3 times with pre-warmed PBS and fresh medium was added. 11 hrs. later, thymidine was added

to a final concentration of 2 mM. After 15 hrs., cells were washed with pre-warmed PBS and again provided with fresh media. Cells were harvested at the indicated time points for western blot and FACs analysis. Exponentially growing HeLa S3 cells (suspension culture) were fractionated by size using centrifugal elutriation in an Avanti™ J-20 XP Centrifuge (Beckman) 11 fractions were obtained and processed for western blot and FACs analysis alongside unfractionated cells.

Fluorescence activated cell sorting (FACS) analysis

Cells were harvested from a 10 cm dish by trypsinization, washed with PBS, and resuspended in 100 µl PBS. Two ml ice cold 70% ethanol was added dropwise while vortexing. Cells were stored at 4°C. For FACS, cells were resuspended in propidium iodide solution (500 µl PBS, 100 µg RNase, 25 µg propidium iodide) and incubated at RT for 30 min. Cells were analyzed on a Becton Dickinson FACS – Scan II.

Immunofluorescence

Cells were plated in dishes on coverslips. Cells were rinsed with PBS, fixed with 2% paraformaldehyde in PBS for 10 min. at RT, wash twice with PBS for 5 min. Cells were either stored in PBS with the addition of 0.02% azide or processed immediately. Cells were permeabilized with 0.5% NP40. If extraction was desired, prior to fixation, cells were treated with Triton X-100 extraction buffer (0.5% Triton X-100, 20 nM HEPES-KOH pH 7.9, 50 mM NaCl, 3 mM $MgCl_2$, 300

mM sucrose). Extracted cells were fixed with 3% paraformaldehyde, 2% sucrose for 10 minute at RT, and washed twice with PBS. If extraction was performed, Triton X-100 buffer was used for permeabilization instead of 0.5% NP-40. After permeabilization, cells were washed three times with PBS and blocked with PBG (0.2% (w/v) cold water fish gelatin (Sigma), 0.5% (w/v) BSA (Sigma) in PBS) for 30 min. at RT. Cells were incubated with primary antibody diluted in PBG overnight at 4°C, washed 3 times with PBG at RT, incubated with secondary antibody diluted 1:250 in PBG for 45 min. at RT, and washed 3 times with PBS. To the second PBS wash 0.1 µg/ml 4,6-diamidino-2-phenylindole (DAPI) was added. Coverslips were sealed onto glass sides with embedding media (ProLong Gold Antifade Reagent, Invitrogen).

Microscopy and image processing

Images were captured using an Axioplan II Zeiss microscope with a Hamamatsu CCD digital camera using Improvision OpenLab software. Images were merged in OpenLab and processed with Adobe Photoshop.

Differential salt extraction

Cells were harvested by trypsinization, washed twice in serum-containing media, and once with cold PBS. Cells were resuspended in 10 times the pellet volume of Buffer C-150 (20 mM HEPES pH 7.9, 25% glycerol, 5 mM MgCl, 0.2% NP-40, 1 mM DTT, 1 mM PMSF, with a complete mini-protease inhibitor tablet [Roche] per 10 ml). Lysates were incubated for 15 min. on ice and then the samples

were centrifuged for 5 min. at 3K rpm at 4°C. The supernatant is the 150 mM fraction and represents the soluble cytoplasmic and nucleoplasmic proteins. Pellets were resuspended in Buffer C-420 (Same as Buffer C-150 but contains 420 mM KCl) and incubated on ice for 15 min. Samples were centrifuged for 10 min. at 14K rpm at 4°C. The supernatant is the 420 mM fraction and contains chromatin bound proteins. The final pellets were resuspended in 2X Laemmli buffer and sonicated.

Preparation of genomic DNA

Cells were harvested by trypsinization and washed with PBS. 0.5 X 10^6 cells for MEFs and 1 x 10^6 cells for HeLa cells were resuspended in 50 µl PBS and incubated at 50°C for 5 min. Using pipette tips with the ends cut off, 50 µl of 2% agarose (prewarmed to 50°C) was added to each sample, mixed, and incubated for 5 min at 50°C. The 100 µl mixture was added to the Bio-Rad plug cast, incubated at RT for 5 min. and at 4°C for 15 min. Solidified plugs were incubated in 0.5 ml Proteinase K digestion buffer (10 mM Tris-HCl pH 7.9, 250 mM EDTA pH 8.0, 0.2% sodium deoxycholate, 1% sodium lauryl sarcosine, and 1 mg/ml fresh Proteinase K) overnight at 50°C. Plugs were washed three times with TE for one hr. each at RT with nutation. Plugs were washed for 1 additional hr. at RT with TE containing 1 mM PMSF and stored at 4°C in this final wash. Prior to digestion, plugs were washed for 1 hr. in fresh TE and 20 min. in H_20. Plugs were equilibrated for 1 hr. in the appropriate restriction enzyme buffer at RT.

Each plug was then digested with 60 units of MboI for MEFs and 60 units of MboI and 60 units AluI for human cells overnight at 37°C. Plugs were washed with TE for 1 hr. and equilibrated in 0.5X TBE for 30 min.

In gel hybridization to detect telomeric DNA from MEFs

DNA from MEFs was fractionated on a CHEF-DRII PFGE (Biorad) in a 1% agarose gel in 0.5X TBE for 24 hrs. at 6 V/cm at 14°C. Gels were stained with ethidium bromide and photographed. Gels were dried and then prehybridized in Church Mix (0.5M Na_2HPO_4 pH 7.2, 1 mM EDTA, 7% SDS, 1% BSA) for 1 hr. at 50°C. Hybridization was performed overnight at 50°C in Church Mix with 4 ng of a γ-32P-ATP end-labeled probe, $[CCCTAA]_4$ (See below for labeling protocol). The gel was washed at 55°C: 3 times for 30 min. each in 4X SSC and one time for 30 min. in 4X SSC, 0.1% SDS and exposed to a PhosphorImager screen. Subsequently, the gel was denatured in 0.5 M NaOH, 1.5 M NaCl for 30 min., neutralized with two 15 minute washes in 0.5 M Tris-HCl pH 7.5, 3 M NaCl, prehybridized in Church mix for 1 hr. at 55°C, and hybridized with the same probe as above overnight at 55°C. The gel was washed and exposed as above.

Southern blot to detect telomeric DNA from human cells

DNA was separated on a 0.7% agarose gel in 0.5X TBE with ethidium bromide by running for 1 hr. at 30 V and then running until the orange G front was at the bottom of the gel (approximately overnight at 45V). Gel was photographed. Gel was then run until the 1.3 kb marker was almost at the bottom of the gel. Gel

was photographed with a ruler next to the markers. Gel was gently shaken in Depurination solution (0.25M HCl) for 30 min., Denaturation solution (1.5 M NaCl; 0.5 M NaOH) for 30 min. twice, and Neutralization solution (1 M Trish pH 7.4, 1.5M NaCl) for 30 min. twice. Gel was then blotted onto a Hybond filter overnight in 20X SSC. Blot was cross-linked, rinsed in H_20, and prehybridized and probed as in the in gel hybridization protocol above.

Chromatin Immunoprecipitation (ChIP)

Cells were washed with PBS, fixed in 1% formaldehyde in PBS for 60 min. at RT, washed in PBS, and lysed in 1% SDS, 50 mM Tris-HCl pH 8.0, 10 mM EDTA at a density of $1x10^7$ cells/ml. Lysates were sonicated on ice for 10 cycles of 20 seconds each (0.5 seconds on/0.5 seconds off) on power setting 5 on a Misonix Sonicator 3000. Two 50 µl aliquots of lysates were set aside at 4°C to represent "Total" DNA. 200 µl of lysate was diluted with 1.2 ml 0.01% SDS, 1.1% Triton X-100, 1.2 mM EDTA, 16.7 mM Tris-HCl pH 8.0, and 150 mM NaCl. Antibody (20 µl crude serum or 4 µl affinity purified antibody or anti-c-myc 9E10, see antibody section below for specifics) was added and cells were nutated overnight at 4°C. 30 µl protein G sepharose beads (Amersham; blocked with 30 µg BSA and 5 µg sheared *E. coli* DNA) was added and samples were nutated for an additional 30 min. at 4°C. Beads were pelleted by centrifugation and pellets were washed with 0.1% SDS, 1% Triton X-100, 2 mM EDTA pH 8.0, 20 mM Tris-HCl pH 8.0, 150 mM NaCl. The second wash was the same except with 500 mM NaCl. Subsequent washes were with 0.25 M LiCl, 1% NP-40, 1% Na-deoxycholate, 1

mM EDTA pH 8.0, 10 mM Tris-HCl pH 8.0, 1 mM EDTA. Chromatin was eluted from beads with 500 µl 1% SDS, 0.1M Na_2CO_3. 450 µl 1% SDS, 0.1M Na_2CO_3 was added to the "Total" fractions, and these were subsequently processed along with the rest of the samples. 20 µl 5M NaCl was added and samples were incubated for 4 hr. at 65°C to reverse cross-links. At this point, 20 µl 1M Tris-HCl pH 6.5, 10 µl 0.5 M EDTA, and 20 µg DNase free RNase A was added and samples were incubated at 37°C for 30 min. 40 µg proteinase K was added and samples were digested for 60 min. at 37°C and extracted with phenol. 20 µg of glycogen was added and samples were mixed. 1 ml ethanol was added and DNA was precipitated overnight at -20°C. Precipitated DNA was dissolved in 100 µl H_20, denatured at 95°C for 5 min., and blotted onto Hybond membranes in 2X SSC (0.3M NaCl, 0.03M Sodium citrate). "Total" fractions were diluted 1/4, 1/8, and 1/16 and blotted as well. Membranes were treated with 1.5M NaCl, 0.5 N NaOH for 10 min. and then with 1 M NaCl, 0.5 M Tris-HCl pH 7.0 for 10 min. Hybridization was performed with a γ^{32}-P endlabeled $[CCCTAA]_4$ probe as described for in gel hybridization of genomic DNA. Membranes were washed 4 times in 2X SSC and exposed overnight to a PhosphorImager screen. Screens were developed using a STORM 820 Phosphorimager (Molecular Dynamics). ImageQuant software was used to quantify the percent of total telomeric DNA that was precipitated by each antibody.

γ-^{32}P end labeling of oligonucleotides with T4 polynucleotide kinase (PNK)

2 µl H_20, 1 µl 10X T4 DNA PNK buffer (NEB), 1 µl 10 U/µl T4 DNA PNK (NEB), 1 µl 50 ng/µl $[CCCTAA]_4$ oligonucleotide and 5 µl 10.0 mCi/ml γ-^{32}P (NEN) were mixed and incubated for 45 min. at 37°C. 80 µl TES (10 mM Tris-HCl pH 8.0, 10 mM EDTA pH 8.0, 0.01% SDS) were added to stop the reaction. The probe was loaded onto a 3 ml G25 Sephadex column equilibrated with TNES (10 mM Tris-HCl pH 7.4, 10 mM EDTA, 100 mM NaCl, 1% SDS). The column was washed with 700 µl TNES and the probe was eluted with 600 µl TNES.

Metaphase spreads

Cells were grown to approximately 40% confluence on 10 cm dishes and incubated for 1-2 hrs. in 0.1 µg/ml colcemide (Sigma). Cells were harvested by trypsinization, centrifuged at 1K for 5 min., and resuspended in 0.075M KCL prewarmed to 37°C. Cells were incubated at 37°C for 15 min. with occasional inversion. Cells were centrifuged at 1K for 5 min. and supernatant was decanted. Cells were resuspended by tapping in the remaining (~200 µl) supernatant. 500 µl of cold 3:1 methanol:glacial acetic acid fixative was added dropwise while cells were mixed gently on a vortexer (<1000 rpm). Another 500 µl fixative was added slowly while cells were being mixed. Tubes were then filled to 10 mL with the fixative and stored at 4°C overnight or longer. Cells were centrifuged at 1K rpm for 5 min. and supernatant was decanted. Cells were resuspended in the remaining fixative (~300 µl) and dropped from approximately 6 inches onto glass

slides which had been soaked in cold water. Slides were washed with fresh fixative and placed on a humidified heating block set to 70°C (42°C for CO-FISH) for 1 minute. Spreading efficiency was checked under a light microscope. Slides were dried overnight. If only DAPI staining was required, slides were rehydrated in PBS for 5 min., stained with DAPI in PBS for 5 min., washed in PBS for 5 min., and allowed to dry before mounting.

CO-FISH

For CO-FISH cells were grown in the presence of BrdU:BrdC (3:1, 10 µM final) for 12-14 hrs. and supplemented with 0.1 µg/ml colcemide (Sigma) for the final two hrs. Metaphases were harvested as described above. Cells were treated with 0.5 mg/ml RNase A (in PBS, DNase free) for 10 min. at 37°C. Slides were then stained with 0.5 µg/ml Hoechst 33258 (Sigma) in 2X SSC for 15 min. at RT. Slides were then exposed to 365-nm UV light in a Stratalinker 1800 UV irradiator for 30 min. (equivalent to $5.4x10^3$ J/m^2). Strands which had incorporated BrdU and BrdC were digested with 80 µl of 10 units/µl Exonuclease III (Promega) under a coverslip for 10 min. at RT. Exonuclease III digestion was repeated. Slides were washed in PBS and dehydrated in an ethanol series: 5 min. each 70%, 85%, 100%, and air dried. Slides were incubated with the TAMRA-TelG 5'-$[TTAGGG]_3$-3' PNA probe (Applied Biosystems) diluted 1:5000 in 80 µl of hybridization mix (10 mM Tris-HCl pH 7.2, 70% deionized formamide, 0.5% blocking reagent [Boehringer Mannheim]) under a coverslip for two hrs. at RT in the dark. Slides were washed for several seconds in Wash I (70% formamide, 10

mM Tris-HCl pH 7.2, 0.1% BSA). Slides were incubated with the FITC-TelC 5'-$[CCCTAA]_3$-3' PNA probe (Applied Biosystems) in hybridization mix as described above. Slides were washed in Wash I twice for 30 min. each with a stir bar on a magnetic stir plate. Slides were then washed three times for 5 min. each in Wash II (0.1M Tris-HCl pH 7.2, 0.15M NaCl, 0.08% Tween-20) with a stir bar on a magnetic stir plate. DAPI was added to the second wash. Slides were dehydrated in an ethanol series: 5 min. each 70%, 95%, 100%, air dried, and mounted.

FISH

FISH was performed according to the same protocol as CO-FISH with the following exceptions. Cells were not incubated with BrdU/BrdC prior to collection of metaphase spreads. After metaphase spreads were dropped, slides were placed on a heating block set to 70°C (not 42°C as for CO-FISH). Hybridization was only performed with the FITC-TelC 5'-$[CCCTAA]_3$-3' PNA probe at 1:1000 and slides were placed on a heating block set to 80°C for 3 min. to denature DNA.

IF-FISH

Cells were plated in dishes with coverslips. Cells were rinsed with PBS, fixed with 2% paraformaldehyde in PBS for 10 min. at RT, washed twice with PBS for 5 min. each. Cells were either stored in PBS with the addition of 0.02% azide or processed immediately. Coverslips were blocked for 30 min. in blocking solution

(1 mg/ml BSA, 3% goat serum, 0.1% Triton X-100, 1 mM EDTA in PBS) and incubated for 1 hr. in primary antibody diluted in blocking solution. Cover slips were washed 3 times 5 min. each in PBS before incubation in secondary antibody diluted in blocking solution. Cover slips were washed 3 times 5 min. each in PBS, dehydrated in an ethanol series: 5 min. each 70%, 95%, 100%, and air dried. Coverslips were transferred (cells facing up) to glass slides and 80 µl of FITC-TelC 5'-$[CCCTAA]_3$-3' (Applied Biosystems) probe at 1:1000 in hybridizing solution (70% formamide, 0.5% blocking reagent [Boehringer Mannheim], 10 mM Tris-HCl pH 7.2) was added. Slides were placed on a heating block set to 70°C for 5 min. and incubated in the dark for 2 hrs. – overnight. Coverslips were washed twice for 15 min. in 70% formamide, 10 mM Tris-HCl pH 7.2 and three times for 5 min. in PBS. DAPI was added to the second PBS wash. Cover slips were sealed on glass slides with embedding media.

siRNA Treatment

Dharmacon ON-TARGETplus™ SMARTpool siRNA against ATR or Dharmacon luciferase siRNA (5'-CGTACGCGGAATACTTCGA-3') and TRF2 were cotransfected into 293T cells using DharmaFECT© Duo transfection reagent according to the manufacturer's instructions. 0.5 x 10^6 293T cells were plated per 6 cm dish the day before transfection. For each 6 cm dish: 5 µl of 1µg/µl TRF2 plasmid DNA, 25 µl 20 µM siRNA and 470 µl DMEM (with no serum or supplements) were mixed gently in one tube. In a second tube, 30 µl of

DharmaFECT© Duo transfection reagent were mixed with 470 µl DMEM (with no serum or supplements). The two tubes were incubated at RT for 5 min. The contents of the two tubes were then mixed together and incubated at RT for 20 min. 4 ml of antibiotic-free media (containing serum and other supplements) was added to the 1 ml transfection mixture. Cells were rinsed once with antibiotic free media and then the media containing the transfection mixture was added. Cells were harvested 48 hrs. after transfection (or at timepoints indicated in text) as described above for cells transfected by calcium phosphate co-precipitation.

shRNA

Oligonucleotides targeting PIKKs were designed by Agnel Sfeir and were obtained from E-oligos, annealed, phosphorylated and cloned into pSuperior-PURO (Oligoengine). Plasmids were sequenced to confirm integrity of the construct. pSuperior-Puro shRNA containing constructs were used to retrovirally infect 293T cells as described above. Subsequent to selection, infected cells were transfected with TRF2 using the calcium phosphate method as described above.

shRNAs were designed to target a 19 nucleotide sequence within the gene of interest in the following format:

sense: 5'-GATC_4(19mer)$T_2C A_2$GAGA(19mer reverse complement)$T_5G_2A_4$-3'

antisense: 5'-AG$CT_4C_2A_5$(19mer)TCTCT_2GA_2(19mer reverse complement)G_2-3'

ATM

1 – GGACTTGTTGAAATACTTA

2 – CGAGATCCTGAAACAATTA

3 – CCAGATGTGTAATACATTA

DNA-PK

1 – GATCGCACCTTACTCTGTT

2 – GCATCTCTTGCCTTTAATA

3 – GCATCCAGCTAAACCTAAA

SMG1

1 – CCAGGACACGAGGAAACTG

2 – GCAGCTGGATTCCATTTAA

3 – GCATCACAGGATAGCAATA

Aphidicolin survival assay

MEFs expressing TRF2 alleles and control MEFs were infected with the pWZL-Cre retrovirus. Subsequent to 7 days of hygromycin selection, cells were plated for aphidicolin treatment. For each dose (0, 0.5 μM, and 1 μM) cells were plated in triplicate in 6 well dishes. 24 hrs. later, media was exchanged for media

containing the appropriate dose a aphidicolin. 24 hrs. later, cells (including untreated cells) were washed once with warm PBS and grown in fresh media for 3-4 days until colonies were visible. Cells were washed with PBS and stained with 50% MeOH, 7% glacial acetic acid, 0.1% Coomassie Brilliant Blue G for 10 min. Cells were rinsed with water and air-dried. Colonies were counted under a light microscope.

Antibodies used

ID	antigen	Type	Applications (h) human (m) mouse	Origin
1254	mTRF2 (GST-FL)	Rb poly	Western (m) 1:5000 ChIP (m) 1:70 (serum)	Celli/de Lange
1252	mRap1 (GST-FL)	Rb poly	Western (m) 1:10000 IF (m) 1:10,000 ChIP (m) 1:70 (serum)	Celli/de Lange
644	mTRF1 (peptide)	Rb poly	IF (m) 1:1000 ChIP (m) 1:350	Karlseder/de Lange
1447	mTIN2 (GST-FL)	Rb poly	IF (m) 1:2000 ChIP (m) 1:350	Donigian/de lange
1151	mTPP1 (GST-250-544)	Rb poly	ChIP (m) 1:350	Ye/de Lange
1220	mPot1a (peptide)	Rb poly	ChIP (m) 1:350	Hockemeyer/ de Lange lab
1223	mPot1b (peptide)	Rb poly	ChIP (m) 1:350	Hockemeyer/ de Lange lab
647	hTRF2 (baculoviral-FL)	Rb poly	Western (h) 1:1000	Zhu/de Lange lab
αhTRF2	hTRF2	Mo	Western (h) 1:1000	Upstate

ID	antigen	Type	Applications (h) human (m) mouse	Origin
	(peptide)	mono		
αhTRF1	hTRF1 (baculoviral-FL)	Mo poly	IF (h): 1:5000	Marrero/ de Lange lab
9E10	c-myc peptide	Mo mono	IF 1:5000	Sigma
9E10	c-myc peptide	Mo mono	Western 1:1000	Calbiochem
M2	Flag peptide	Mo mono	Western 1:10,000	Sigma
HA.11	HA peptide	Mo mono	Western 1:1000	Covance
α53BP1	Human 53BP1	Mo mono	IF (h,m) 1:50	Halazonetis, The Wistar Institute, PA
α53BP1	53BP1 (peptide)	Rb poly	IF (m) 1:1000	Novus
α-γH2AX	γH2AX (phospho peptide S139)	Mo mono	IF (h) 1:1000	Upstate
GTU88	γTubulin (peptide)	Mo mono	Western (h,m) 1:5000	Sigma
PG-M3	PML (peptide)	Mo mono	IF (h) 1:100	Santa Cruz
αATM-P	ATM (phospho peptide S1981)	Mo Mono	Western (h) 1:1000	Cell Signaling
αChk1-P	Chk1-P (phospho peptide S345)	Rb mono	Western (h,m) 1:1000	Cell Signaling

ID	antigen	Type	Applications (h) human (m) mouse	Origin
αp70 S6 kinase-P	p70 S6 kinase (phospho peptide T389)	Rb mono	Western (h) 1:1000	Cell Signaling
αTRF2 S368-P	TRF2 (phospho peptide S368)	Rb poly	Western (h) 1:1000 IF (h,m) 1:1000	AnaSpec/de Lange
αTRF2 T188-P	TRF2 (phospho peptide T188)	Rb poly	IF (h,m) 1:200	AnaSpec/ Gilley
2G2	hMMS19	Mo mono	Western (h) 1:1000	Hoeijmakers, Erasmus Medical Center, The Netherlands
FRP1(N19) 1887	ATR	Gt poly	Western (h) 1:500	Santa Cruz
MAT3	ATM	Mo mono	Western (h) 1:6000	Sigma
DNA-PK(C19) 1552	DNA-PK	Gt poly	Western (h) 1:500	Santa Cruz
αSMG1	SMG1	Rb poly	Western (h) 1:2000	Bethyl Labs
D16.11	ATM	M mono	Immunoprecipitation	Alligood/ Glaxo

Rb: Rabbit; Mo: mouse; Gt: goat; poly: polyclonal; mono: monoclonal

REFERENCES

1. Morris, C. A. & Moazed, D. Centromere assembly and propagation. *Cell* **128**, 647-650 (2007).
2. Henikoff, S. & Dalal, Y. Centromeric chromatin: what makes it unique? *Curr Opin Genet Dev* **15**, 177-184 (2005).
3. Todorovic, V., Falaschi, A. & Giacca, M. Replication origins of mammalian chromosomes: the happy few. *Front Biosci* **4**, D859-68 (1999).
4. Watson, J. D. Origin of concatemeric T7 DNA. *Nat New Biol* **239**, 197-201 (1972).
5. Olovnikov, A. M. A theory of marginotomy. The incomplete copying of template margin in enzymic synthesis of polynucleotides and biological significance of the phenomenon. *J Theor Biol* **41**, 181-190 (1973).
6. Klobutcher, L. A., Swanton, M. T., Donini, P. & Prescott, D. M. All gene-sized DNA molecules in four species of hypotrichs have the same terminal sequence and an unusual 3' terminus. *Proc Natl Acad Sci USA* **78**, 3015-3019 (1981).
7. Richards, E. J. & Ausubel, F. M. Isolation of a higher eukaryotic telomere from Arabidopsis thaliana. *Cell* **53**, 127-136 (1988).
8. Okazaki, S., Tsuchida, K., Maekawa, H., Ishikawa, H. & Fujiwara, H. Identification of a pentanucleotide telomeric sequence, (TTAGG)n, in the silkworm Bombyx mori and in other insects. *Mol Cell Biol* **13**, 1424-1432 (1993).
9. de Lange, T. et al. Structure and variability of human chromosome ends. *Mol Cell Biol* **10**, 518-527 (1990).
10. Harley, C. B., Futcher, A. B. & Greider, C. W. Telomeres shorten during ageing of human fibroblasts. *Nature* **345**, 458-460 (1990).
11. Starling, J. A., Maule, J., Hastie, N. D. & Allshire, R. C. Extensive telomere repeat arrays in mouse are hypervariable. *Nucleic Acids Res* **18**, 6881-6888 (1990).
12. Prowse, K. R. & Greider, C. W. Developmental and tissue-specific regulation of mouse telomerase and telomere length. *Proc Natl Acad Sci USA* **92**, 4818-4822 (1995).
13. Makarov, V. L., Hirose, Y. & Langmore, J. P. Long G tails at both ends of human chromosomes suggest a C strand degradation mechanism for telomere shortening. *Cell* **88**, 657-666 (1997).
14. Sfeir, A. J., Chai, W., Shay, J. W. & Wright, W. E. Telomere-end processing the terminal nucleotides of human chromosomes. *Mol Cell* **18**, 131-138 (2005).
15. Griffith, J. D. et al. Mammalian telomeres end in a large duplex loop. *Cell* **97**, 503-14. (1999).
16. Stansel, R. M., de Lange, T. & Griffith, J. D. T-loop assembly in vitro involves binding of TRF2 near the 3' telomeric overhang. *EMBO J* **20**, 5532-5540 (2001).
17. Munoz-Jordan, J. L., Cross, G. A., de Lange, T. & Griffith, J. D. t-loops at trypanosome telomeres. *Embo J* **20**, 579-88. (2001).
18. Nikitina, T. & Woodcock, C. L. Closed chromatin loops at the ends of chromosomes. *J Cell Biol* **166**, 161-165 (2004).
19. Murti, K. G. & Prescott, D. M. Telomeres of polytene chromosomes in a ciliated protozoan terminate in duplex DNA loops. *Proc Natl Acad Sci USA* **96**, 14436-14439 (1999).

20. Verdun, R. E. & Karlseder, J. The DNA damage machinery and homologous recombination pathway act consecutively to protect human telomeres. *Cell* **127**, 709-720 (2006).
21. Wang, R. C., Smogorzewska, A. & de Lange, T. Homologous recombination generates T-loop-sized deletions at human telomeres. *Cell* **119**, 355-368 (2004).
22. Makarov, V. L., Lejnine, S., Bedoyan, J. & Langmore, J. P. Nucleosomal organization of telomere-specific chromatin in rat. *Cell* **73**, 775-787 (1993).
23. Lejnine, S., Makarov, V. L. & Langmore, J. P. Conserved nucleoprotein structure at the ends of vertebrate and invertebrate chromosomes. *Proc Natl Acad Sci USA* **92**, 2393-2397 (1995).
24. Tommerup, H., Dousmanis, A. & de Lange, T. Unusual chromatin in human telomeres. *Mol Cell Biol* **14**, 5777-5785 (1994).
25. Greider, C. W. & Blackburn, E. H. Identification of a specific telomere terminal transferase activity in Tetrahymena extracts. *Cell* **43**, 405-413 (1985).
26. Greider, C. W. & Blackburn, E. H. The telomere terminal transferase of Tetrahymena is a ribonucleoprotein enzyme with two kinds of primer specificity. *Cell* **51**, 887-898 (1987).
27. Feng, J. et al. The RNA component of human telomerase. *Science* **269**, 1236-1241 (1995).
28. Lingner, J. & Cech, T. R. Purification of telomerase from Euplotes aediculatus: requirement of a primer 3' overhang. *Proc Natl Acad Sci USA* **93**, 10712-10717 (1996).
29. Lingner, J. et al. Reverse transcriptase motifs in the catalytic subunit of telomerase. *Science* **276**, 561-567 (1997).
30. Lendvay, T. S., Morris, D. K., Sah, J., Balasubramanian, B. & Lundblad, V. Senescence mutants of Saccharomyces cerevisiae with a defect in telomere replication identify three additional EST genes. *Genetics* **144**, 1399-1412 (1996).
31. Meyerson, M. et al. hEST2, the putative human telomerase catalytic subunit gene, is up- regulated in tumor cells and during immortalization. *Cell* **90**, 785-95. (1997).
32. Nakamura, T. M. et al. Telomerase catalytic subunit homologs from fission yeast and human. *Science* **277**, 955-959 (1997).
33. Lundblad, V. & Szostak, J. W. A mutant with a defect in telomere elongation leads to senescence in yeast. *Cell* **57**, 633-643 (1989).
34. Evans, S. K. & Lundblad, V. Est1 and Cdc13 as comediators of telomerase access. *Science* **286**, 117-120 (1999).
35. Reichenbach, P. et al. A human homolog of yeast est1 associates with telomerase and uncaps chromosome ends when overexpressed. *Curr Biol* **13**, 568-574 (2003).
36. Snow, B. E. et al. Functional conservation of the telomerase protein est1p in humans. *Curr Biol* **13**, 698-704 (2003).
37. Cohen, S. et al. Protein Composition of Catalytically Active Human Telomerase from Immortal Cells. *Science* **315**, 1850-1853 (2007).
38. Smogorzewska, A. & de Lange, T. Regulation of telomerase by telomeric proteins. *Ann Rev Biochem* **73**, 177-208 (2004).
39. HAYFLICK, L. & MOORHEAD, P. S. The serial cultivation of human diploid cell strains. *Exp Cell Res* **25**, 585-621 (1961).

40. Bodnar, A. G. et al. Extension of life-span by introduction of telomerase into normal human cells. *Science* **279**, 349-352 (1998).
41. Greider, C. W. Telomeres. *Curr Opin Cell Biol* **3**, 444-451 (1991).
42. Wright, W. E., Piatyszek, M. A., Rainey, W. E., Byrd, W. & Shay, J. W. Telomerase activity in human germline and embryonic tissues and cells. *Dev Genet* **18**, 173-179 (1996).
43. Kim, N. W. et al. Specific association of human telomerase activity with immortal cells and cancer. *Science* **266**, 2011-205. (1994).
44. Bryan, T. M., Englezou, A., Dalla-Pozza, L., Dunham, M. A. & Reddel, R. R. Evidence for an alternative mechanism for maintaining telomere length in human tumors and tumor-derived cell lines. *Nat Med* **3**, 1271-1274 (1997).
45. Lee, H. W. et al. Essential role of mouse telomerase in highly proliferative organs. *Nature* **392**, 569-574 (1998).
46. Rudolph, K. L. et al. Longevity, stress response, and cancer in aging telomerase-deficient mice. *Cell* **96**, 701-712 (1999).
47. Herrera, E. et al. Disease states associated with telomerase deficiency appear earlier in mice with short telomeres. *Embo J* **18**, 2950-2960 (1999).
48. Herrera, E., Martinez, A. C. & Blasco, M. A. Impaired germinal center reaction in mice with short telomeres. *Embo J* **19**, 472-81. (2000).
49. Wyllie, F. S. et al. Telomerase prevents the accelerated cell ageing of Werner syndrome fibroblasts. *Nat Genet* **24**, 16-17 (2000).
50. Ouellette, M. M., McDaniel, L. D., Wright, W. E., Shay, J. W. & Schultz, R. A. The establishment of telomerase-immortalized cell lines representing human chromosome instability syndromes. *Hum Mol Genet* **9**, 403-11. (2000).
51. Chang, S. et al. Essential role of limiting telomeres in the pathogenesis of Werner syndrome. *Nat Genet* **36**, 877-882 (2004).
52. Crabbe, L., Verdun, R. E., Haggblom, C. I. & Karlseder, J. Defective telomere lagging strand synthesis in cells lacking WRN helicase activity. *Science* **306**, 1951-1953 (2004).
53. Dokal, I. Dyskeratosis congenita in all its forms. *Br J Haematol* **110**, 768-779 (2000).
54. Vulliamy, T. et al. The RNA component of telomerase is mutated in autosomal dominant dyskeratosis congenita. *Nature* **413**, 432-435 (2001).
55. Heiss, N. S. et al. X-linked dyskeratosis congenita is caused by mutations in a highly conserved gene with putative nucleolar functions. *Nat Genet* **19**, 32-8. (1998).
56. Mitchell, J. R., Wood, E. & Collins, K. A telomerase component is defective in the human disease dyskeratosis congenita. *Nature* **402**, 551-55. (1999).
57. Vulliamy, T., Marrone, A., Dokal, I. & Mason, P. J. Association between aplastic anaemia and mutations in telomerase RNA. *Lancet* **359**, 2168-2170 (2002).
58. de Lange, T. Shelterin: the protein complex that shapes and safeguards human telomeres. *Genes Dev* **19**, 2100-2110 (2005).
59. Chong, L. et al. A human telomeric protein. *Science* **270**, 1663-1667 (1995).
60. Broccoli, D., Smogorzewska, A., Chong, L. & de Lange, T. Human telomeres contain two distinct Myb-related proteins, TRF1 and TRF2. *Nat Genet* **17**, 231-235 (1997).

61. Bianchi, A., Smith, S., Chong, L., Elias, P. & de Lange, T. TRF1 is a dimer and bends telomeric DNA. *Embo J* **16**, 1785-1794 (1997).
62. Bilaud, T. et al. Telomeric localization of TRF2, a novel human telobox protein. *Nat Genet* **17**, 236-239 (1997).
63. van Steensel, B., Smogorzewska, A. & de Lange, T. TRF2 protects human telomeres from end-to-end fusions. *Cell* **92**, 401-413 (1998).
64. Ye, J. Z. et al. TIN2 binds TRF1 and TRF2 simultaneously and stabilizes the TRF2 complex on telomeres. *J Biol Chem* **279**, 47264-47271 (2004).
65. Kim, S. H. et al. TIN2 mediates functions of TRF2 at human telomeres. *J Biol Chem* **279**, 43799-43804 (2004).
66. Ye, J. Z. et al. POT1-interacting protein PIP1: a telomere length regulator that recruits POT1 to the TIN2/TRF1 complex. *Genes Dev* **18**, 1649-1654 (2004).
67. Liu, D. et al. PTOP interacts with POT1 and regulates its localization to telomeres. *Nat Cell Biol* **6**, 673-680 (2004).
68. Hockemeyer, D. et al. Telomere protection by mammalian POT1 requires interaction with TPP1. *Nat Struct Mol Biol* **14**, 754-761 (2007).
69. Baumann, P. & Cech, T. R. Pot1, the putative telomere end-binding protein in fission yeast and humans. *Science* **292**, 1171-115. (2001).
70. Loayza, D., Parsons, H., Donigian, J., Hoke, K. & de Lange, T. DNA binding features of human POT1: A nonamer 5'-TAGGGTTAG-3' minimal binding site, sequence specificity, and internal binding to multimeric sites. *J Biol Chem* **279**, 13241-13248 (2004).
71. Liu, D., O'Connor, M. S., Qin, J. & Songyang, Z. Telosome, a mammalian telomere-associated complex formed by multiple telomeric proteins. *J Biol Chem* **279**, 51338-51342 (2004).
72. Mattern, K. A. et al. Dynamics of protein binding to telomeres in living cells: implications for telomere structure and function. *Mol Cell Biol* **24**, 5587-5594 (2004).
73. Karlseder, J. et al. Targeted deletion reveals an essential function for the telomere length regulator Trf1. *Mol Cell Biol* **23**, 6533-6541 (2003).
74. Bianchi, A. et al. TRF1 binds a bipartite telomeric site with extreme spatial flexibility. *Embo J* **18**, 5735-5744 (1999).
75. van Steensel, B. & de Lange, T. Control of telomere length by the human telomeric protein TRF1. *Nature* **385**, 740-743 (1997).
76. Smogorzewska, A. et al. Control of human telomere length by TRF1 and TRF2. *Mol Cell Biol* **20**, 1659-1668 (2000).
77. Fairall, L., Chapman, L., Moss, H., de Lange, T. & Rhodes, D. Structure of the TRFH dimerization domain of the human telomeric proteins TRF1 and TRF2. *Molecular Cell* **8**, 351-361 (2001).
78. Li, B., Oestreich, S. & de Lange, T. Identification of human Rap1: implications for telomere evolution. *Cell* **101**, 471-483 (2000).
79. Celli, G. & de Lange, T. DNA processing not required for ATM-mediated telomere damage response after TRF2 deletion. *Nat Cell Biol* **7**, 712-718 (2005).
80. Li, B. & de Lange, T. Rap1 affects the length and heterogeneity of human telomeres. *Mol Biol Cell* **14**, 5060-5068 (2003).

81. de Lange, T. Protection of mammalian telomeres. *Oncogene* **21**, 532-540 (2002).
82. Conrad, M. N., Wright, J. H., Wolf, A. J. & Zakian, V. A. RAP1 protein interacts with yeast telomeres in vivo: overproduction alters telomere structure and decreases chromosome stability. *Cell* **63**, 739-750 (1990).
83. Konig, P., Giraldo, R., Chapman, L. & Rhodes, D. The crystal structure of the DNA-binding domain of yeast RAP1 in complex with telomeric DNA. *Cell* **85**, 125-136 (1996).
84. Kanoh, J. & Ishikawa, F. spRap1 and spRif1, recruited to telomeres by Taz1, are essential for telomere function in fission yeast. *Curr Biol* **11**, 1624-1630 (2001).
85. Marcand, S., Gilson, E. & Shore, D. A protein-counting mechanism for telomere length regulation in yeast. *Science* **275**, 986-990 (1997).
86. Shore, D. RAP1: a protean regulator in yeast. *Trends Genet* **10**, 408-412 (1994).
87. Kim, S. H., Kaminker, P. & Campisi, J. TIN2, a new regulator of telomere length in human cells. *Nat Genet* **23**, 405-412 (1999).
88. Houghtaling, B. R., Cuttonaro, L., Chang, W. & Smith, S. A dynamic molecular link between the telomere length regulator TRF1 and the chromosome end protector TRF2. *Curr Biol* **14**, 1621-1631 (2004).
89. Gottschling, D. E. & Zakian, V. A. Telomere proteins: specific recognition and protection of the natural termini of Oxytricha macronuclear DNA. *Cell* **47**, 195-205 (1986).
90. Gray, J. T., Celander, D. W., Price, C. M. & Cech, T. R. Cloning and expression of genes for the Oxytricha telomere-binding protein: specific subunit interactions in the telomeric complex. *Cell* **67**, 807-814 (1991).
91. Horvath, M. P., Schweiker, V. L., Bevilacqua, J. M., Ruggles, J. A. & Schultz, S. C. Crystal structure of the Oxytricha nova telomere end binding protein complexed with single strand DNA. *Cell* **95**, 963-974 (1998).
92. Loayza, D. & de Lange, T. POT1 as a terminal transducer of TRF1 telomere length control. *Nature* **424**, 1013-1018 (2003).
93. Wang, F. et al. The POT1-TPP1 telomere complex is a telomerase processivity factor. *Nature* **445**, 506-510 (2007).
94. Xin, H. et al. TPP1 is a homologue of ciliate TEBP-beta and interacts with POT1 to recruit telomerase. *Nature* **445**, 559-562 (2007).
95. Takai, H., Smogorzewska, A. & de Lange, T. DNA damage foci at dysfunctional telomeres. *Curr Biol* **13**, 1549-1556 (2003).
96. d'Adda di Fagagna, F. et al. A DNA damage checkpoint response in telomere-initiated senescence. *Nature* **426**, 194-198 (2003).
97. Denchi, E. L. & de Lange, T. Protection of telomeres through independent control of ATM and ATR by TRF2 and POT1. *Nature* (2007).
98. Burma, S., Chen, B. P., Murphy, M., Kurimasa, A. & Chen, D. J. ATM phosphorylates histone H2AX in response to DNA double-strand breaks. *J Biol Chem* **276**, 42462-42467 (2001).
99. Canman, C. E., Wolff, A. C., Chen, C. Y., Fornace, A. J., Jr. & Kastan, M. B. The p53-dependent G1 cell cycle checkpoint pathway and ataxia- telangiectasia. *Cancer Res* **54**, 5054-508. (1994).
100. Khanna, K. K. & Lavin, M. F. Ionizing radiation and UV induction of p53 protein by different pathways in ataxia-telangiectasia cells. *Oncogene* **8**, 3307-312. (1993).

101. Kastan, M. B. et al. A mammalian cell cycle checkpoint pathway utilizing p53 and GADD45 is defective in ataxia-telangiectasia. *Cell* **71**, 587-597 (1992).
102. Karlseder, J., Broccoli, D., Dai, Y., Hardy, S. & de Lange, T. p53- and ATM-dependent apoptosis induced by telomeres lacking TRF2. *Science* **283**, 1321-1325 (1999).
103. Smogorzewska, A. & de Lange, T. Different telomere damage signaling pathways in human and mouse cells. *Embo J* **21**, 4338-4348 (2002).
104. Karlseder, J., Smogorzewska, A. & de Lange, T. Senescence induced by altered telomere state, not telomere loss. *Science* **295**, 2446-2449 (2002).
105. Smogorzewska, A., Karlseder, J., Holtgreve-Grez, H., Jauch, A. & de Lange, T. DNA Ligase IV-Dependent NHEJ of Deprotected Mammalian Telomeres in G1 and G2. *Curr Biol* **12**, 1635 (2002).
106. Celli, G. B., Lazzerini Denchi, E. & de Lange, T. Ku70 stimulates fusion of dysfunctional telomeres yet protects chromosome ends from homologous recombination. *Nat Cell Biol* **8**, 885-890 (2006).
107. Zhu, X. D. et al. ERCC1/XPF Removes the 3' Overhang from Uncapped Telomeres and Represses Formation of Telomeric DNA-Containing Double Minute Chromosomes. *Mol Cell* **12**, 1489-1498 (2003).
108. Godhino Ferreira, M. & Promisel Cooper, J. The fission yeast Taz1 protein protects chromosomes from Ku-dependent end-to-end fusions. *Mol Cell* **7**, 55-63. (2001).
109. Ancelin, K. et al. Targeting assay to study the cis functions of human telomeric proteins: evidence for inhibition of telomerase by TRF1 and for activation of telomere degradation by TRF2. *Mol Cell Biol* **22**, 3474-3487 (2002).
110. Li, B. & Lustig, A. J. A novel mechanism for telomere size control in Saccharomyces cerevisiae. *Genes Dev* **10**, 1310-1326 (1996).
111. Lustig, A. J. Clues to catastrophic telomere loss in mammals from yeast telomere rapid deletion. *Nat Rev Genet* **4**, 916-923 (2003).
112. Nakamura, T. M., Cooper, J. P. & Cech, T. R. Two modes of survival of fission yeast without telomerase. *Science* **282**, 493-496 (1998).
113. Tarsounas, M. et al. Telomere maintenance requires the RAD51D recombination/repair protein. *Cell* **117**, 337-347 (2004).
114. Jaco, I. et al. Role of mammalian Rad54 in telomere length maintenance. *Mol Cell Biol* **23**, 5572-5580 (2003).
115. Karlseder, J. et al. The telomeric protein TRF2 binds the ATM kinase and can inhibit the ATM-dependent DNA damage response. *PLoS Biol* **2**, E240 (2004).
116. Michelson, R. J., Rosenstein, S. & Weinert, T. A telomeric repeat sequence adjacent to a DNA double-stranded break produces an anticheckpoint. *Genes Dev* **19**, 2546-2559 (2005).
117. Hockemeyer, D., Sfeir, A. J., Shay, J. W., Wright, W. E. & de Lange, T. POT1 protects telomeres from a transient DNA damage response and determines how human chromosomes end. *EMBO J.* **24**, 2667-2678 (2005).
118. Hockemeyer, D., Daniels, J. P., Takai, H. & de Lange, T. Recent expansion of the telomeric complex in rodents: Two distinct POT1 proteins protect mouse telomeres. *Cell* **126**, 63-77 (2006).
119. Zou, L. & Elledge, S. J. Sensing DNA damage through ATRIP recognition of RPA-ssDNA complexes. *Science* **300**, 1542-1548 (2003).

120. Smith, S., Giriat, I., Schmitt, A. & de Lange, T. Tankyrase, a poly(ADP-ribose) polymerase at human telomeres. *Science* **282**, 1484-1487 (1998).
121. Smith, S. & de Lange, T. Tankyrase promotes telomere elongation in human cells. *Curr Biol* **10**, 1299-302. (2000).
122. Donigian, J. R. & de Lange, T. The role of the poly(ADP-ribose) polymerase tankyrase1 in telomere length control by the TRF1 component of the shelterin complex. *J Biol Chem* **282**, 22662-22667 (2007).
123. Sbodio, J. I. & Chi, N. W. Identification of a tankyrase-binding motif shared by IRAP, TAB182, and human TRF1 but not mouse TRF1. NuMA contains this RXXPDG motif and is a novel tankyrase partner. *J Biol Chem* **277**, 31887-31892 (2002).
124. Zhou, X. Z. & Lu, K. P. The Pin2/TRF1-Interacting Protein PinX1 Is a Potent Telomerase Inhibitor. *Cell* **107**, 347-59. (2001).
125. Guglielmi, B. & Werner, M. The yeast homolog of human PinX1 is involved in rRNA and small nucleolar RNA maturation, not in telomere elongation inhibition. *J Biol Chem* **277**, 35712-35719 (2002).
126. Hsu, H. L., Gilley, D., Blackburn, E. H. & Chen, D. J. Ku is associated with the telomere in mammals. *Proc Natl Acad Sci USA* **96**, 12454-12458 (1999).
127. Hsu, H. L. et al. Ku acts in a unique way at the mammalian telomere to prevent end joining. *Genes Dev* **14**, 2807-212. (2000).
128. d'Adda di Fagagna, F. et al. Effects of DNA nonhomologous end-joining factors on telomere length and chromosomal stability in mammalian cells. *Curr Biol* **11**, 1192-116. (2001).
129. Zhu, X. D., Kuster, B., Mann, M., Petrini, J. H. & de Lange, T. Cell-cycle-regulated association of RAD50/MRE11/NBS1 with TRF2 and human telomeres. *Nat Genet* **25**, 347-352 (2000).
130. Weemaes, C. M. et al. A new chromosomal instability disorder: the Nijmegen breakage syndrome. *Acta Paediatr Scand* **70**, 557-64. (1981).
131. Seemanova, E. et al. Familial microcephaly with normal intelligence, immunodeficiency, and risk for lymphoreticular malignancies: a new autosomal recessive disorder. *Am J Med Genet* **20**, 639-648 (1985).
132. Ranganathan, V. et al. Rescue of a telomere length defect of Nijmegen breakage syndrome cells requires NBS and telomerase catalytic subunit. *Curr Biol* **11**, 962-96. (2001).
133. Uziel, T. et al. Requirement of the MRN complex for ATM activation by DNA damage. *Embo J* **22**, 5612-5621 (2003).
134. Lee, J. H. & Paull, T. T. ATM activation by DNA double-strand breaks through the Mre11-Rad50-Nbs1 complex. *Science* **308**, 551-554 (2005).
135. Falck, J., Coates, J. & Jackson, S. P. Conserved modes of recruitment of ATM, ATR and DNA-PKcs to sites of DNA damage. *Nature* **434**, 605-611 (2005).
136. Wu, Y., Xiao, S. & Zhu, X. D. MRE11-RAD50-NBS1 and ATM function as co-mediators of TRF1 in telomere length control. *Nat Struct Mol Biol* **14**, 832-840 (2007).
137. Opresko, P. L. et al. Telomere binding protein TRF2 binds to and stimulates the Werner and Bloom syndrome helicases. *J Biol Chem* **277**, 41110-41119 (2002).

138. Machwe, A., Xiao, L. & Orren, D. K. TRF2 recruits the Werner syndrome (WRN) exonuclease for processing of telomeric DNA. *Oncogene* **23**, 149-156 (2004).
139. Hickson, I. D. RecQ helicases: caretakers of the genome. *Nat Rev Cancer* **3**, 169-178 (2003).
140. Laud, P. R. et al. Elevated telomere-telomere recombination in WRN-deficient, telomere dysfunctional cells promotes escape from senescence and engagement of the ALT pathway. *Genes Dev* **19**, 2560-2570 (2005).
141. van Overbeek, M. & de Lange, T. Apollo, an Artemis-related nuclease, interacts with TRF2 and protects human telomeres in S phase. *Curr Biol* **16**, 1295-1302 (2006).
142. Lenain, C. et al. The Apollo 5' exonuclease functions together with TRF2 to protect telomeres from DNA repair. *Curr Biol* **16**, 1303-1310 (2006).
143. Cooper, J. P., Nimmo, E. R., Allshire, R. C. & Cech, T. R. Regulation of telomere length and function by a Myb-domain protein in fission yeast. *Nature* **385**, 744-747 (1997).
144. Henson, J. D., Neumann, A. A., Yeager, T. R. & Reddel, R. R. Alternative lengthening of telomeres in mammalian cells. *Oncogene* **21**, 598-610 (2002).
145. Bryan, T. M., Englezou, A., Gupta, J., Bacchetti, S. & Reddel, R. R. Telomere elongation in immortal human cells without detectable telomerase activity. *Embo J* **14**, 4240-4248 (1995).
146. Murnane, J. P., Sabatier, L., Marder, B. A. & Morgan, W. F. Telomere dynamics in an immortal human cell line. *Embo J* **13**, 4953-4962 (1994).
147. Dunham, M. A., Neumann, A. A., Fasching, C. L. & Reddel, R. R. Telomere maintenance by recombination in human cells. *Nat Genet* **26**, 447-450 (2000).
148. Yeager, T. R. et al. Telomerase-negative immortalized human cells contain a novel type of promyelocytic leukemia (PML) body. *Cancer Res* **59**, 4175-4179 (1999).
149. Abraham, R. T. PI 3-kinase related kinases: 'big' players in stress-induced signaling pathways. *DNA Repair* **3**, 883-887 (2004).
150. Shiloh, Y. ATM and related protein kinases: safeguarding genome integrity. *Nat Rev Cancer* **3**, 155-168 (2003).
151. Kim, S. T., Lim, D. S., Canman, C. E. & Kastan, M. B. Substrate specificities and identification of putative substrates of ATM kinase family members. *J Biol Chem* **274**, 37538-37543 (1999).
152. Bakkenist, C. J. & Kastan, M. B. Initiating cellular stress responses. *Cell* **118**, 9-17 (2004).
153. Osborn, A. J., Elledge, S. J. & Zou, L. Checking on the fork: the DNA-replication stress-response pathway. *Trends Cell Biol* **12**, 509-516 (2002).
154. Stiff, T. et al. ATR-dependent phosphorylation and activation of ATM in response to UV treatment or replication fork stalling. *EMBO J* **25**, 5775-5782 (2006).
155. Adams, K. E., Medhurst, A. L., Dart, D. A. & Lakin, N. D. Recruitment of ATR to sites of ionising radiation-induced DNA damage requires ATM and components of the MRN protein complex. *Oncogene* **25**, 3894-3904 (2006).
156. Cuadrado, M. et al. ATM regulates ATR chromatin loading in response to DNA double-strand breaks. *J Exp Med* **203**, 297-303 (2006).
157. Jazayeri, A. et al. ATM- and cell cycle-dependent regulation of ATR in response to DNA double-strand breaks. *Nat Cell Biol* **8**, 37-45 (2006).

158. Myers, J. S. & Cortez, D. Rapid activation of ATR by ionizing radiation requires ATM and Mre11. *J Biol Chem* **281**, 9346-9350 (2006).
159. Smith, G. C. & Jackson, S. P. The DNA-dependent protein kinase. *Genes Dev* **13**, 916-934 (1999).
160. Meek, K., Gupta, S., Ramsden, D. A. & Lees-Miller, S. P. The DNA-dependent protein kinase: the director at the end. *Immunol Rev* **200**, 132-141 (2004).
161. Yamashita, A., Ohnishi, T., Kashima, I., Taya, Y. & Ohno, S. Human SMG-1, a novel phosphatidylinositol 3-kinase-related protein kinase, associates with components of the mRNA surveillance complex and is involved in the regulation of nonsense-mediated mRNA decay. *Genes Dev* **15**, 2215-2228 (2001).
162. Brumbaugh, K. M. et al. The mRNA surveillance protein hSMG-1 functions in genotoxic stress response pathways in mammalian cells. *Mol Cell* **14**, 585-598 (2004).
163. Dann, S. G. & Thomas, G. The amino acid sensitive TOR pathway from yeast to mammals. *FEBS Lett* **580**, 2821-2829 (2006).
164. Lustig, A. J. & Petes, T. D. Identification of yeast mutants with altered telomere structure. *Proc Natl Acad Sci USA* **83**, 1398-1402 (1986).
165. Takata, H., Kanoh, Y., Gunge, N., Shirahige, K. & Matsuura, A. Reciprocal association of the budding yeast ATM-related proteins Tel1 and Mec1 with telomeres in vivo. *Mol Cell* **14**, 515-522 (2004).
166. Hector, R. E. et al. Tel1p preferentially associates with short telomeres to stimulate their elongation. *Mol Cell* **27**, 851-858 (2007).
167. Sabourin, M., Tuzon, C. T. & Zakian, V. A. Telomerase and Tel1p preferentially associate with short telomeres in S. cerevisiae. *Mol Cell* **27**, 550-561 (2007).
168. Bianchi, A. & Shore, D. Increased association of telomerase with short telomeres in yeast. *Genes Dev* **21**, 1726-1730 (2007).
169. Ritchie, K. B., Mallory, J. C. & Petes, T. D. Interactions of TLC1 (which encodes the RNA subunit of telomerase), TEL1, and MEC1 in regulating telomere length in the yeast Saccharomyces cerevisiae. *Mol Cell Biol* **19**, 6065-6075 (1999).
170. Dahlen, M., Olsson, T., Kanter-Smoler, G., Ramne, A. & Sunnerhagen, P. Regulation of telomere length by checkpoint genes in Schizosaccharomyces pombe. *Mol Biol Cell* **9**, 611-621 (1998).
171. Naito, T., Matsuura, A. & Ishikawa, F. Circular chromosome formation in a fission yeast mutant defective in two ATM homologues. *Nat Genet* **20**, 203-206 (1998).
172. Tseng, S. F., Lin, J. J. & Teng, S. C. The telomerase-recruitment domain of the telomere binding protein Cdc13 is regulated by Mec1p/Tel1p-dependent phosphorylation. *Nucleic Acids Res* **34**, 6327-6336 (2006).
173. Goudsouzian, L. K., Tuzon, C. T. & Zakian, V. A. S. cerevisiae Tel1p and Mre11p are required for normal levels of Est1p and Est2p telomere association. *Mol Cell* **24**, 603-610 (2006).
174. Nugent, C. I. et al. Telomere maintenance is dependent on activities required for end repair of double-strand breaks. *Curr Biol* **8**, 657-660 (1998).
175. Ritchie, K. B. & Petes, T. D. The Mre11p/Rad50p/Xrs2p complex and the Tel1p function in a single pathway for telomere maintenance in yeast. *Genetics* **155**, 475-479 (2000).

176. Herbig, U., Jobling, W. A., Chen, B. P., Chen, D. J. & Sedivy, J. M. Telomere shortening triggers senescence of human cells through a pathway involving ATM, p53, and p21(CIP1), but not p16(INK4a). *Mol Cell* **14**, 501-513 (2004).
177. Savitsky, K. et al. A single ataxia telangiectasia gene with a product similar to PI-3 kinase. *Science* **268**, 1749-1753 (1995).
178. Chun, H. H. & Gatti, R. A. Ataxia-telangiectasia, an evolving phenotype. *DNA Repair (Amst)* **3**, 1187-1196 (2004).
179. Metcalfe, J. A. et al. Accelerated telomere shortening in ataxia telangiectasia. *Nat Genet* **13**, 350-353 (1996).
180. Smilenov, L. B. et al. Influence of ATM function on telomere metabolism. *Oncogene* **15**, 2659-2665 (1997).
181. Espejel, S. et al. Functional interaction between DNA-PKcs and telomerase in telomere length maintenance. *Embo J* **21**, 6275-6287 (2002).
182. Goytisolo, F. A., Samper, E., Edmonson, S., Taccioli, G. E. & Blasco, M. A. The absence of the DNA-dependent protein kinase catalytic subunit in mice results in anaphase bridges and in increased telomeric fusions with normal telomere length and G-strand overhang. *Mol Cell Biol* **21**, 3642-351. (2001).
183. Bailey, S. M., Cornforth, M. N., Ullrich, R. L. & Goodwin, E. H. Dysfunctional mammalian telomeres join with DNA double-strand breaks. *DNA Repair (Amst)* **3**, 349-357 (2004).
184. Bailey, S. M. et al. DNA double-strand break repair proteins are required to cap the ends of mammalian chromosomes. *Proc Natl Acad Sci USA* **96**, 14899-1904. (1999).
185. Myung, K. et al. Regulation of telomere length and suppression of genomic instability in human somatic cells by Ku86. *Mol Cell Biol* **24**, 5050-5059 (2004).
186. Burge, S., Parkinson, G. N., Hazel, P., Todd, A. K. & Neidle, S. Quadruplex DNA: sequence, topology and structure. *Nucleic Acids Res* **34**, 5402-5415 (2006).
187. Arthanari, H. & Bolton, P. H. Functional and dysfunctional roles of quadruplex DNA in cells. *Chem Biol* **8**, 221-230 (2001).
188. Mirkin, S. M. Expandable DNA repeats and human disease. *Nature* **447**, 932-940 (2007).
189. Neylon, C., Kralicek, A. V., Hill, T. M. & Dixon, N. E. Replication termination in Escherichia coli: structure and antihelicase activity of the Tus-Ter complex. *Microbiol Mol Biol Rev* **69**, 501-526 (2005).
190. Ohki, R. & Ishikawa, F. Telomere-bound TRF1 and TRF2 stall the replication fork at telomeric repeats. *Nucleic Acids Res* **32**, 1627-1637 (2004).
191. Fouche, N., Ozgur, S., Roy, D. & Griffith, J. D. Replication fork regression in repetitive DNAs. *Nucleic Acids Res* **34**, 6044-6050 (2006).
192. Ivessa, A. S., Zhou, J. Q., Schulz, V. P., Monson, E. K. & Zakian, V. A. Saccharomyces Rrm3p, a 5' to 3' DNA helicase that promotes replication fork progression through telomeric and subtelomeric DNA. *Genes Dev* **16**, 1383-1396 (2002).
193. Makovets, S., Herskowitz, I. & Blackburn, E. H. Anatomy and dynamics of DNA replication fork movement in yeast telomeric regions. *Mol Cell Biol* **24**, 4019-4031 (2004).

194. Bakkenist, C. J. & Kastan, M. B. DNA damage activates ATM through intermolecular autophosphorylation and dimer dissociation. *Nature* **421**, 499-506 (2003).
195. Pellegrini, M. et al. Autophosphorylation at serine 1987 is dispensable for murine Atm activation in vivo. *Nature* **443**, 222-225 (2006).
196. Berkovich, E., Monnat, R. J. J. & Kastan, M. B. Roles of ATM and NBS1 in chromatin structure modulation and DNA double-strand break repair. *Nat Cell Biol* **9**, 683-690 (2007).
197. Kozlov, S. V. et al. Involvement of novel autophosphorylation sites in ATM activation. *EMBO J* **25**, 3504-3514 (2006).
198. Bradshaw, P. S., Stavropoulos, D. J. & Meyn, M. S. Human telomeric protein TRF2 associates with genomic double-strand breaks as an early response to DNA damage. *Nat Genet* **37**, 193-197 (2005).
199. Amiard, S. et al. A topological mechanism for TRF2-enhanced strand invasion. *Nat Struct Mol Biol* **14**, 147-154 (2007).
200. Fouche, N. et al. The basic domain of TRF2 directs binding to DNA junctions irrespective of the presence of TTAGGG repeats. *J Biol Chem* **281**, 37486-37495 (2006).
201. Williams, E. S. et al. DNA double-strand breaks are not sufficient to initiate recruitment of TRF2. *Nat Genet* **39**, 696-8; author reply 698-9 (2007).
202. O'Neill, T. et al. Utilization of oriented peptide libraries to identify substrate motifs selected by ATM. *J Biol Chem* **275**, 22719-22727 (2000).
203. Traven, A. & Heierhorst, J. SQ/TQ cluster domains: concentrated ATM/ATR kinase phosphorylation site regions in DNA-damage-response proteins. *Bioessays* **27**, 397-407 (2005).
204. Ward, I. M. & Chen, J. Histone H2AX is phosphorylated in an ATR-dependent manner in response to replicational stress. *J Biol Chem* **276**, 47759-47762 (2001).
205. Wang, H., Wang, M., Wang, H., Bocker, W. & Iliakis, G. Complex H2AX phosphorylation patterns by multiple kinases including ATM and DNA-PK in human cells exposed to ionizing radiation and treated with kinase inhibitors. *J Cell Physiol* **202**, 492-502 (2005).
206. Stiff, T. et al. ATM and DNA-PK function redundantly to phosphorylate H2AX after exposure to ionizing radiation. *Cancer Res* **64**, 2390-2396 (2004).
207. Stucki, M. et al. MDC1 directly binds phosphorylated histone H2AX to regulate cellular responses to DNA double-strand breaks. *Cell* **123**, 1213-1226 (2005).
208. Kishi, S. et al. Telomeric protein Pin2/TRF1 as an important ATM target in response to double strand DNA breaks. *J Biol Chem* **276**, 29282-29291 (2001).
209. Tanaka, H. et al. DNA damage-induced phosphorylation of the human telomere-associated protein TRF2. *Proc Natl Acad Sci U S A* **102**, 15539-15544 (2005).
210. Sarkaria, J. N. et al. Inhibition of phosphoinositide 3-kinase related kinases by the radiosensitizing agent wortmannin. *Cancer Res* **58**, 4375-4382 (1998).
211. Reiling, J. H. & Sabatini, D. M. Stress and mTORture signaling. *Oncogene* **25**, 6373-6383 (2006).
212. Sabatini, D. M. mTOR and cancer: insights into a complex relationship. *Nat Rev Cancer* **6**, 729-734 (2006).

213. Sarbassov, D. D., Guertin, D. A., Ali, S. M. & Sabatini, D. M. Phosphorylation and regulation of Akt/PKB by the rictor-mTOR complex. *Science* **307**, 1098-1101 (2005).
214. Hresko, R. C. & Mueckler, M. mTOR.RICTOR is the Ser473 kinase for Akt/protein kinase B in 3T3-L1 adipocytes. *J Biol Chem* **280**, 40406-40416 (2005).
215. Jacinto, E. et al. Mammalian TOR complex 2 controls the actin cytoskeleton and is rapamycin insensitive. *Nat Cell Biol* **6**, 1122-1128 (2004).
216. Sarbassov, D. D. et al. Rictor, a novel binding partner of mTOR, defines a rapamycin-insensitive and raptor-independent pathway that regulates the cytoskeleton. *Curr Biol* **14**, 1296-1302 (2004).
217. Sarbassov, D. D. et al. Prolonged rapamycin treatment inhibits mTORC2 assembly and Akt/PKB. *Mol Cell* **22**, 159-168 (2006).
218. Petermann, E. & Caldecott, K. W. Evidence that the ATR/Chk1 pathway maintains normal replication fork progression during unperturbed S phase. *Cell Cycle* **5**, 2203-2209 (2006).
219. Stokes, M. P., Van Hatten, R., Lindsay, H. D. & Michael, W. M. DNA replication is required for the checkpoint response to damaged DNA in Xenopus egg extracts. *J Cell Biol* **158**, 863-872 (2002).
220. Fernandez, J. J., Candenas, M. L., Souto, M. L., Trujillo, M. M. & Norte, M. Okadaic acid, useful tool for studying cellular processes. *Curr Med Chem* **9**, 229-262 (2002).
221. Goodarzi, A. A. et al. Autophosphorylation of ataxia-telangiectasia mutated is regulated by protein phosphatase 2A. *EMBO J* **23**, 4451-4461 (2004).
222. Ward, I. M., Minn, K., Jorda, K. G. & Chen, J. Accumulation of checkpoint protein 53BP1 at DNA breaks involves its binding to phosphorylated histone H2AX. *J Biol Chem* **278**, 19579-19582 (2003).
223. Seroz, T. et al. Cloning of a human homolog of the yeast nucleotide excision repair gene MMS19 and interaction with transcription repair factor TFIIH via the XPB and XPD helicases. *Nucleic Acids Res* **28**, 4506-4513 (2000).
224. Greider, C. W. Telomerase activity, cell proliferation, and cancer. *Proc Natl Acad Sci USA* **95**, 90-92 (1998).
225. Matsuoka, S. et al. ATM and ATR substrate analysis reveals extensive protein networks responsive to DNA damage. *Science* **316**, 1160-1166 (2007).
226. Verdun, R. E., Crabbe, L., Haggblom, C. & Karlseder, J. Functional human telomeres are recognized as DNA damage in G2 of the cell cycle. *Mol Cell* **20**, 551-561 (2005).
227. Longhese, M. P., Paciotti, V., Neecke, H. & Lucchini, G. Checkpoint proteins influence telomeric silencing and length maintenance in budding yeast. *Genetics* **155**, 1577-1591 (2000).
228. Brown, E. J. & Baltimore, D. ATR disruption leads to chromosomal fragmentation and early embryonic lethality. *Genes Dev* **14**, 397-402 (2000).
229. Paulsen, R. D. & Cimprich, K. A. The ATR pathway: fine-tuning the fork. *DNA Repair (Amst)* **6**, 953-966 (2007).
230. Cobb, J. A., Bjergbaek, L., Shimada, K., Frei, C. & Gasser, S. M. DNA polymerase stabilization at stalled replication forks requires Mec1 and the RecQ helicase Sgs1. *EMBO J* **22**, 4325-4336 (2003).

231. Lucca, C. et al. Checkpoint-mediated control of replisome-fork association and signalling in response to replication pausing. *Oncogene* **23**, 1206-1213 (2004).
232. Cobb, J. A. et al. Replisome instability, fork collapse, and gross chromosomal rearrangements arise synergistically from Mec1 kinase and RecQ helicase mutations. *Genes Dev* **19**, 3055-3069 (2005).
233. Zachos, G., Rainey, M. D. & Gillespie, D. A. Chk1-dependent S-M checkpoint delay in vertebrate cells is linked to maintenance of viable replication structures. *Mol Cell Biol* **25**, 563-574 (2005).
234. Heller, R. C. & Marians, K. J. Replisome assembly and the direct restart of stalled replication forks. *Nat Rev Mol Cell Biol* **7**, 932-943 (2006).
235. Lisby, M., Barlow, J. H., Burgess, R. C. & Rothstein, R. Choreography of the DNA damage response: spatiotemporal relationships among checkpoint and repair proteins. *Cell* **118**, 699-713 (2004).
236. Meister, P. et al. Temporal separation of replication and recombination requires the intra-S checkpoint. *J Cell Biol* **168**, 537-544 (2005).
237. Boddy, M. N. et al. Replication checkpoint kinase Cds1 regulates recombinational repair protein Rad60. *Mol Cell Biol* **23**, 5939-5946 (2003).
238. Boddy, M. N. et al. Damage tolerance protein Mus81 associates with the FHA1 domain of checkpoint kinase Cds1. *Mol Cell Biol* **20**, 8758-8766 (2000).
239. Kai, M., Boddy, M. N., Russell, P. & Wang, T. S. Replication checkpoint kinase Cds1 regulates Mus81 to preserve genome integrity during replication stress. *Genes Dev* **19**, 919-932 (2005).
240. Wu, L. & Hickson, I. D. The Bloom's syndrome helicase suppresses crossing over during homologous recombination. *Nature* **426**, 870-874 (2003).
241. Ira, G., Malkova, A., Liberi, G., Foiani, M. & Haber, J. E. Srs2 and Sgs1-Top3 suppress crossovers during double-strand break repair in yeast. *Cell* **115**, 401-411 (2003).
242. Karow, J. K., Constantinou, A., Li, J. L., West, S. C. & Hickson, I. D. The Bloom's syndrome gene product promotes branch migration of holliday junctions. *Proc Natl Acad Sci U S A* **97**, 6504-6508 (2000).
243. Cortez, D. Unwind and slow down: checkpoint activation by helicase and polymerase uncoupling. *Genes Dev* **19**, 1007-1012 (2005).
244. Walter, J. & Newport, J. Initiation of eukaryotic DNA replication: origin unwinding and sequential chromatin association of Cdc45, RPA, and DNA polymerase alpha. *Mol Cell* **5**, 617-627 (2000).
245. Byun, T. S., Pacek, M., Yee, M. C., Walter, J. C. & Cimprich, K. A. Functional uncoupling of MCM helicase and DNA polymerase activities activates the ATR-dependent checkpoint. *Genes Dev* **19**, 1040-1052 (2005).
246. Gruber, M., Wellinger, R. E. & Sogo, J. M. Architecture of the replication fork stalled at the 3' end of yeast ribosomal genes. *Mol Cell Biol* **20**, 5777-5787 (2000).
247. Lambert, S., Watson, A., Sheedy, D. M., Martin, B. & Carr, A. M. Gross chromosomal rearrangements and elevated recombination at an inducible site-specific replication fork barrier. *Cell* **121**, 689-702 (2005).
248. Nishiyama, A. et al. Cell-cycle-dependent Xenopus TRF1 recruitment to telomere chromatin regulated by Polo-like kinase. *EMBO J* **25**, 575-584 (2006).

249. Bai, Y. & Murnane, J. P. Telomere instability in a human tumor cell line expressing a dominant-negative WRN protein. *Hum Genet* **113**, 337-347 (2003).
250. Miller, K. M., Rog, O. & Cooper, J. P. Semi-conservative DNA replication through telomeres requires Taz1. *Nature* **440**, 824-828 (2006).
251. Ye, J. Z. & de Lange, T. TIN2 is a tankyrase 1 PARP modulator in the TRF1 telomere length control complex. *Nat Genet* **36**, 618-623 (2004).
252. O'Driscoll, M., Ruiz-Perez, V. L., Woods, C. G., Jeggo, P. A. & Goodship, J. A. A splicing mutation affecting expression of ataxia-telangiectasia and Rad3-related protein (ATR) results in Seckel syndrome. *Nat Genet* **33**, 497-501 (2003).
253. Silver, D. P. & Livingston, D. M. Self-excising retroviral vectors encoding the Cre recombinase overcome Cre-mediated cellular toxicity. *Mol Cell* **8**, 233-243 (2001).